Multi-omics studies of thermal response towards the development of heat-tolerant bread wheat

(高温耐性パンコムギの開発に向けた高温応答のマルチオミクス研究)

The United Graduate School of Agricultural Sciences,

Tottori University, Japan

Sachiko Matsunaga

松永 幸子

2022

Table of contents

1. Introduction

The world's cereal production must be sustainably increased to meet the growing food demand of a rising global population under increasing climate change. Rice, maize, and wheat account for about 90% of the current total cereal production (FAOSTAT, 2021). Of these, wheat is the most susceptible to heat stress. Asseng *et al.* (2011) reported a 6% reduction in yield for every 1°C increase in temperature. On the basis of the analysis of temperature effects on yield in Sudan, the hottest wheat-growing area in the world, Iizumi *et al.* (2021) concluded that the development of heat-tolerant wheat cultivars is essential.

Plants show a variety of morphological, physiological, biochemical, and molecular changes when exposed to high temperatures. Typical responses include growth disorders, inhibition of photosynthesis, accumulation or reduction of plant hormones, production of heat shock proteins and accumulation of reactive oxygen species (Qu *et al.* 2013); and wheat shows such responses (Abdelrahm *et al.*, 2020). Reduction of photosynthetic capacity caused by chlorophyll loss and sterility caused by abnormal development of pollen grains or tubes greatly reduce grain yield (Abdelrahm *et al.*, 2020). To overcome heat stress, wheat plants can lower canopy temperature by opening stomata to activate transpiration (Fisher *et al.*, 1998). Winter wheat grows where the temperature rises with the stage of crop growth. Previous studies of the effect of high temperatures on wheat have focused on the most sensitive stage, *i.e.*, the reproductive stage (Rezaei *et al.*, 2018; Telfer *et al.*, 2018; Zampieri *et al.*, 2018). However, in future global warming scenarios, temperatures will increase in all growth stages (Stocker *et al.*, 2021). Heat-stress effects might depend on the growth stage (Wahid *et al.*, 2007). Thus, it is necessary to consider responses to high temperatures during other growth stages as well. To breed cultivars that

maintain yield even under high warming conditions, it is necessary to analyze the effects of heat on grain yield.

Wheat is a general term for several species, and the main cultivated wheat species are bread wheat (*Triticum aestivum* L., genome constitution AABBDD) and durum wheat (*Triticum turgidum ssp. durum* (Desf.) Husn, genome constitution AABB). Durum wheat is suitable for Mediterranean climates and shows high yields in this environment. Bread wheat, on the other hand, has a broad adaptability and can be grown in areas other than the Mediterranean climate. As a result, about 90% of the world's wheat is now bread wheat. Bread wheat originated as a hybrid plant about 8,000 to 10,000 years ago, when pollen from *Aegilops tauschii* ssp. *strangulata* (the D genome donor) pollinated the pistils of the cultivated species of durum wheat (Kihara, 1944; McFadden and Sears, 1944). With this hybridization, bread wheat obtained the high productivity derived from durum wheat and the environmental adaptability derived from *Aegilops tauschii* Coss. (genome constitution DD), giving bread wheat the ability to adapt to a wide area of the world. In the process of cultivation around the world, a group of varieties suitable for various climates were selected. In modern breeding, aggressive crossbreeding has taken place leading to the selection of plant types desired by man. In particular, the semi-dwarf varieties developed during the Green Revolution have shown much higher yields than conventional varieties and have supported the food supply of people around the world (Gale and Youssefian, 1985).

In recent years, global warming has had a negative impact on wheat production. To develop wheat varieties that can adapt to global warming, it is necessary to find and utilize high-temperature related genes. However, the diversity of current bread wheat cultivars is too narrow, thereby hindering the creation of new tolerant lines suited to

environments with severe heat stress by crossing among the cultivars. Therefore, there is a need to utilize unconventional genetic resources to advance wheat breeding, especially for abiotic stress tolerance. It was reported that crossbreeding between durum wheat (AB genome donor) and *Ae. tauchii* ssp. *strangulata* (D genome donor) in northern Iran occurred to generate hexaploidy bread wheat. On the other hand, the genetic diversity of *Ae. tauchii* is widely distributed in many regions including West Asia, Central Asia, South Caucasus and Northern Iran (Matsuoka, 2011). Therefore, it is believed that D genome derived from the wild wheat relative contains stress tolerance genes for adaptation to different environmental niches such as salt tolerance and cold hardiness (Schachtman *et al*., 1992; Babben *et al.*, 2018). This suggests that various genes underlying tolerance to harsh environments, which have not yet been used in bread wheat breeding, can be introduced from wild wheat relatives such as the D genome donorto provide additional tolerance to bread wheat.

Synthetic wheat is a hybrid derived from the artificial crossing of durum wheat and *Ae. tauschii* in a combination similar to the evolution of bread wheat. Matsuoka and Nasuda (2004) developed synthetic wheat by crossing a durum wheat cv. 'Langdon' with 51 lines of *Ae. tauschii*. However, these synthetic wheat lines have strong characteristics of wild species derived from *Ae. tauschii*, such as hard spikes, which makes threshing, and measurement of yield and seed traits difficult. Therefore, a group of lines were developed by crossing these synthetic wheat lines with practical bread wheat cultivars and then backcrossing with the practical bread wheat cultivars. These lines were self-pollinated in bulk to fix the genes. This wheat diversity population is called the multiple synthetic derivatives (MSD) population (Tsujimoto *et al.,* 2015). Although this population incorporate intraspecific variation in *Ae. tauschii*, three-fourths of its D genome is derived

from practical bread wheat varieties, making it as easy to thresh as conventional bread wheat, and serves as an advanced population that can be evaluated from a variety of bread wheat traits including D genome diversity and yield potential (Tsujimoto *et al.,* 2015; Gorafi *et al.,* 2018).

Elbashir *et al.* (2017a, b) cultivated MSD populations with a genetic background of the practical wheat cultivar 'Norin 61' in experimental plots in Sudan and selected lines that could maintain or increase yield under high-temperature conditions. However, the molecular mechanisms underlying resistance to heat stress remains unclear, as it is still limited to plant observations and physiological response analysis in the field and simulated environmental conditions. Elucidation of the molecular mechanisms underlying heat tolerance will enable us to understand the tolerance mechanisms in terms of molecular behavior and contribute to the precise selection of desirable plant types via molecular breeding approaches.

Omics-analysis is a method directed toward comprehensively elucidating the molecular behavior in plants. Omics-analysis includes genomics, transcriptomics, proteomics, and metabolomics, which comprehensively analyze genomic sequences (DNA), gene expressions with alternative splicing (mRNA), proteins and metabolites, respectively. Comprehensive phenotypic analysis and elemental analysis are also sometimes called phenomics and ionomics.

Living organisms have DNA which encodes genetic information. From this DNA, mRNA is transcribed followed by translation into proteins. The resulting proteins function as enzymes that speed up biochemical reactions and synthesis of chemical compounds to sustain life in the organism. Individual metabolites produced by metabolism are divided into two types: primary metabolites and secondary metabolites. Primary metabolites are

necessary to produce substances essential for biological activities and include sugars, amino acids, nucleic acids and organic acids. Secondary metabolites are substances that are not directly involved in essential activities for normal growth and development but have important ecological functions such as protecting from abiotic and biotic stresses (Obata *et al.*, 2015; Avila-Ospina, Clément and Masclaux-Daubresse, 2017; Templer *et al.*, 2017; Todaka *et al.*, 2017; Nguyen *et al.*, 2019; Shi *et al.*, 2020). They include pigments and antioxidants and can be broadly classified into three categories: terpenes, phenols, and nitrogen compounds. Metabolites also include plant hormones, which act as signal transmitters within the plant to regulate their growth. These metabolites belong to various but connected metabolic pathways, and when one metabolic pathway fluctuates, other metabolic pathways can be affected leading to various metabolites accumulation and consequently their phenotype associations. It is our expectation that a comprehensive investigation of these metabolic pathways in wheat would reveal important molecular mechanisms underlying high-temperature tolerance. For this reason, a detailed metabolomic analysis of plants subjected to high-temperature stress was conducted in this doctoral thesis.

The qualitative and quantitative analysis of the metabolites was performed using LC-MS/MS, which stands for high-performance liquid chromatography-tandem mass spectrometry. It is a system composed of (1) High-performance liquid chromatograph (HPLC); (2) Ionization process to lead chemical compounds into mass spectrometer; (3) Tandem mass spectrometer (MS/MS) for qualitative and quantitative analysis of chemical compounds. Firstly, ion-exchange chromatography is used to mutually separate the sample components according to their retention time in the column by utilizing the difference in affinity of the solute for the stationary phase and mobile phase (liquid) based

on their polarity. Then, the separated column eluate is passed to ionization by spraying the eluate under atmospheric pressure using the electrospray ionization (ESI) method followed by the mass separation section. In the mass separation section, there are two sets of ionization sections with DC and AC voltages (quadrupole mass spectrometer), and the ionized compounds are separated according to specific m/z (m: mass of ion divided by unified atomic mass unit, z: charge number of ion) values and reach the detector for mass analysis. The ions produced in the first mass spectrometry (MS1) are called precursor ions, and the precursor ions are further decomposed by colliding with an inert gas (*e.g.* nitrogen) to produce product ions. Product ions are transferred to the second mass spectrometry (MS2) to identify their m/z and quantify them. By performing mass spectrometry in two stages, it is possible to qualify compounds with higher accuracy. The results of mass spectrometry are presented in the form of a mass spectrum, which is represented by m/z on the horizontal axis and ion intensity on the vertical axis. A compound is quantified by comparing the peak with the highest ion intensity. Since mass spectrometry results are multivariate data, multivariate analysis such as principal component analysis (PCA) and hierarchical clustering were used to observe changes in metabolite content due to high-temperature stress treatment, and to pick up metabolites that show significant changes in different environments and analyze their trends. Also, metabolites with significant changes can be mapped in the metabolic pathways to find the pathways responding to experimental factors such as stress environments. It is expected that this metabolite analysis would reveal novel molecular markers for stress response and tolerance mechanisms in wheat.

2. Materials and Methods

2.1. Plant materials and growth conditions

The bread wheat (*Triticum aestivum* L.) cultivar 'Norin 61' is facultative wheat grown in Japan and is generally used as the standard check in breeding programs. The MSD population were produced by crossing and backcrossing of the Japanese bread wheat cultivar 'Norin 61' with 43 synthetic hexaploid wheat lines derived from crosses between 43 accessions of *Ae. tauschii* and *T. turgidum var. durum* cv. 'Langdon' (Kajimura *et al.*, 2011; Matsuoka and Nasuda, 2004). The BC_1F_4 seeds of the selected lines and 'Norin 61' were sown at Gezira Research Farm, Agricultural Research Corporation, Sudan in the 2015/2016 season. Seeds were sown either in the third week of November (optimum sowing; OS) or in the second week of December (late sowing; LS), which was used to expose plants to heat stress at the reproductive stage. The yields of 234 different MSD lines and 'Norin 61' were plotted and five lines (MSD296, MSD34, MSD392, MSD417 and MSD54) that increased or maintained their yields at LS compared to OS were selected (Figure 1). In addition to these lines, MNH2, which has been reported as a line that may have heat tolerance genes (Elbashir *et al.*, 2017b) was also selected. Fully matured seeds of both 'Norin 61' and the selected six lines, were harvested in 2016 in the field of the Agricultural Research Corporation, Wad Medani, Sudan. The harvested seeds had >99% germination rate.

Plants were grown in climate chambers in which temperature, humidity and light were controlled as below (Espec, Japan: W 1800 mm × D 1800 mm × H 2500 mm) at the Arid Land Research Center, Tottori University, Japan. Owing to limited space in the

chambers, plants were grown in two seasons (Mar – Jul 2019 and Jan – May 2020). In the first experiment, one planter (46.5 cm × 23.7 cm × 17.5 cm) with six plants was used for each heat treatment. In the second experiment, two planters with six plants each were used. A control treatment was used in both seasons to standardize experimental fluctuations. Seeds were placed on a sheet of filter paper in Petri dishes and soaked in tap water. The seeds were stratified at 4°C for 7 days and incubated for germination at room temperature for 72 h. Six 1-cm sprouts were transplanted into a planter filled with a commercial soil mixture made of composted bark, granular clay-like mineral, pumice, peat moss, perlite and vermiculite (Cainz, Honjo City, Saitama, Japan). The planters were placed in the growth chambers. In the control treatment, the air temperature was controlled at 22°C maximum in the daytime and 18°C continuously at night. In the heat environments, it was controlled at 38°C maximum during the day and 18°C continuously at night (Figure 2A). The temperature shift slope was set at 4°C per hour until these temperatures were reached. The light duration was 14 h light and 10 h dark. The relative humidity was 30% day / 50% night. The photosynthetic photon flux density was 1000 μmol s^{-1} m^{-2}. Three growth stages were designated: GS1, heat exposure from two-leaf to tillering (Zadoks's scale, Z12–Z19); GS2, heat exposure from budding to flowering (Z20–Z61), and GS3, from flowering to full maturity (Z62–Z95) (Figure 2B) (Acevedo *et al.*, 2002, Zadoks *et al.*, 1974). Six selected MSD lines and 'Norin 61' were exposed to heat at GS3. The plants were transferred from the control chamber to the heating chamber during the respective periods. At the beginning of GS3, 10 g of NPK fertilizer (MC Ferticom Co., Ltd., Chiyoda Ward, Tokyo, Japan) containing 13% N, 16% P, and 16% K by total weight (present as water-soluble ammonium phosphate dibasic and water-soluble potassium) was supplied.

2.2. Measurement of plant traits

Plant height was measured in centimeters from the soil surface to the top of the spike, excluding awns. The number of tillers with spikes was counted as tiller number. The dry weight of the entire aboveground part was defined as biomass, and that of the aboveground part without spikes was defined as culm and leaf weight. Total grain yield from one plant was defined as grain yield. Grain weight per spike, grain number per spike and spikelet number per spike were measured using five representative spikelets. Harvest index was calculated as grain yield ÷ biomass. Fertility was defined as grain number per spike ÷ spikelet number per spike.

In the 'Norin 61' study, all six plants were measured independently in the same condition. Six plants in the same planter of the first and second experiments were measured separately. After standardizing the values based on the average in the two different experiments, the values from the total of 12 plants served as replications.

To observe seed maturation, seeds at 10, 20, 30, 40, and 50 days post-anthesis were excised from the first and second florets of the ten spikelets above four or six spikelets, which may contain immature seeds, from the spike basal end. Fresh weight (FW) was measured immediately after collecting immature seeds and dry weight (DW) after complete desiccation in an oven at 80°C. One spike per plant was collected randomly from three of the six plants on each date. FW and DW are presented as the average of the three spikes. In the study about MSD lines, six plants in the same planter were measured separately. PCA, heat map and barplot of agronomic traits were created using R version 4.0.3 (https://www.R-project.org/).

2.3. Mineral analysis

Ten matured seeds or 500 mg of crushed matured plants from individuals in each condition were used. The samples (10 seeds or 500 mg of powdered matured individual plant straw and leaves in each condition) were placed in quartz glass bottles with 5 mL of 70% nitric acid (electronics industry grade: FUJIFILM Wako cat# 143-09741) followed by digestion at 190°C for 20 min. Insoluble material was removed from the solution by centrifugation and then the supernatant was diluted 2000 times with 1% nitric acid for ICP-MS analysis. The concentration of each element was calculated based on counts per second (CPS) with standard curves using dilution series of a standard mixture (SPEX XSTC-331 and XSTC-8) to contain 42 different elements. Quantifications for each element between replications was validated with a relative standard deviation (RSD) less than 30%.

2.4. Gas exchange rate measurements

The CO_2 exchange rate of one flag leaf per plant selected from three of the six plants was measured with an LI-6800XT portable gas exchange system (Li-Cor, Lincoln, Nebraska, USA) at CO_2 concentrations of 0, 50, 100, 200, 400, 500, 800, 1000, 1500, and 2000 ppm. The leaf temperature was 22°C in the control and 38°C in the heat treatment. Other settings were fixed: humidity, 18%; light intensity, 1000 μmol s^{-1} m^{-2} with 90% red and 10% blue light source; and flow rate, 500 μmol s^{-1}. Three biological replicates in each environment were measured at 14 days post-anthesis. From the measurements, photosynthetic CO_2 assimilation (*A*) and leaf intercellular CO_2 concentration (*Ci*) (*A–Ci*

curve) were plotted. Through curve fitting, *Vcmax*, *J,* and *TPU* were obtained as per Sharkey et al. (2007). Data could not be collected from two GS3 replicates, which had completely senesced.

2.5. Metabolite analysis

Six flag leaves were collected from two plants (three from each plant) at 7 days post-anthesis, and flash-frozen in liquid nitrogen. The flash-frozen samples were pulverized using a Multi-Beads Shocker (Yasui Kikai, Osaka, Japan) without thawing, and then stored at −80°C. The powder was dehydrated using a VD-550R freeze-dryer (TITEC, Saitama, Japan), and then 4 mg of the dry powdered sample was extracted with 400 μL of 80% v/v methanol (MeOH, LC/MS grade; FUJIFILM Wako Chemicals, Osaka, Japan; cat# 138-14521) overnight at room temperature in the dark.

After centrifugation (15,000 rpm, 5 min, 4°C), the supernatant was collected, and then centrifuged again to remove any insoluble material. The concentrations of 69 metabolites (Table 1) were quantified from the supernatant using a triple-quadrupole LC-MS/MS system (Agilent 6420, Santa Clara, CA, USA) and a Discovery HS-F5 column (2.1 × 250 mm, 5 μm i.d.; Sigma-Aldrich, Allentown, PA, USA). Metabolites were identified utilizing multiple reaction monitoring analysis. The product ions used to characterize each metabolite are shown in Table 1.

The metabolite levels were standardized in each sample per unit sample dry weight and then calculated *z*-scores relative to the control value. Standard curves for the metabolites were established using laboratory standard solutions at different concentrations (0.00, 0.08, 0.40, 2.00, and 10.00 ppm). Compounds with similar

molecular weights or retention times were not included in the same mixture. The mobile phase consisted of 0.1% v/v formic acid (LC/MS grade; FUJIFILM Wako; cat# 067-04531) and acetonitrile (LC/MS grade; FUJIFILM Wako; cat# 018-19853) as the A and B solutions, respectively. Four A:B ratio gradient flows: (1) 100% A:0% B for 2 min, (2) 75% A:25% B for 8 min, (3) 65% A:35% B for 4 min, and (4) 5% A:95% B for 3 min were then applied. The peaks derived from the metabolites with a high signal-to-noise ratio were evaluated to exclude unreliable peaks. Quantifications for each metabolite between replications were validated with relative standard deviation (RSD) less than 30%. The metabolite concentrations obtained from each condition was divided by the mean value of the control, and the fold change from the control was calculated. The values were used for enrichment analysis and multivariate analysis.

2.6. Statistical analysis

The dataset was analyzed using MetaboAnalyst 5.0 (https://www.metaboanalyst.ca/), which is a Web-based metabolomics data analysis software. Metabolites with missing values even in one replication under each condition were excluded and analyses was performed using only metabolites that were stably detected in all replicates with RSD less than 30%. One of the three iterations of GS2 showed clear outliers for all metabolites, and so it was excluded from the analysis.

Univariate analysis was applied to calculate the change in metabolite concentrations between each heat-stressed condition and the control. To assess the statistical significance of our results, *t*-tests and one-way ANOVA were performed using R version 4.1.0. (https://www.R-project.org/). *P* values less than 0.05 were considered

statistically significant. The multivariate method principal component analysis was applied to provide additional insights into the relationships among the variables. For the metabolites that showed a significant change ($p < 0.05$), pathway analysis and enrichment analysis were performed using MetaboAnalyst 5.0. The enrichment analysis selected the metabolic pathways with false discovery rate (FDR) less than 0.05.

Pearson correlation coefficients were used to evaluate relationships between metabolites and agricultural traits and tested whether the correlation coefficients were significantly different from 0 ($p < 0.05$). The Benjamini-Hochberg correction was applied to adjust the significance level in a multiple test. The values of the abundance of 69 metabolites and 15 agronomic traits of the corresponding samples were used in the analysis.

2.7. Network analysis and multiple regression analysis

In estimating causal relationships among agronomic traits, agronomic traits measured in each growth treatment as well as dummy variables indicating which growth stage was exposed to the high-temperature environment (GS1, GS2, GS3) were included to estimate the effect of high-temperature stress. Since some phenotypic distributions of the traits were found to be far from the normal distribution, the bootstrap method, which does not specify the shape of the distribution, was used for the estimation. Three types of inappropriate causal relationships were pre-blacklisted to ensure that uninterpretable causal relationships were not included in the estimation results: (1) agronomic traits as causes and dummy variables representing high-temperature stress as outcomes; (2) yield-related traits (grain yield, grain number per spike, spikelet number per spike, grain weight

per spike, spike length, grain number, thousand kernel weight, fertility) as the cause and biomass-related traits (other than those listed) as the outcome, and (3) grain yield as the cause and other agronomic traits as the outcome. The estimation results include innumerable causal relationships. To extract useful causal relationships among them, the strength of the relationships was drawn, and the threshold was visually defined. The R package bnlearn (ver. 4.7) was used for the analysis.

Next, the impact of the ionome and metabolome on each trait was estimated by regression analysis, considering the obtained causal relationships. The regression analysis was repeated with the ionome and metabolome as the explanatory variable and one agricultural trait as the objective variable. However, since there are interactions among agricultural traits, the influence of the ionome metabolome through other agricultural traits cannot be eliminated. Therefore, a regression analysis was conducted to eliminate indirect effects by using Bayesian networks and including traits that have relationships with the target variable as explanatory variables. Specifically, it is known that indirect effects can be eliminated by considering variables that have the following relationships with the objective variable on the Bayesian network (called Markov blankets) (Bishop, 2006): (1) parent node of the objective variable, (2) child node of the objective variable, (3) parent node of (2).

Note that LASSO was used as the method for estimating the regression coefficients because the usual multiple regression cannot be used when the number of samples is larger than the number of traits.

3. Results

3.1. Stage-specific response to heat treatment on agronomic traits

The agronomic traits were investigated after exposure of plants to high temperatures during GS1, GS2, GS3, or all stages (GS1–3). Stage-specific alterations in plant and seed morphology were observed (Figure 3); seed size of plants exposed to heat during ripening (GS3 and GS1–3) was significantly reduced, while that of plants exposed during GS1 was significantly increased (Figures 3C and 5B). The traits formed three clusters (Figure 4A): agronomic cluster 1) those positively affected by heat during GS1, agronomic cluster 2) those negatively affected by heat during all stages, and agronomic cluster 3) those affected negatively by heat during GS1 and positively during GS3.

Heat during GS1 increased harvest index (by 12% relative to control), thousand kernel weight (by 7.5%), and fertility (by 10%) (Figure 5A–C). Heat during GS2 increased harvest index (to the same level as in GS1), but did not affect thousand kernel weight or fertility. Heat during GS3, on the other hand, reduced these values (harvest index, −15%; thousand kernel weight, −30%; fertility, −11%). Heat during all three stages (GS1–3) decreased harvest index (by −5%) and thousand kernel weight (by −27%), indicating that the decreases caused by heat during GS3 canceled the increases caused by heat during GS1.

Heat during GS1 had little or no effect on grain yield, grain weight per spike, grain number per spike, or spike length. Heat during GS2, GS3, and GS1–3, however, it significantly reduced these values (Figure 5D–G). Heat during GS2 and GS3 similarly reduced grain yield (GS2, by −24%; GS3, by −28%) and spike length (GS2, by −6%;

GS3, by −9%), but differentially reduced grain weight per spike (GS2, by −23%; GS3, by −43%) and grain number per spike (GS2, by −26%; GS3, by −15%). Thus, heat affected these traits during GS1–3. All growth stages had cumulative effects on grain yield (−49%), but GS3 explained most of the effect on grain weight per spike (−46%), and GS2 explained most of the effect on grain number per spike (−27%).

Heat during GS1, GS2, and GS1–3 reduced spikelet number per spike, biomass, culm and leaf weight, plant height, and grain number, but heat during GS3 did not (Figure 5H–L). The effect was greater during GS2 than during GS1. The effects were additive. Heat during GS2 reduced spikelet number per spike by 27%, biomass by 31%, culm and leaf weight by 43%, plant height by 26%, and grain number by 26%. Heat during GS1 also reduced spikelet number per spike, culm and leaf weight, and plant height. Heat during GS1 and GS2 reduced plant height, while heat during GS1–3 had an effect on heat during GS2, as can be seen from plant morphology (Figure 3A). On the other hand, heat during GS2 and GS3 reduced biomass, with a multiplier effect during GS1–3. Since culm and leaf weight did not differ significantly between GS3 and the control, biomass decrease during GS3 is attributable to grain yield.

Heat during GS3 increased flag leaf length but not node number or tiller number. Heat during GS1 and GS2 reduced node number, and heat during GS2 reduced flag leaf length (Figure 5M, N) but had no significant effect on tiller number (Figure 5O).

Principal component analysis (PCA) showed that each condition was separated, but GS2 and GS1–3 were placed close to each other (Figure 4B). GS2 and other traits were separated along with agronomic traits such as biomass, grain yield, and grain number per spike in PC1, and GS3 was separated along with harvest index in PC2 (Figure 4C).

There were strong phenotypic correlations of grain yield with biomass (r = 0.95) and grain weight per spike (0.82); of plant height with culm and leaf weight (0.83) and flag leaf length (0.85); of biomass with culm and leaf weight (0.93) and grain number (0.91); and of harvest index with thousand kernel weight (0.83) (Figure 5). There were negative correlations of harvest index with flag leaf length (−0.56), and of fertility with tiller number (−0.51). It is noteworthy that node number and harvest index were negatively correlated (−0.66), though these two traits seem not to be directly related. Physiological traits related to photosynthetic rate are also included in Figure 6 (See in Section 3.5).

3.2. Positive effect of heat treatment at the seedling stage on agronomic traits

Bayesian network was created using 15 agronomic traits and each high-temperature treatment condition (Figure 7) to estimate the causal relationships among the agronomic traits.

The endpoints of the arrows were divided into grain yield and grain weight per spike. Grain yield was positively controlled by grain number and thousand kernel weight, while grain number per spike was positively controlled by thousand kernel weight and grain number per spike. Thousand kernel weight, which was involved in both, was highly positively correlated with harvest index, indicating that node number positively controlled harvest index. On the other hand, grain number was found to be mainly influenced by biomass-related traits such as tiller number, plant height and culm and leaf weight. The grain number per spike was also explained by fertility and spikelet number per spike.

As for the correlation between agronomic traits and each high-temperature treatment, it was found that high-temperature treatment at GS1 had a strong effect on plant height, harvest index and fertility; high temperature at GS2 affected spike length, spikelet number per spike and plant height; and high temperature at GS3 affected harvest index. The high-temperature treatments at all stages (GS1−3) were not correlated with any of the studied traits, indicating that there was no independent effect of treatment at GS1–3, but that the effect at each of the growth stages was additive.

3.3. Effect of heat treatment on translocation efficiency

In relation to agronomic traits, it was observed that high temperature at each growth stage affected the seed formation process, and the network analysis showed that the node number was highly correlated with the harvest index, an indicator of grain yield (Figure 5, 6, 7). The mineral contents in seeds are the result of translocation, and some minerals remained in the culm and leaf. Therefore, I tried to indirectly evaluate the translocation of assimilation products in plants by observing the behavior of minerals in plants. For this purpose, I sampled seeds and other plant parts separately and investigated the mineral content in each. In addition, the effect of high temperatures during different the growing seasons on the absorption and translocation of various minerals was investigated.

PCA was used to get an overall picture of each sample based on the stability of the replications and the distribution of each condition (Figure 8). In both seed and straw, the four treatments and controls were well replicated, with all six replicates of each condition distributed relatively close to each other. Mineral analysis in single grains

revealed that four different treatments and control were well separated between GS1 and others with magnesium, phosphorus, and sulfur on PC1. The level of specific elements such as strontium and zinc separated between heat-treated plants in GS3 and others on PC2 (Figure 8A). In the straw, PC1 separated each condition and showed a stratified distribution from samples grown under normal conditions in the order of GS1, GS2, GS3, and GS1–3 samples (Figure 8B). In PC2, two major separations occurred: GS2 and GS1–3 samples and normally grown samples at GS1 and GS3 stages.

Multiple regression analysis by LASSO was conducted to search for elements that could explain the difference between harvest index and node number from 11 elements. When the node number was used as the objective variable, phosphorus in the grain was the only element found to have a significant regression coefficient (=−0.185) (Figure 9A). There was a high correlation coefficient between phosphorus content in the grain and node number (r=−0.681) (Figure 9C), suggesting that the phosphorus content in the grain decreased as the number of nodes increased. On the other hand, when harvest index was used as the objective variable, manganese in the grain (=−0.060) and phosphorus (=−0.096) and chromium (=−0.020) in the culm and leaf showed high regression coefficients, with phosphorus having the highest regression coefficient (Figure 9B). The correlation between phosphorus content in the straw and harvest index was r=−0.581, showing a clear distribution for each condition; and the phosphorous content in the grain decreased as the harvest index increased (Figure 9D).

3.4. Effect of heat treatment on seed development

Both fresh and dry seed weight (FW, DW) were measured in the course of

accumulated. The FW of seeds in the control plants increased up to 30 days post-anthesis and then decreased until 50 days post-anthesis (Figure 10A). The seeds gained 42% of the final DW between 10 and 20 days post-anthesis, and a further 16% between 30 and 40 days post-anthesis despite desiccation. This indicates that the translocation of anabolic products continued into this period. FW equalled DW at 50 days post-anthesis with the completion of desiccation.

FW of seeds on plants exposed to heat during GS1 showed a similar trend to the control (Figure 10B), but decreased between 40 and 50 days post-anthesis (Figure 10B). Heat during GS1 thus delayed the start of desiccation. This delay may cause an increase in harvest index, thousand kernel weight and fertility in those plants (Figure 5). As in the control, FW of seeds on plants exposed to heat during GS2 increased till 30 days post-anthesis and began decreasing from 40 days post-anthesis (Figure 10C). Filling of seeds continued even between 30 and 40 days post-anthesis.

In contrast, seeds of plants exposed to heat during the seed formation stage (GS3 and GS1–3) had the highest FW and DW at 20 days post-anthesis. In this short period (10–20 days post-anthesis), the seeds gained as much as 76% and 57%, respectively, of the final DW at 50 days post-anthesis. DW increased till 30 days post-anthesis, but FW decreased from 20 days post-anthesis (Figure 10D, E). The decrease of harvest index, thousand kernel weight and fertility is attributed to this short period.

3.5. Extension of carbon assimilation period by heat treatment at seedling stage

The above results show that heat exposure during GS1 prolongs the seed maturation period. To understand the basis of this phenomenon, photosynthetic CO_2

assimilation (*A*) was measured at 14 days post-anthesis in plants exposed to heat treatment at different stages (Figure 11A). Plants exposed to heat during GS1 tended to have a higher *A* than the control at 400 ppm CO_2 (Figure 11B). Plants exposed during GS2 had a similar *A* to the control. However, plants exposed during GS3 had extremely low *A*: two of the three replicates reached complete leaf senescence (Figure 3B) and the other had extremely low *A* at 14 days post-anthesis. Interestingly, plants exposed to heat during GS1–3 had similar *A* to the control (Figure 11A) despite the measurement of photosynthesis in the hot chamber during GS3. This trend was apparent under high CO_2 concentrations, and the *A* of plants exposed to heat during GS1 remained higher than the control at all concentrations (Figure 12).

I calculated the triose phosphate utilization (*TPU*), the rate of photosynthetic electron transport (*J*), and the maximum carboxylation rate of rubisco (*Vcmax*) at 400 ppm (Sharkey, 2007) from the photosynthetic values (Figure 11C–E). *TPU* and *J* were significantly higher than the control in the GS1 sample. All three were zero in the GS3 sample. *A* was significantly lower in the control and GS3 at 14 days post-anthesis than at 7 days post-anthesis, and GS2 also showed a decreasing trend (Figure 11F). However, GS1 and GS1–3 maintained their photosynthetic activity. This indicates that heat during GS1 and GS2 acclimatizes the plants to heat in the early seed maturation stage.

There were strong positive correlations in each physiological trait related to photosynthetic rate ($r > 0.8$). Additionally, there were strong correlations of harvest index with *A* ($r = 0.79$) and *Vcmax* (0.72) and *J* (0.85) and *TPU* (0.86); of thousand kernel weight with *J* (0.72) and *TPU* (0.71) (Figure 6).

3.6. Analysis of metabolite trends under different high-temperature timings

The previous section suggested that high temperature during certain growth stages affects the senescence rate during seed formation. Therefore, to explore the metabolic changes during the seed formation period under each temperature condition, I quantified the stably detected metabolites (amino acids, organic acids, nucleic acids, and hormones) in the youngest flag leaves at 7 days post-anthesis (Table 1).

All replicates of each condition were distributed close to each other in the PCA plot of the first two principal components, PC1 and PC2, which accounted for a high proportion (89.9%) of the variance (Figure 13A). The GS2 and GS3 samples were distributed far from the control samples, whereas the GS1 samples were distributed close to the control samples in PC1. For both PC1 and PC2, the GS1–3 samples, which were treated at high temperature during all growth stages, showed a distribution closer to the control than the samples treated only in GS2 or GS3. However, for PC3 (which explained only 4.1% of the variance) the values for GS1–3 samples differed from those for control and GS2, as well as GS3 samples (Figure 13B).

3.7. Clustering and heat map based on the metabolic response in each high-temperature treatment

Clustering based on the quantified metabolite contents revealed three major clusters (Figure 14). In the GS1 samples, the levels of most metabolites were lower than in the control samples, especially in metabolite cluster 1. Metabolite cluster 1 contained many nucleic acids such as deoxyuridine, deoxycytidine and adenosine, and amino acids such as tryptophan, proline and phenylalanine. Metabolite cluster 2 contained ascorbic

acid putrescine, and abscisic acid (ABA). Metabolite cluster 3 contained more branched-chain amino acids synthesized from pyruvate and amino acids such as glycine and serine, synthesized from glycerate triphosphate.

3.8. Metabolites that differed significantly from the control and growth stage-specific behavior

In the GS1, GS2, GS3 and GS1–3 samples, 6, 30, 19 and 14 metabolites were found, respectively, that significantly ($p < 0.05$) decreased (less than two-thirds) or increased (more than one and a half fold) compared to the control (Table 2, 3, Figure 15, 16). Samples treated at high temperature only during GS2 accumulated the most growth stage-specific metabolites (18 metabolites). The metabolites that increased most (as a multiple of the control value) in GS2 were asparagine, followed by citrulline, argininosuccinic acid, serine, betaine, valine, isoleucine, nicotinamide adenine dinucleotide (NAD), tartaric acid, cytosine, aspartic acid, glycine, tyrosine, threonine, leucine, arginine and tyramine. On the other hand, the metabolites that decreased most compared to the control were shikimic acid, followed by 4-hydroxyproline, malic acid, trigonelline, citric acid and ABA (Table 2). The samples treated at high temperature during GS3 showed alteration of the concentrations of nine metabolites: 2-oxoglutaric acid, beta-alanine, galacturonic acid, gamma-aminobutyric acid (GABA), guanosine, methionine sulfoxide, phenylalanine and proline increased, whereas sinapic acid decreased. In GS1–3, only kynurenic acid decreased compared with the control. No metabolites were observed in the samples treated at high temperature only during GS1.

Sixteen metabolites changed relative to the control in two or more conditions: Citrulline changed in all four treatments (decreased in GS3 and GS1–3, and increased in

GS1 and GS2). Argininosuccinic acid and glutamic acid were altered in GS2, GS3, and GS1–3, with an increase observed in GS2. Ascorbic acid decreased by similar amounts in GS2, GS3 and GS1–3. Putrescine decreased in GS2, GS3 and GS1–3, with the greatest decrease in GS1–3. Tartaric acid increased by comparable amounts in GS2, GS3 and GS1–3. Pyroglutamic acid increased in GS1, GS2 and GS1–3, with the greatest increase in GS2. Cytosine increased in GS2 and GS1–3, with the greatest increase observed in GS2. Histidine increased by similar amounts in GS2 and GS3. Hypoxanthine and inosine decreased by comparable amounts in GS1 and GS1–3. NAD increased in GS1 and GS2 and decreased in GS3. Serotonin and tryptophan increased in GS3 and GS1–3, with the greatest increase in GS3. Succinic acid increased by comparable amounts in GS2 and GS1–3.

GS2 and GS3 plants accumulated free amino acids but with different trends. Of the 27 amino acids, 22 showed changes relative to the control under one or more conditions (Table 2). Sixteen were altered by the treatment at GS2, and all except hydroxyproline increased. Only histidine showed the same increase at GS2 and GS3 stages, but three amino acids (argininosuccinic acid, citrulline and glutamic acid) responded differently between GS2 and GS3 plants. The remaining six amino acids (beta-alanine, GABA, methionine sulfoxide, phenylalanine, proline, and tryptophan) were increased by the treatment in GS3. The GS1–3 plants responded differently from the GS2 and GS3 plants, and were not significantly different from the control, except for four amino acids (argininosuccinic acid, citrulline, glutamic acid, and tryptophan), which showed similar behavior to that in the GS3 plants. Pyroglutamic acid showed more than 2 times the control value in all treatments except GS3.

3.9. Enrichment analysis of differentially accumulated metabolites corresponding to stage-specific heat stress

To understand how high temperature at different growth stages altered metabolic pathways during the reproductive stage, I conducted enrichment analysis using differentially accumulated metabolites (DAMs) and mapped the metabolites showing interesting behavior in the associated metabolic pathways (Table 4, Figure 15, 16).

The urea cycle was commonly affected in GS1, GS2 and GS3, but not in GS1–3. Eight metabolites (argininosuccinic acid, fumaric acid, glutamic acid, aspartic acid, 2-oxoglutaric acid, arginine, nicotinamide dinucleotide (NAD), and citrulline) were included in the urea cycle. Both at GS2 and GS3 stages, arginine and proline metabolism (glutamic acid, proline, argininosuccinic acid, glycine, fumaric acid, aspartic acid, succinic acid, arginine, NAD, and citrulline), aspartate metabolism (argininosuccinic acid, beta-alanine, fumaric acid, glutamic acid, asparagine, aspartic acid, 2-oxoglutaric acid, arginine, and citrulline), the malate–aspartate shuttle (glutamic acid, aspartic acid and malic acid), and ammonia recycling (glycine, glutamic acid, asparagine, histidine, aspartic acid, 2-oxoglutaric acid, and NAD) were detected (Table 4). Some pathways reacted only in a specific treatment group: purine metabolism in GS1 (fumaric acid, hypoxanthine, inosine, and NAD), carnitine synthesis (ascorbic acid, glycine, succinic acid, and NAD), and tyrosine metabolism in GS2 (ascorbic acid, fumaric acid, glutamic acid, tyrosine, aspartic acid, tyramine, and NAD). In GS3, metabolites involved in beta-alanine metabolism (beta-alanine, glutamic acid, histidine, 2-oxoglutaric acid, and NAD), the glucose–alanine cycle (glutamic acid, 2-oxoglutaric acid, and NAD), and tryptophan metabolism (glutamic acid, 2-oxoglutaric acid, serotonin, NAD, and tryptophan) changed significantly.

3.10. Correlation with the altered metabolite concentrations and agronomic traits

The changes in metabolite concentrations described in the previous sections were correlated with the values of the agronomic traits obtained (Figure 17, Table 5, 6). In section 3.1., I divided agronomic traits into three clusters based on the response to high-temperature treatment: in agronomic cluster 1, traits were positively affected by heat during GS1; in agronomic cluster 2, traits were negatively affected by heat during all stages; and in agronomic cluster 3, traits were affected negatively by heat during GS1 but positively during GS3.

Many metabolites showed strong correlations with the agronomic traits classified in agronomic cluster 1 (harvest index, thousand kernel weight and fertility). These metabolites were negatively correlated with the harvest index: methionine sulfoxide, proline, beta-alanine, tryptophan, guanosine, deoxyguanosine, thymidine, guanine, deoxyuridine, deoxycytidine, deoxyadenosine, galacturonic acid, malic acid, hydroxyproline and serotonin, and only NAD showed a positive correlation with this trait. In contrast, putrescine and glutamic acid were positively correlated with the thousand kernel weight, whereas methionine sulfoxide, beta-alanine, tryptophan, guanosine, thymidine, malonic acid and serotonin were negatively correlated. Beta-alanine, deoxyuridine, deoxycytidine, deoxyadenosine and hydroxyproline were negatively correlated with fertility.

Many metabolites showed strong correlations (with the agronomic traits classified in agronomic cluster 2 (grain weight per spike, grain number per spike, spike length, spikelet number per spike, culm and leaf weight, and plant height). For grain weight per

spike, putrescine and ascorbic acid were positively correlated, whereas histidine, beta-alanine, GABA, tryptophan, guanosine, deoxyguanosine, thymidine and tartaric acid were negatively correlated. For grain number per spike, putrescine and ascorbic acid showed a positive correlation, whereas histidine, GABA and tartaric acid showed negative correlations. For spike length, methionine sulfoxide, proline, beta-alanine, tryptophan, guanosine, deoxyguanosine, thymidine, deoxyuridine, 2-oxoglutaric acid and serotonin showed negative correlations, and no metabolites showed a positive correlation. For spikelet number per spike, putrescine, ascorbic acid, and succinic acid showed positive correlations, whereas cytosine, pyroglutamic acid, tartaric acid, 4-hydroxybenzoic aldehyde, and 1-aminocyclopropane-1-carboxylic acid (ACC) showed negative correlations. For culm and leaf weight, succinic acid showed a positive correlation and there were no negative correlations. For plant height, succinic acid, ABA and hydroxyproline showed positive correlations, whereas cytosine, pyroglutamic acid and 4-hydroxybenzoic aldehyde showed negative correlations.

In the agronomic traits classified as agronomic cluster 3 (flag leaf length and node number), many metabolites showed strong correlations: aspartic acid, glycine, pyro-glutamic acid, 4-hydroxybenzoic acid and sinapic acid were negatively correlated with flag leaf length, whereas many metabolites were positively correlated with this trait: methionine sulfoxide, proline, beta-alanine, choline, methionine, deoxyguanosine, thymidine, guanine, cytidine, deoxyuridine, deoxycytidine, deoxyadenosine, galacturonic acid, malic acid, pyruvic acid, 2-oxoglutaric acid, hydroxyproline and serotonin. For node number, only lysine showed a correlation and it was positive.

No metabolites that were significantly correlated with grain yield, tiller number, biomass and grain number were found.

3.11. Heat response of the multiple synthetic derivative (MSD) lines in agronomic traits

Agronomic traits in MDS lines were investigated after exposure of plants to high temperatures during GS3 (Figure 2B). The results showed lineage-specific changes in plant and seed morphology (Figure 19): seed size of 'Norin 61' was obviously reduced, while that of MSD392 was increased (Fig. 19B). As a result of cluster analysis based on the agronomic traits of seven lines in two environments, MSD34, MNH2, MSD296, and MSD417 formed close clusters in two environments (Figure 20). Among them, MSD296 and MNH2 showed a more similar trend, and these two lines had significantly higher plant height in the two environments. MSD34 significantly increased grain number per spike and spikelet number per spike in a gene-specific change by high temperature. The trends of MSD392, 'Norin 61' and MSD54 in their respective environments were similar, and most of the agronomic traits were reduced by high-temperature treatments. However, MSD392 was the only one among the seven lines that did not show any reduction in thousand kernel weight due to high temperature.

Tiller number and culm and leaf weight and fertility were not significantly different between the two environments in all seven lines (Figure 21). For grain number, 'Norin 61', MSD417 and MSD54 were significantly reduced by the high-temperature environment, while the other four lines (MSD296, MSD34, MSD392 and MNH2) showed a decreasing trend but were not significantly different.

3.12. Metabolite analysis in MSD lines

I quantified the metabolites (amino acids, organic acids, nucleic acids and

hormones) stably detected in the youngest flag leaf at 7 days post-anthesis to explore metabolic changes during GS3 in each line (‘Norin 61’, MSD296, MSD34, MSD392, MSD417, MSD54, MNH2) (Table 2). Then, I evaluated the trend of metabolite content in the two environments for each strain and the response of each line to high-temperature treatment.

3.12.1. Trends of metabolites in overall MSD lines

In each condition, repetitions originating from the same environment were distributed close to each other. In the PC1 and PC2 of the PCA plot, MSD296, MSD417 and MSD34 were distributed close to each other in the two environments; and in the cluster analysis, the two environments were classified into the same cluster. In PC2 and PC3, only ‘Norin 61’ showed separation of the two environments along with PC2, and the other six strains showed separation of the two environments in PC3. However, MSD296 had a shorter distance of separation and showed a similar trend of metabolite accumulation between the two environments.

Clustering based on the quantified metabolite content revealed three major metabolic clusters (Figure 22C). Metabolic cluster 1, the most distant, contained nucleic acids derived from RNA and DNA. Metabolic cluster 2 contained tryptophan, proline, urea and beta-alanine. Metabolic cluster 3 contained ornithine, citrulline and argininosuccinic acid from the urea cycle, and amino acids such as glycine and serine, synthesized from glycerol triphosphate. On the other hand, the sample clusters were divided into four clusters. Sample cluster 1, in which the accumulation of almost all metabolites was low, contained control and a heat-treated sample of MSD296 and control sample of MNH2; while sample cluster 2, in which specific accumulation was observed

in metabolite cluster 1, contained control and a heat-treated sample of MSD34 and a heat-treated sample of 'Norin 61'. In sample clusters 3 and 4, control and a heat-treated sample of MSD392, MSD417, MSD54 and MNH2 were separated. In the behavior of metabolites, as well as agronomic traits, control and a heat-treated sample of MSD296 and MSD34 were classified into the same cluster.

3.12.2. Metabolites that differed from the control in each MSD lines

According to the metabolic tendency of high-temperature response, MNH2 formed an independent cluster, and 'Norin 61' and MSD392 were distributed in the same cluster (Figure 23). The other four lines (MSD296, MSD34, MSD417 and MSD54) were classified as close clusters, and MSD54 and MSD417 formed close clusters.

The metabolites divided by the six major clusters showed characteristic behaviors in each line. Cluster 1 contained amino acids, and almost all lines showed a decrease in these metabolites associated with high temperature, while MNH2 showed an increasing trend in some metabolites. Nucleic acids derived from RNA and DNA, classified in cluster 2, were markedly increased in 'Norin 61' and MSD396. Cluster 3 included beta-alanine, GABA, and pyroglutamic acid, which increased in MNH2 and 'Norin 61' and MSD392 but decreased in MSD34. Cluster 4 included ornithine, citrulline and argininosuccinic acid, which functions in the urea cycle, and these were particularly increased in MSD296. Urea, tryptophan, and NAD, classified as cluster 5, were particularly increased in MNH2, and tryptophan was increased in all MSD lines except MSD296. MSD54 had a low accumulation of all metabolites under high temperature.

In summary, MSD296 and MSD34 seemed to be the lines that showed low sensitivity to high temperatures, whereas 'Norin 61' was most sensitive. MSD392 showed

the most similar high-temperature response to ‘Norin 61’, while MNH2 showed the most different heat response from the other six lines. MSD54 was a unique line whose metabolite content was reduced by the high-temperature treatment.

3.12.3. Multiple regression analysis of metabolite concentrations and agronomic traits

I conducted a multiple regression analysis using LASSO to search for molecular markers that influence agronomic traits from the measured metabolites (Figure 24A). Thirteen agronomic traits were used as objective variables, and 48 metabolites were used as explanatory variables. In the regression with grain yield as the objective variable, argininosuccinate (regression coefficient =2.53), guanosine (=1.76), threonine (=−2.49), and pyro-glutamic acid (=−1.87) were detected as metabolites with high regression coefficients. The correlation coefficients between each metabolite and grain yield were 0.292, −0.21, −0.108, and −0.448, in the order aforementioned (Figure A−D). No line showed altered threonine content by the heat treatment (Figure 26A−C). Argininosuccinic acid was significantly decreased in ‘Norin 61’ and significantly increased in MSD417 by heat treatment (Figure 25A).

Multiple regression analysis of grain number and thousand kernel weight detected as factors controlling grain yield in the network analysis in the previous section showed that argininosuccinic acid (=21.72) and NAD (=17.61), beta-alanine (=−5.76) and adenosine (=3.94), respectively (Figure 24B, C). The correlation coefficients of argininosuccinic acid and NAD with grain number were low (0.296 and 0.27, respectively), while the correlation coefficients of beta-alanine and adenosine with thousand kernel weight were −0.562 and 0.062, respectively, indicating a high correlation between beta-alanine and thousand kernel weight (Figure 26E−H). Among them,

argininosuccinic acid, NAD and beta-alanine were highly correlated with grain yield in multiple regression analysis (Figure 26I, J).

NAD content was highest in MSD417 and a significant increase was observed in MSD34 and MNH2 under high temperature (Figure 25E). All lines except MSD296 were divided into control and high temperature on the beta-alanine contents, and MSD392, which did not show any decrease in thousand kernel weight under a high-temperature environment, had high content as well as ‘Norin 61’ (Figure 25F, 26G). Adenosine was poorly correlated with thousand kernel weight (r=0.062) though its level increased specifically in MSD392 under high-temperature conditions (Figure 25G, 26H).

4. Discussion

4.1. Agronomic traits related to grain yield

Grain yield was reduced by reduction of biomass, plant height and grain number due to heat during GS2 and by reduction of grain weight per spike, grain number per spike, fertility, harvest index and thousand kernel weight due to heat during GS3 (Figures 2 and 3). The similar losses caused by heat during GS2 and GS3 were additive; therefore, heat during GS1–3 had a more severe effect. Most traits were positively correlated with each other such as plant height-spikelet number per spike, but some were negatively correlated, such as harvest index–node number as shown in Figure 5. 'Norin 61' has the photoperiod-insensitive *Ppd-D1a* allele and the semi-dwarfing *Rht-D1b* allele (Shimizu *et al.*, 2021). *Rht-D1b* is associated with high-temperature tolerance in Europe (Barber *et al.*, 2017). Gibberellic acid (GA)-sensitive (*Rht8*, *Rht12*, *rht*), semi-dwarf (*Rht-D1b*) plants at a high temperature below 36°C at booting and anthesis stages maintained grain number per spikelet, while severely dwarf (*Rht-D1c*) plants had fewer grains (Alghabari *et al.*, 2014). However, heat stress above 36°C eroded tolerance regardless of the *Rht* allele. Our heat stress condition (38°C) may erode the regulatory system for GA sensitivity of plant height and spikelet number regardless of *Rht* allele. Genetic analyses of near-isogenic wheat lines differing in plant height on account of *Ppd1* and *Rht* alleles showed pleiotropic effects on spikelet number per spike and plant height (Worland *et al.*, 1998; Matsuyama *et al.*, 2015). The higher correlation between plant height and spikelet number per spike obtained here suggests that the same mechanism regulates both traits (Figure 6).

Vegetative growth was strongly suppressed, leading to a reduction of biomass in plants that were heat stressed during GS2. Decrease in vegetative biomass limits source translocation to sink tissue during seed development. However, heat stress during GS2 down-regulated the volume of sink tissue by decreasing spikelet number per spike. As a result, thousand kernel weight remained at the control level, and the harvest index was improved.

Heat treatment before anthesis reduced grain number (Fischer, 1985; Wheeler *et al.*, 1996a, b). At the double-ridge stage (the beginning of GS2), primordial spikelet begins to form in each spike (Hyles *et al.*, 2020). A longer double-ridge phase increased the spikelet number per spike, but higher temperature above 19°C decreased it (Rawson 1971; Slafer and Rawson, 1994). GS1 does not span this period, which may be why the grain number was not reduced.

Balla *et al.* (2019) reported that heat treatment of 101 wheat cultivars at the booting stage decreased plant height by about 10%, but that it had a much smaller effect at heading and later growth stages, and that a great reduction of thousand kernel weight by heat stress after heading might decrease harvest index. Other studies reported the reduction of harvest index, grain yield and fertility by heat stress during anthesis and grain development in wheat and rice (Ferris *et al.*, 1998; Hasegawa *et al.*, 2011). A similar behavior was observed in this study: heat during GS2 (from double ridge to heading) reduced plant height, and heat during GS3 significantly decreased harvest index, thousand kernel weight, fertility, and grain yield (Figure 5A–D, K).

In the network analysis, thousand-grain weight and yield index are directly bound to each other, and indicated that this correlation was maintained even when the high-temperature environment is diversified. Furthermore, the node number was independently

bound to the harvest index, and controlling node number may lead to improved grain yield potential in the future. It should be noted that only the heat treatment at GS1 has the greatest impact on grain yield in the high-temperature treatment, as the arrows connect the two routes of grain number and thousand kernel weight that control grain yield.

4.2. Relationship between the number of nodes and translocation efficiency

Node number had a high negative correlation with harvest index (Figure 6). The harvest index is an indirect indicator of the translocation of nutrients and assimilates via the culm and leaf to seeds. Nodes in grasses play the role of hubs in distributing nutrients taken up by the roots to various organs (Yamaji and Ma, 2014) and thus control the efficiency of translocation to grains. The reduction of node number might have eased the control of translocation to the grain. To confirm the control of translocation by nodes, I observed the distribution of element accumulation in plants.

Mineral analysis showed that both node number and harvest index were related to phosphorus content (Figure 9). Yamaji *et al.* (2017) reported that the phosphorus transporter is intrinsic to each node and contributes to the preferential distribution of newly absorbed phosphorus from the roots to new leaves and spikes. Nodes are junctional regions of stems, leaves and axillary buds, and one node is always accompanied by one leaf. The transporter is believed to function as a switch that distributes the attached leaf to the higher nodes and spikes, and this function in the node is largely responsible for the efficiency of translocation to the seed. Therefore, it is inferred that when transporter expression is constant, the amount of elements transported to seeds is highly increased when the node number is less.

The fact that the trend of correlation between harvest index and phosphorus content in the culm and leaf was different in GS2 and GS1–3 than in the other three conditions may be attributed to the low culm and leaf weight in these two conditions (Figure 9E). The high temperature treatment at GS2 significantly inhibited growth and caused a reduction in culm and leaf weight. Because these conditions are source-limited, it is likely that the proportion of elemental transfer from the stems and leaves increased relatively to allow sufficient translocation of mineral elements from there to the seeds.

4.3. Duration of grain development affected by different heat stress periods

The grains in the control treatment started desiccating at a mean of 609.9°C·d (cumulative average daily temperature) (30 days post-anthesis) and were completely desiccated at 1016.5°C·d (50 days post-anthesis). Those in the GS3 and GS1–3 treatments started desiccating at 593.4°C·d (20 days post-anthesis) and were completely desiccated at 890.1°C·d (30 days post-anthesis) (Soltani *et al.*, 2012). The difference suggests that the start of desiccation depends on the accumulated average temperature during seed development. On the other hand, GS1 and GS2 extended the desiccation phase, even though they had the same temperature during seed development as the control (Figure 6). I consider that the timing of seed desiccation in the GS1 and GS2 treatments is regulated by mechanisms other than the cumulative average daily temperature. Yamasaki *et al.* (2017) reported that the difference in the starch accumulation period between two wheat cultivars was regulated by a difference in abscisic acid (ABA) sensitivity at the start of desiccation. In addition, epigenetic changes due to histone methylation and acetylation and expression changes due to retrotransposon insertion can alter the regulation of heat

priming effects of wheat (Wang *et al.*, 2016; Hu *et al.*, 2015; Ito *et al.*, 2011). For example, a heat-activated retrotransposon, *ONSEN* (*ATCOPIA78*), in Arabidopsis, generated a mutation of an ABA-responsive gene, leading to ABA insensitivity (Ito *et al.*, 2016). These studies suggest that heat stress treatment during GS1 and GS2 can remodel phytohormone sensitivity, thus changing seed development.

4.4. Extension of grain development by high-temperature treatment at the seedling stage

Heat stress during GS1 increased grain development duration and improved thousand kernel weight and harvest index (Figures 5A, B and 10). Previous studies of stress-related priming showed a short-term improvement of germination and emergence and a long-term improvement of yield and grain development by osmo-hardening, selenium or salicylic acid treatment in rice (Farooq *et al.*, 2006; Wang *et al.*, 2016; Mendanha *et al.*, 2018). Mendanha *et al.* (2018) showed that 48 h of heat priming at the 3- or 5- leaf stage improved grain yield and thousand kernel weight. Iizumi *et al.* (2021) predicted that the optimal wheat sowing date under future global warming in Sudan is about 6 days earlier than at present. Our results show that even if earlier sowing before winter increases the risk of exposure to high temperatures, heat stress at the seedling stage does not significantly affect grain yield or yield-related traits, but rather improves seed formation.

4.5. Improved senescence of heat-primed plants

As well as grain-filling in GS3 heat-treated plants, leaf senescence was accelerated,

resulting in significantly reduced carbon assimilation, *J* and *TPU* during 7 to 14 days post-anthesis (Figure 11B–E). This phenomenon is well characterized by loss of chlorophyll, low PSII activity and reduced electron transport (Harding *et al.*, 1990). Control plants also reduced assimilation between 7 and 14 days post-anthesis, which accelerated leaf senescence. On the other hand, *A* was not significantly different between Control and GS1, but *TPU* and *J* had the highest values at 14 days post-anthesis in GS1 heat-treated plants. Time-series differences also suggest that senescence was delayed in GS1 heat-treated plants (Figure 6F). Tobacco lines with delayed senescence maintained significantly higher *J* and *TPU* and maintained rubisco activity (Rivero *et al.*, 2009). This suggests that heat priming during GS1 suppresses the decrease in the final carbon assimilation rate by maintaining rubisco activity even at 14 days post-anthesis.

GS1–3 plants maintained higher photosynthetic activity than GS3 plants, maybe owing to acclimatization to a high temperature by exposure before the ripening stage. Fan *et al.* (2018) reported that *A* decreased less in heat-primed plants than in unprimed plants, indicating that primed plants retain higher photosynthetic capacity under stress.

These behaviors may have led to the delayed senescence and prolonged starch deposition of source tissues during grain formation of GS1 plants, and ultimately contributed to the improvement of thousand kernel weight.

4.6. Metabolites involved in aging that can explain heat priming and acclimation

In section 4.5., I suggested that control plants grown under standard conditions showed the onset of leaf senescence at 14 days post-anthesis and that the plants treated with high temperature during GS3 showed apparent leaf senescence by 14 days post-

anthesis after losing carbon assimilation capacity. On the other hand, plants treated with a high temperature during all growth stages (GS1–3) were able to maintain high photosynthetic activity even at 14 days post-anthesis. This suggests that high-temperature exposure during the seedling stage (GS1), vegetative stage (GS2), or both induced high-temperature acclimation during the seed maturation stage (GS3). Moreover, plants treated with the high temperature only in GS1 showed higher photosynthetic activity than the control. Thus, I regarded treatment during GS1 as a "priming effect" that delayed senescence during the seed maturation stage.

In metabolite analysis, the metabolomic dynamics behind this phenomenon was investigated. The GS3 plants showed alterations of levels of metabolites involved in beta-alanine synthesis (Figure 15) and accumulated more beta-alanine (Figure 18A). However, its accumulation in GS1–3 plants was significantly lower than that in GS3 plants. Moreover, the amount of beta-alanine in GS1 plants was significantly lower than that in the control. In the DNA and RNA degradation pathways, nucleotidases catalyze the transformation of nucleotides into nucleosides and phosphates, followed by nucleosidase activity to generate purines and pyrimidines (Witte *et al.*, 2020; Ashihara *et al.*, 2018). Generally, purines and pyrimidines are either regenerated into nucleic acids through salvage and phosphorylation, or are degraded into amino acids, urea, ribose, NH_4^+, and CO_2 under nitrogen starvation and during leaf senescence. In section 3.5., I determined the rate of carbon assimilation at 14 days post-anthesis by photosynthesis measurement and found a decrease in the order GS3 > GS1–3 > GS2 > control > GS1. I found that the accumulation of beta-alanine at 7 days post-anthesis showed the same trend (Figure 18A). Beta-alanine results from the degradation of uracil produced during pyrimidine degradation by dihydropyrimidine dehydrogenase, dihydropyrimidinase and beta-

ureidopropionase. Therefore, the higher accumulation of beta-alanine during GS3 may indicate that nucleotide degradation leading to pyrimidine degradation under heat stress has already occurred. This is consistent with the findings of Avila-Ospina *et al.* (2017), who reported that beta-alanine accumulates in the flag leaves of barley during leaf senescence. Therefore, beta-alanine accumulation can be a biomarker for the degree of senescence.

Similar to the response of pyrimidine catabolism to heat stress, the accumulation of hypoxanthine in GS1 and GS1–3 plants were remarkably lower than in the control (Table 2). Hypoxanthine, which is generated from inosine by inosine nucleosidase, represents a turning point in the salvage pathway of this metabolite for regeneration of purine nucleotides or degradation of purine (Ashihara *et al.*, 2018). Hesberg *et al.* (2004) reported that the production of the enzyme xanthine dehydrogenase/oxidase (XDH), which is responsible for uric acid synthesis from hypoxanthine, is up-regulated in response to ABA. Inhibition of XDH may play an essential role in the maintenance of plant growth and development by inducing various effects such as growth retardation, reduced fertility and premature maturation (Hesberg *et al.*, 2004; Nakagawa *et al.*, 2007; Watanabe *et al.*, 2010). The low accumulation of hypoxanthine in GS1 and GS1–3 plants may therefore result from increasing activity of XDH in purine degradation. It may also be related to the delayed senescence observed in GS1 plants compared to the control and in GS1–3 plants compared to GS3 plants.

Alteration of metabolite levels related to the amino acids also appeared in addition to the nucleic acid pathways mentioned above. Plants exposed to high temperature during the seedling stage (GS1) accumulated the least tryptophan and serotonin (Figure 18B, C) in the tryptophan metabolic pathway. In contrast, plants exposed to high temperatures at

the sampling time (GS3 and GS1–3) had higher levels of both metabolites, and the difference was significant in the case of the GS3 plants. The accumulation of these amino acids in GS3 plants was more than twice that in GS1–3 plants. The trend of these accumulations was consistent with the senescence levels at 14 days post-anthesis.

The tryptophan metabolic pathway diverges at tryptamine and is divided into the synthesis of indole-3-acetic acid via indole-3-pyruvic acid and the synthesis of serotonin (Kang *et al.*, 2007). Tryptamine biosynthesis involves tryptophan decarboxylase (TDC), whose gene expression increases during senescence and is thought to be the rate-limiting factor for serotonin accumulation (Pelagio-Flores *et al.*, 2011). Serotonin plays a protective role against reactive oxygen species in plants, and by regulating cell division and elongation, it delays senescence (Kang *et al.*, 2009). Furthermore, Ishihara *et al.* (2008) reported that serotonin is involved in establishing a physical defense against pathogens in rice. However, this does not mean that plants with a high accumulation of serotonin exhibit delayed senescence, but rather that senescent plants increase their serotonin levels to resist the effects of senescence. In any case, the serotonin accumulation (Figure 18C) could be an indicator of the degree of senescence.

I observed similar behavior for proline, whose accumulation was lowest in GS1 plants and highest in GS3 plants (Figure 18D). Yuan *et al.* (2017) reported that photosynthetic activity was reduced by high temperature in *Brassica napus*, and that proline showed the opposite accumulation tendency to that of several amino acids, and explicitly increased under stress. Proline is known to be a compatible solute that increases cell osmotic pressure under drought stress (Itam *et al.*, 2020). However, the role of proline in high-temperature stress is evident but not yet fully understood (Shin *et al.*, 2016).

The results of the present study indicated that the amino acids beta-alanine,

tryptophan, serotonin and proline will be useful molecular markers for indicating senescence.

4.7. Metabolites involved in ammonia recycling and urea cycle that can explain recovery from heat stress

This study demonstrated that high temperatures during the vegetative stage (GS2) and reproductive stage (GS3) led to the accumulation of different amino acids. Plants exposed to high temperatures during GS3 showed increased beta-alanine, tryptophan, serotonin, and proline levels, as described in the previous section. On the other hand, those exposed to high temperature during GS2 accumulated other amino acids (*e.g.* leucine, isoleucine, threonine, tyrosine and valine). The increase in these amino acids may be due to a stress-induced decrease in protein synthesis or an increase in protein degradation (Glaubiz *et al.*, 2015). The amino acids that increased in GS3 plants were those that accumulated during senescence, whereas the amino acids that increased in GS2 plants were those that accumulated after the effects of high temperature before flowering. NH_4^+, as a protein degradation product, is consumed by glutamic acid dehydrogenase (GDH) and glutamine synthase (GS) and in the urea cycle (Figure 15). Plants exposed to high temperature during GS2 accumulated significantly more arginine, argininosuccinic acid and citrulline, which are three of the four major metabolites in the urea cycle (the fourth is ornithine), indicating that detoxification of NH_4^+ by conversion into urea in this metabolic pathway is particularly active in the GS2 plants. In the urea cycle, NH_4^+ is consumed during the synthesis of citrulline from ornithine. Therefore, the metabolic activity of ornithine conversion to citrulline may be accelerated in the GS2 plants and NH_4^+ consumption may be increased.

Blume *et al.* (2019) reported that ornithine and citrulline serve as alternative sinks for excess nitrogen, and that these may be also alternative sinks for nitrogen produced during photorespiration. NH_4^+ produced by protein degradation accumulates in metabolites in the form of nitrogen. Arginine, which plays a role in the urea cycle, functions as a major nitrogen storage compound in plants. The observed increase in arginine and argininosuccinic acid in the GS2 plants in the present study suggests that nitrogen accumulation is occurring in these plants at 7 days post-anthesis. However, among the four metabolites involved in the urea cycle, the content of argininosuccinic acid was by far the highest, suggesting that nitrogen accumulation is likely to occur in this acid rather than in arginine.

Other ammonium recycling pathways include the GDH pathway and the GS–glutamine oxoglutarate aminotransferase (GOGAT) cycle (Figure 15). In the GDH pathway, NH_4^+ is consumed by the catalytic action of GDH during the synthesis of glutamate from 2-oxoglutarate in the tricarboxylic acid cycle. In the GS–GOGAT cycle, NH_4^+ is consumed by GS during the synthesis of glutamine from glutamate, and NH_4^+ is released from glutamine during the synthesis of glutamic acid catalyzed by glutamine oxoglutarate aminotransferase. In the present study, glutamate accumulated in plants exposed to high temperature during GS2 but accumulated less in plants treated with high temperature during the reproductive stage (GS3 and GS1–3). The reduced accumulation of glutamic acid in GS3 plants may be due to increased GDH activity and decreased GS–GOGAT activity caused by exposure to high temperature during the reproductive stage. Yuan *et al.* (2017) and Liang *et al.* (2011) reported that heat-sensitive wheat lines showed a decrease in GS–GOGAT activity and an increase in GDH activity under high temperature, whereas resistant lines showed a smaller reduction.

Furthermore, glutamic acid is converted to aspartic acid by aspartic acid aminotransferase, and aspartic acid is converted to asparagine by asparagine synthase and asparaginase (Figure 15). Glutamine, glutamic acid and aspartic acid are used in the synthesis of nitrogenous compounds. Asparagine is synthesized from aspartic acid, and functions not only as a protein amino acid but also as a major nitrogen transporter (Oliveira *et al.*, 2001). In the present study, aspartic acid, asparagine and glutamate accumulated in plants exposed to high temperature during GS2. This suggests that nitrogen assimilation, metabolism and transport are activated by high-temperature exposure during GS2. In addition, GS2 plants may be preparing to resume protein synthesis at 7 days post-anthesis, and accumulated nitrogen stores in asparagine and arginine would be the materials consumed by this process.

In healthy plants, when photosynthesis is active during the daytime, glutamine, glutamic acid and aspartic acid are used to synthesize other amino acids required for protein synthesis. These are converted to asparagine at night, which functions as nitrogen storage and transport compound (Morot-Gaudry *et al.*, 2001). On the other hand, in carbon-starved plants, glutamine and glutamic acid are converted to sugars, and the nitrogen released in this process is stored in nitrogen-rich metabolites such as asparagine and arginine (https://biocyclopedia.com/index/plant_pathways/glutamine_glutamate_aspartate_and_asparagine.php). In this study, plants exposed to high temperatures during GS2 accumulated particularly high levels of asparagine and arginine, suggesting that these plants are carbon-starved. In carbon-starved plants where the stomata are closed and CO_2 is not supplied, the CO_2 concentration in the leaves decreases significantly, resulting in increased photorespiration (Bauwe *et al.*, 2010). Photorespiration functions to prevent the

accumulation of reactive oxygen species due to excessive photosynthetic light reactions (Voss *et al.*, 2013).

Timm *et al.* (2013) reported that accumulation of glycine, serine and glyceric acid are converted from the toxic compound, 2-phosphoglycolate by photorespiration. Thus, plants exposed to high temperatures during GS2 may cause an increase of photorespiration at 7 days post-anthesis as a post-heat stress feature. The NH_4^+ emitted by photorespiration is assimilated by GS in the GS–GOGAT cycle (Bauwe *et al.*, 2010). In addition, since nitrogen assimilation, metabolism and transport appear to be activated in GS2 plants, the mechanism for removing the NH_4^+ generated by photorespiration may also be activated.

These facts indicate that the impact of high temperature in GS2 plants continued into the GS3 stage even though the plants grew 7 days under controlled conditions. These plants are recovered from the adverse effects of temperature stress by actively mobilizing nitrogen metabolism and photorespiration to remove NH_4^+ and reactive oxygen species.

4.8. Metabolites that explain changes in agronomic traits due to stage-specific heat stress

Many of the metabolites were strongly correlated with agronomic traits. Especially, four metabolites (beta-alanine, serotonin, tryptophan and proline) showed strong negative correlations with harvest index and spike length, and a strong positive correlation with flag leaf length (Figure 17). Beta-alanine, serotonin and tryptophan were also negatively correlated with thousand kernel weight and grain weight per spike, and beta-alanine showed a negative correlation with fertility. These metabolites were regarded as indicators of senescence. The results suggest that senescence affects grain formation.

In addition to plant senescence, starch accumulation is another factor that affects grain formation. Lu *et al.* (2019) and Yang *et al.* (2018) reported that heat stress during the grain-filling stage affects the activities of starch biosynthesis genes responsible for enzymes such as sucrose synthase, AGPase, glucokinase, soluble starch synthase and starch branching enzyme that are involved in starch accumulation in wheat and maize. Furthermore, at 7 days post-anthesis, the GS3 heat treatment at 38°C/18°C reached 200 cumulative degree-days of heat, indicating that 7 days post-anthesis in GS3 overlaps the timing of A-type starch granule synthesis (Bechtel *et al.*, 2003; Guo *et al.*, 2012). Thus, translocation of nutrients from senescing leaf tissue accelerated at 7 days post-anthesis and may have led to the highest fresh weight accumulation in the grains at 10 days post-anthesis in GS3 plants even though the grain dry weight did not increase significantly. This suggests a possible defect of starch synthesis in hot environments rather than a problem with nutrient translocation from the source (senescing tissue). It is possible that less-effective starch biosynthesis during grain development under heat stress may lead to the use of sugars and nutrients for flag leaf growth, thereby leading to increased flag leaf length.

As for the other metabolites, putrescine showed a strong positive correlation with four agronomic traits: thousand kernel weight, grain weight per spike, grain number per spike and spikelet number per spike (Figure 17). The accumulation of putrescine was significantly less in all plants that experienced high temperatures than in the control, and the order was GS1 > GS2 > GS3 > GS1–3 (Table 2).

Chen *et al.* (2019) reported that putrescine is the major polyamine in plants and is involved in the regulation of a variety of physiological processes including senescence and embryogenesis. Polyamine metabolic enzyme activities and polyamine content

change throughout a plant's growth stages. Duan (2000) and Duan *et al.* (2006) reported that senescence could be inhibited by the application of exogenous polyamines and indicated that this change in the polyamine content could be a signal of or prelude to senescence. Polyamines are regulators of embryonic development. Putrescine is abundant in immature embryos and reduced concentrations of putrescine would therefore result in fewer somatic embryos. Few reports have mentioned the relationship between high-temperature stress and polyamines. Shao *et al.* (2015) reported that the heat tolerance of alfalfa is associated with a high spermidine content and low putrescine and spermine contents. Yang *et al*. (2002) reported that high-temperature treatment also affected polyamine synthesis in Chinese kale leaves, and the total amount of polyamines and the content of putrescine increased after 6 days of high-temperature treatment, but the increase was not sustained as the treatment time increased. These results suggest that putrescine is also useful as an indicator of senescence and indirectly explains the status of embryogenesis at 7 days post-anthesis. However, there have been no reports that could fully explain the high-temperature priming effect and the behavior of high-temperature acclimation seen in GS1–3 plants in the present study. Although beta-alanine (the end product of polyamine synthesis, Parthasarathy *et al.*, 2019) and putrescine were significantly correlated, the correlation coefficient was −0.52, indicating that there was a moderate or indirect relationship between them.

The correlation with agronomic traits indicates that the behavior of these metabolites at 7 days post-anthesis influences subsequent seed development, suggesting that these substances are essential for the expressed traits. I hypothesize that metabolites analysis can be used to estimate yield in the future.

4.9. Genotype-specific heat responses in agronomic traits

The high-temperature tolerant candidate lines MSD296, MSD34, MSD392, MSD417, MSD54 and MNH2) suppressed the extent of grain yield reduction by high-temperature treatment during the reproductive stage than 'Norin 61'. However, the traits leading to maintenance of yield potential differed among the individual lines. When classified by the two yield-contributing traits identified in the network analysis (thousand kernel weight and grain number), MSD392 and MSD296 had traits that maintained thousand kernel weight, while all lines except 'Norin 61' maintained grain number. In terms of grain number, all lines except 'Norin 61' maintained it and no genotype-specific differences were observed. These two lines (MSD296 and MSD392) originated from the same synthetic wheat (Syn32) during the breeding process, and I expect that the genes involved in the maintenance of thousand kernel weight were introduced from the D genome of this synthetic wheat.

4.10. Metabolic responses of MSD lines

In a study on 'Norin 61', I estimated senescence, acclimation to high temperature, and recovery from heat stress by the trend of metabolites in the flag leaves at 7 days post-anthesis. The results were highly correlated with the measured agronomic traits. I attempted to characterize the candidate lines for high-temperature tolerance based on (1) the findings in the 'Norin 61' study and (2) the high-temperature response behavior specific in MSD lines.

4.10.1 Metabolic responses that can be described by the findings from 'Norin 61'

Among the trend of tryptophan, beta-alanine, putrescine and proline detected as molecular markers for senescence in response to high temperature in 'Norin 61', MSD296 did not show any change in accumulation due to high temperature in these four metabolites (Figure 25F, H−J). In particular, tryptophan, which showed specific behavior in MSD 296, is located at the junction of serotonin, another senescence indicator, and IAA, a growth hormone, in the metabolic pathway (Figure 15, 25H). As mentioned in previous section, since the behavior of tryptophan and serotonin accumulation in plants is similar, it is expected that MSD296 also suppresses the serotonin accumulation. In beta-alanine, five lines ('Norin 61', MSD392, MSD417, MSD54 and MNH2) showed a significant increase under high-temperature treatment (Figure 25F), suggesting that these five lines have already undergone nucleotide degradation leading to pyrimidine degradation under heat stress, and senescence was accelerated at the time of sampling. Among the senescence indices detected in 'Norin 61', tryptophan and beta-alanine reflected the differences among lines.

In summary, high temperature induced senescence in four lines (MSD392, MSD417, MSD54 and MNH2) just as in 'Norin 61', while MSD296 was the least sensitive to high temperature and was identified as a unique line that did not show senescence induction by high-temperature treatment. Putrescine is a versatile marker of high-temperature response that behaves similarly in all genotypes.

4.10.2. Genotype-specific metabolic response

Four metabolites (argininosuccinic acid, NAD, beta-alanine and adenosine) were

detected by their high regression coefficients in the multiple linear regression analysis using grain number and thousand kernel weight as objective variables, which were detected as factors controlling grain yield in the network analysis of 'Norin 61' (Figure 7, 24B, C). Among these metabolites, argininosuccinic acid, NAD and beta-alanine showed peaks in the multiple linear regression with grain yield as the objective variable (Figure 24A), suggesting that these metabolites may be useful as molecular markers for yield.

Argininosuccinic acid showed significant accumulation in high temperature treated samples at GS2 in 'Norin 61' as a factor for the activity of ammonia detoxification leading to recovery from high-temperature treatments (Table 2). Among the heat-tolerant candidate lines, MSD417 significantly accumulated this metabolite under high-temperature treatment, while in other metabolites in the urea cycle (ornithine and citrulline and arginine), ornithine and citrulline accumulated under high-temperature treatment (Figure 15, 25K−M). NAD had high regression coefficients in multiple linear regression analysis with fertility as the objective variable (Figure 24D), and the contribution of NAD in grain number may indirectly explain the involvement of fertility and grain number.

The high correlation between fertility and NAD suggests that NAD may be a predictive marker of fertility that can almost independently explain fertility (Figure 26K). The scatter plots of NAD and fertility showed a close distribution of each strain in the two environments (Figure 26K), suggesting that they are controlled by genetic factors. In both factors, MSD417 showed a high tendency in the two environments (Figure 25E, 26I), suggesting that MSD417 has the potential to increase grain number.

Thousand kernel weight and beta-alanine were highly related to each other in multiple and single regressions, respectively (Figure 24C, 26G), indicating that they are

useful factors for describing environmental responsiveness. However, only beta-alanine contents were not able to explain the characteristics of MSD392, a line with increased thousand kernel weight (Figure 21F, 25F). Adenosine, which showed high regression coefficients along with beta-alanine in multiple linear regression of thousand kernel weight (Figure 24C), may be a factor that fills in the gaps left by beta-alanine. The analysis of adenosine based on its biochemical properties in the future is suggested in future studies.

The correlation between these three metabolites (argininosuccinic acid, NAD and beta-alanine) and grain yield is low (Figure 26A, I, J), suggesting that these metabolites have an additive effect on grain yield. In addition, thousand kernel weight and fertility are agronomic traits that indirectly explain grain yield and are expected to contain useful genes in MSD392 and MSD417, respectively.

5. Conclusion

I first elucidated the effects of high-temperature stress on agronomic traits and physiological responses during seed formation using ‘Norin 61’ and found the stage-specific heat response. Furthermore, I assessed the genotype-specific differences in yield potential by integrating agronomic traits and metabolomic analysis.

High temperature during the seedling and vegetative stages decreased plant height and the number of grains, whereas this stress imposed during the reproductive stage significantly shortened the seed formation period and reduced grain weight. Interestingly, however, high temperature during the seedling stage delayed senescence and extended the starch deposition period, and reduced the number of nodes which caused an increase in translocation efficiency which contributes to the maintenance of thousand kernel weight, thereby increasing the harvest index and thousand kernel weight rather than reducing yield. I called the response to this treatment during the seedling stage the “heat priming” effect. Also, the plants exposed to high temperature continuously from seedling to maturity showed delayed senescence compared with those exposed to high temperature only at maturity. I called this phenomenon “acclimation” to maintain photosynthetic activity longer. I explained the priming effect caused by high temperature, accelerated senescence and high-temperature acclimation based on the dynamics of many metabolites. Beta-alanine, tryptophan, serotonin, proline and putrescine in the flag leave at 7 days post-anthesis appear to be suitable biomarkers that can be used to evaluate senescence and acclimation. Especially, accumulation of beta-alanine in the flag leaves could indicate the level of leaf senescence in response to heat stress, while the increase in tryptophan and serotonin appeared concomitantly with heat stress but disappeared in the acclimated

sample. These metabolites were strongly correlated with agronomic traits such as thousand kernel weight. Changes in metabolite concentrations during the recovery from the damage caused by heat stress were also observed. Also, several metabolites that positively affect thousand kernel weight and fertility, which directly affect yield were identified. It is expected that the accumulation tendency of metabolites can be used for the selection of suitable parental lines for the breeding of useful varieties. In this study, MSD392 and MSD417 were identified as lines that may have heat tolerance genes.

The complete genome sequence of ‘Norin 61’, the backcross parent of MSD, has been assembled, and much information is available in this wheat cultivar. Metabolomic quantitative trait loci (mQTL) analysis, in which metabolomic information is used as an independent phenotype for QTL analysis, is a method to elucidate plant metabolites and the genetic background that controls them. If we can discover mQTLs for metabolites that affect agronomic traits using metabolomics technology, we can expect to produce high-temperature tolerant bread wheat varieties by molecular breeding. The findings in this study might give significant insights into the development of heat-tolerant wheat cultivars.

Table 1. Reaction monitoring conditions for detected metabolites.

Compound name	Formula	Mw.	Polarity	Precursor ion	Fragmentor 1	Fragmentor 2	Fragmentor 3	Product ion 1 (CE)	Product ion 2 (CE)	Product ion 3 (CE)	Retention Time
Abscisic acid	C15H20O4	264.3	Negative	263.1	130	130	130	153.1(5)	219.1(9)	203.8(21)	17.3
Adenosine	C10H13N5O4	267.1	Positive	268.1	90	90	90	136(13)	119(55)	94.1(53)	7.7
Alanine	C3H7NO2	89.1	Positive	90.1	40	40	40	29.2(45)	44.2(9)	45.1(41)	3.2
1-Aminocyclopropanecarboxylic acid	C4H7NO2	101.1	Positive	102.1	50	50	50	56.2(9)	28.3(25)	61.2(5)	3.6
Arginine	C6H14N4O2	174.2	Positive	175.1	100	100	100	60.2(13)	70.2(25)	116(13)	4.5
Argininosuccinic acid	C10H18N4O6	290.1	Positive	291.1	120	120	120	43.2(55)	70.2(37)	116(17)	4.4
Ascorbic acid	C6H8O6	176.0	Negative	175.0	100	100	0	115(9)	87.1(21)	0	3.9
Asparagine	C4H8N2O3	132.1	Positive	133.1	80	80	80	87.1(5)	74.1(13)	28.3(29)	2.8
Aspartic acid	C4H7NO4	133.1	Positive	134.0	70	70	70	74.1(13)	88.1(5)	43.2(25)	2.9
beta-Alanine	C3H7NO2	89.1	Positive	90.1	50	50	50	30.3(9)	45.2(45)	72.2(5)	4.0
Betaine	C5H11NO2	117.1	Positive	118.1	120	120	120	42.2(55)	58.2(33)	59.2(17)	3.5
Choline	C5H14NO	104.1	Positive	105.1	110	110	110	61.2(17)	45.2(21)	46.2(25)	6.1
Citric acid	C6H8O7	192.0	Negative	191.0	90	90	0	111.0(9)	112.3(21)	0	5.1
Citrulline	C6H13N3O3	175.1	Positive	176.1	80	80	80	70.2(25)	113.0(13)	159.0(5)	3.4
Cytidine	C9H13N3O5	243.1	Positive	244.1	90	90	90	112(9)	95.1(49)	42.2(55)	7.3
Cytosine	C4H5N3O	111.0	Positive	112.1	130	130	130	95.1(21)	40.2(45)	52.2(37)	4.8
Deoxyadenosine	C10H13N5O3	251.1	Positive	252.1	90	90	90	136(9)	119(49)	43.2(37)	8.0
Deoxycytidine	C9H13N3O4	227.1	Positive	228.1	50	50	50	112(5)	95.1(45)	42.2(55)	7.7
Deoxyguanosine	C10H13N5O4	267.1	Positive	268.1	90	90	90	152(5)	135(41)	110(41)	7.2
Deoxyuridine	C9H12N2O5	228.1	Positive	229.1	50	50	0	112.9(15)	116.9(5)	0	7.1
Fumaric acid (trans-butenedioic acid)	C4H4O4	116.0	Nega	115.0	50	50		71.1(5, 10^2)	27.2(10)		9.8
Galacturonic acid	C6H10O7	194.0	Nega	193.0	90			113.1(9)			2.7
Gamma-aminobutyric acid	C4H9NO2	103.1	Positive	104.1	70	70	70	43.2(17)	45.2(25)	87.1(9)	5.1
Glutamic acid	C5H9NO4	147.1	Positive	148.1	80	80	80	84.1(17)	56.2(33)	130(5)	3.3
Glutamine	C5H10N2O3	146.1	Positive	147.1	70	70	70	56.2(33)	84.2(17)	130(5)	3.0
Glyceric acid	C3H6O4	106.0	Negative	107.0	90	0	0	75.1(9)	0	0	3.0
Glycine	C2H5NO2	75.1	Positive	76.0	20	20	0	30.3(5)	48.2(5)	0	2.9
Guanine	C5H5N5O	151.1	Positive	152.1	130	130	130	135(21)	110(21)	43.2(33)	7.1
Guanosine	C10H13N5O5	283.1	Positive	284.1	90	90	90	152(9)	135(41)	110(49)	7.1
Histidine	C6H9N3O2	155.2	Positive	156.1	100	100	100	83.1(29)	93.1(25)	110(13)	3.9
4-Hydroxybenzoic aldehyde	C7H6O2	122.0	Negative	121.0	120	0	0	92.2(25)	0	0	14.6
Hydroxyproline	C5H9NO3	131.1	Positive	132.1	90	90	90	41.2(33)	68.2(21)	86.2(13)	2.9
Hypoxanthine	C5H4N4O	136.0	Positive	137.1	130	130	130	110(21)	119(21)	55.2(37)	7.1
Inosine	C10H12N4O5	268.1	Positive	269.1	90	90	90	137(5)	110(45)	119(53)	7.1
Isoleucine	C6H13NO2	131.2	Positive	132.1	80	80	80	30.3(21)	44.2(25)	86.2(9)	8.7
Kynurenic acid	C10H7NO3	189.0	Posi	190.0	90	90	90	144.1(21,29838)	89.1(49,21833)	116(37,17250)	9.9
Leucine	C6H13NO2	131.2	Positive	132.1	70	70	70	30.3(17)	43.2(25)	86.2(5)	9.1
Lysine	C6H14N2O2	146.2	Positive	147.1	80	80	80	56.2(33)	84.2(17)	130(5)	3.8
Malic acid	C4H6O5	134.0	Negative	133.0	90	90	0	115.0(9)	71.1(13)	0	3.7
Malonic acid	C3H4O4	104.0	Negative	103.0	50	50	0	59.2(5)	41.2(33)	0	4.7
Methionine	C5H11NO2S	149.2	Positive	150.1	80	80	80	56.2(17)	104(9)	133(5)	7.2
Methionine Sulfoxide	C5H11NO3S	165.1	Positive	166.1	80	80	80	56.2(25)	74.1(13)	75.1(5)	3.3
Nicotinamide adenine dinucleotide	C21H27N7O14P2	663.1	Positive	664.1	170	170	170	136(53)	428(25)	524(17)	7.1
Nicotinic acid	C6H5NO2	123.0	Positive	124.0	130	130	130	80.1(21)	78.1(25)	53.2(33)	6.0
Ornithine	C5H12N2O2	132.1	Positive	133.1	80	80	80	43.2(37)	70.2(17)	116.0(5)	3.6
2-Oxoglutaric acid	C5H6O5	146.1	Negative	145.0	50	0	0	101.1(5)	0	0	4.2
Phenylalanine	C9H11NO2	165.2	Positive	166.1	80	80	80	77.1(45)	103(29)	120(9)	9.8
Proline	C5H9NO2	115.1	Positive	116.1	90	90	90	28.3(41)	43.2(37)	70.2(17)	3.8
Putrescine	C4H12N2	88.1	Positive	89.1	70	70	0	30.3(21)	72.2(5)	0	5.5
4-Pyridoxic acid	C8H9NO4	183.1	Posi	184.1	90	90	90	148(21,24717)	166.1(9,23244)	65.2(41,9649)	7.4
Pyro-glutamic acid	C5H7NO3	129.0	Positive	130.1	90	90	90	84.1(13)	41.2(25)	56.2(29)	5.8
Pyruvic acid	C3H4O3	88.1	Negative	87.0	100	0	0	43.2(5)			3.9
Salicylic acid (o-hydroxybenzoic acid)	C7H6O3	138.1	Negative	137.0	100	100	100	93.1(35)	65.2(35)	39.2(35)	18.8
Serine	C3H7NO3	105.1	Positive	106.1	70	70	70	42.2(25)	60.2(9)	88.1(5)	2.8
Serotonin	C10H12N2O	176.1	Positive	177.1	50	50	50	160.1(9)	115.1(33)	117.1(29)	14.3
Shikimic acid	C7H10O5	174.1	Negative	172.9	100	100	120	136.8(15)	110.9(15)	93.1(15)	3.7
Sinapic acid	C11H12O5	224.1	Negative	223.1	110	110	110	208(9)	121(29)	164.1(13)	14.7
Succinic acid	C4H6O4	118.0	Negative	117.0	60	0	0	73.1(9)	0	0	6.5
Tartaric acid	C4H6O6	150.1	Negative	149.0	100	100	100	72.8(20)	43.0(20)	87.1(20)	3.0
Threonine	C4H9NO3	119.1	Positive	120.1	70	70	70	56.2(17)	74.1(9)	102(5)	3.1
Thymidine	C10H14N2O5	242.1	Positive	243.1	50	50	50	127(9)	117(5)	109.9(37)	7.3
Trigonelline	C7H7NO2	137.1	Positive	138.1	130	130	130	92.1(21)	94.1(21)	39.2(55)	4.3
Tryptophan	C11H12N2O2	204.2	Positive	205.1	90	90	90	118(29)	146(13)	188(5)	12.6
Tyramine	C8H11NO	137.1	Positive	138.1	50	50	50	121.1(9)	77.2(33)	51.2(53)	12.5
Tyrosine	C9H11NO3	181.2	Positive	182.1	80	80	80	91.1(33)	136(9)	165(5)	8.0
Uridine	C9H12N2O6	244.1	Positive	245.1	50	50	50	113(5)	96(41)	70.1(37)	7.3
Valine	C5H11NO2	117.2	Positive	118.1	70	70	70	42.2(49)	55.2(21)	72.2(9)	6.6
Vanillin	C8H8O3	152.1	Negative	151.0	90	0	0	136(13)	0	0	15.1
Xanthosine	C10H12N4O6	284.1	Positive	285.1	90	90	90	153(5)	136(37)	43.2(55)	7.1

Table 2. Changes compared with the control for all metabolites in the heat-stressed plants. Growth stages: C = control, with normal temperatures; 1 = heating from germination to tillering; 2 = heating from tillering to flowering; and 3 = heating from flowering to full maturity. Values that represent a significant increase (more than one and a half fold) or decrease (less than two-thirds) the control values are shown in bold. Abbreviations: ABA, abscisic acid; ACC, 1-aminocyclopropane-1-carboxylic acid; GABA, gamma-aminobutyric acid; NAD, nicotinamide adenine dinucleotide.

Metabolites	GS1	GS2	GS3	GS 1–3	Metabolites	GS1	GS2	GS3
ABA	0.92	**0.63**	1.09	0.76	Kynurenic acid	0.78	0.98	1.01
ACC	0.84	1.36	1.07	1.38	Leucine*	0.92	**1.78**	0.93
Adenosine	0.88	1.12	1.13	0.97	Lysine*	1.02	1.03	1.00
Alanine*	0.91	1.39	1.36	1.14	Malic acid	0.77	**0.49**	1.22
Arginine*	1.16	**1.61**	1.17	1.01	Malonic acid	1.19	1.01	1.30
Argininosuccinic acid*	1.42	**3.26**	**0.55**	**0.52**	Methionine*	1.08	1.20	1.40
Ascorbic acid	1.04	**0.48**	**0.59**	**0.60**	Methionine sulfoxide*	0.68	0.73	**1.89**
Asparagine*	0.97	**3.78**	0.96	1.00	NAD	**2.07**	**2.30**	**0.57**
Aspartic acid*	1.10	**1.93**	0.76	1.10	Nicotinic acid	0.82	1.10	0.98
Beta-alanine*	0.70	0.93	**1.90**	1.23	Ornithine*	1.12	0.87	0.97
Betaine	1.00	**3.00**	1.22	1.31	2-Oxoglutaric acid	1.18	1.25	**2.01**
Choline	1.12	1.13	1.06	0.89	Phenylalanine*	0.96	1.26	**1.53**
Citric acid	0.93	**0.60**	1.16	1.30	Proline*	0.80	1.12	**3.78**
Citrulline*	**1.66**	**3.45**	**0.37**	**0.28**	Putrescine	0.77	**0.59**	**0.41**
Cytidine	0.86	1.11	1.22	0.90	4-Pyridoxic acid	1.15	1.25	1.00
Cytosine	1.08	**2.14**	1.27	**1.70**	Pyroglutamic acid*	**2.25**	**8.55**	0.98
Deoxyadenosine	0.83	1.03	1.27	0.95	Pyruvic acid	1.04	1.21	1.20
Deoxycytidine	0.78	0.92	1.37	0.94	Salicylic acid	0.98	1.36	0.70
Deoxyguanosine	0.82	1.13	1.46	1.06	Serine*	1.20	**3.10**	0.79
Deoxyuridine	0.79	0.90	1.32	0.97	Serotonin	0.84	1.36	**8.69**
Fumaric acid	**0.65**	**0.46**	1.40	1.37	Shikimic acid	1.19	**0.25**	1.07
GABA*	0.97	1.39	**1.66**	1.44	Sinapic acid	0.80	0.77	**0.43**
Galacturonic acid	1.00	0.82	**1.71**	1.10	Succinic acid	0.75	**0.35**	0.85
Glutamic acid*	1.06	**1.53**	**0.63**	**0.65**	Tartaric acid	0.80	**2.24**	**2.14**
Glutamine*	1.00	1.06	0.96	0.82	Threonine*	1.10	**1.87**	0.90
Glyceric acid	1.02	1.45	0.78	0.82	Thymidine	0.87	1.05	1.49
Glycine*	1.33	**1.88**	0.76	1.02	Trigonelline	0.85	**0.59**	0.88
Guanine	0.76	1.05	1.38	1.00	Tryptophan*	0.79	0.98	**3.23**
Guanosine	0.88	0.99	**1.60**	1.29	Tyramine	1.22	**1.56**	1.19
Histidine*	0.84	**1.54**	**1.78**	1.37	Tyrosine*	1.01	**1.87**	1.27
4-Hydroxybenzaldehyde	0.95	1.42	0.89	1.29	Uridine	0.81	1.09	1.14
Hydroxyproline*	0.68	**0.39**	1.28	0.68	Valine*	1.06	**2.39**	0.89
Hypoxanthine	**0.60**	1.39	0.79	**0.62**	Vanillin	0.85	0.73	0.84
Inosine	**0.61**	1.25	0.72	**0.66**	Xanthosine	1.04	1.35	0.83
Isoleucine*	0.93	**2.39**	1.04	0.94				

Note: Metabolites labeled with an asterisk are amino acids.

Table 3. A *p*-value of fold change between control and each condition.

	GS1	GS2	GS3	GS1–3		GS1	GS2	GS3	GS1–3
Abscisic acid	0.22	1.46E-03	0.48	0.07	Kynurenic acid	0.01	0.77	0.89	2.92E-04
Adenosine	0.02	0.02	1.38E-03	0.53	Leucine	0.19	7.31E-05	0.31	0.55
Alanine	0.12	4.57E-03	2.87E-05	0.03	Lysine	0.66	0.25	0.91	2.01E-03
1-Aminocyclopropanecarboxylic acid	0.01	4.33E-03	0.13	1.84E-04	Malic acid	7.28E-05	3.96E-06	2.22E-03	0.36
Arginine	1.16E-03	9.76E-06	8.24E-05	0.85	Malonic acid	5.93E-04	0.80	1.05E-05	6.08E-04
Argininosuccinic acid	2.17E-03	8.22E-09	1.77E-03	7.14E-04	Methionine	0.32	3.73E-03	4.97E-05	0.10
Ascorbic acid	0.34	1.30E-08	1.53E-05	5.37E-07	Methionine sulfoxide	2.72E-04	2.70E-05	6.88E-04	0.10
Asparagine	0.64	2.34E-04	0.54	1.00	Nicotinamide adenine dinucleotide	1.18E-03	4.33E-03	3.61E-05	3.74E-03
Aspartic acid	0.07	9.76E-06	7.54E-04	0.16	Nicotinic acid	1.41E-05	0.13	0.58	0.01
beta-Alanine	5.27E-05	0.43	5.89E-09	0.01	Ornithine	0.66	0.56	0.84	0.06
Betaine	0.96	3.36E-09	1.73E-05	2.40E-04	2-Oxoglutaric acid	2.13E-03	7.34E-04	3.91E-10	0.02
Choline	2.22E-03	3.07E-05	0.05	2.89E-03	Phenylalanine	0.69	0.01	0.02	0.58
Citric acid	0.21	6.65E-05	0.05	5.98E-04	Proline	0.02	0.17	1.05E-05	0.39
Citrulline	0.04	6.73E-04	7.54E-04	5.37E-04	Putrescine	3.44E-03	6.79E-04	9.94E-08	1.70E-10
Cytidine	2.08E-05	0.04	5.53E-05	0.01	4-Pyridoxic acid	2.17E-03	4.33E-03	0.98	0.11
Cytosine	0.09	2.68E-07	0.01	1.18E-06	Pyroglutamic acid	2.92E-06	2.14E-11	0.45	5.98E-04
Deoxyadenosine	1.27E-03	0.60	1.51E-06	0.08	Pyruvic acid	0.22	1.59E-03	1.82E-04	2.40E-04
Deoxycytidine	1.27E-03	0.17	5.92E-08	0.06	Salicylic acid (o-hydroxybenzoic acid)	0.91	0.05	4.24E-03	0.38
Deoxyguanosine	0.01	0.09	2.75E-06	0.36	Serine	0.01	2.36E-06	2.60E-03	0.03
Deoxyuridine	5.93E-04	0.05	1.35E-06	0.38	Serotonin	0.32	0.07	5.59E-05	1.94E-03
Fumaric acid	0.02	0.01	0.04	5.35E-04	Shikimic acid	0.21	4.51E-04	0.55	0.05
Galacturonic acid	0.98	1.67E-03	5.46E-08	0.55	Sinapic acid	0.01	4.34E-03	5.89E-09	0.58
Gamma-aminobutyric acid	0.82	2.67E-03	3.81E-05	5.98E-04	Succinic acid	3.41E-03	3.57E-05	0.08	5.37E-04
Glutamic acid	0.03	2.70E-05	2.73E-07	2.97E-08	Tartaric acid	1.27E-03	2.16E-08	5.46E-08	2.05E-07
Glutamine	0.98	0.24	0.36	0.01	Threonine	0.01	9.47E-06	0.03	0.01
Glyceric acid	0.85	8.50E-04	1.89E-03	0.02	Thymidine	0.07	0.49	5.89E-09	1.84E-04
Glycine	0.02	2.73E-05	2.89E-07	0.82	Trigonelline	0.36	0.01	0.06	0.01
Guanine	1.27E-03	0.44	1.65E-04	1.00	Tryptophan	0.04	0.86	9.43E-04	0.01
Guanosine	0.01	0.74	1.46E-06	5.98E-04	Tyramine	0.04	2.77E-05	0.01	0.55
Histidine	0.01	3.35E-04	1.35E-06	3.00E-03	Tyrosine	0.84	3.07E-07	1.87E-04	0.30
4-hydroxybenzaldehyde	0.34	3.35E-04	0.11	1.22E-03	Uridine	0.02	0.30	0.29	0.05
Hydroxyproline	0.02	1.10E-03	1.89E-03	2.89E-03	Valine	0.20	5.10E-07	1.04E-03	0.06
Hypoxanthine	0.02	0.02	0.13	2.01E-03	Vanillin	0.01	3.02E-04	0.20	0.38
Inosine	5.93E-04	0.01	0.01	2.08E-05	Xanthosine	0.56	9.76E-06	7.77E-05	1.00
Isoleucine	0.14	4.35E-05	0.25	0.41					

Table 4. Result of enrichment analysis in each condition.

Growth stage	Pathway	total	expected	hits	Raw p	Holm p	FDR	Contain metabolites
GS1	Purine Metabolism	74	0.43	4	3.39E-04	3.32E-02	1.89E-02	Adenine; Adenosine monophosphate; Adenosine; Ammonia; Cyclic AMP; Deoxyinosine; Deoxyguanosine; Deoxyadenosine; Glycine; Guanine; Guanosine; **Fumaric acid**; L-Glutamic acid; **Hypoxanthine**; Inosinic acid; Inosine triphosphate; L-Aspartic acid; **Inosine**; NADP; NADPH; Pyrophosphate; Phosphoribosyl pyrophosphate; Uric acid; Xanthine; Xanthosine; Calcium; Adenylsuccinic acid; Adenosine triphosphate; Magnesium; Potassium; L-Glutamine; SAICAR; **NAD**; Deoxyadenosine monophosphate; dGDP; 10-Formyltetrahydrofolate; Phosphoribosylformylglycineamidine; 2'-Deoxyguanosine 5'-monophosphate; 5-Phosphoribosylamine; Adenosine diphosphate ribose; Guanosine diphosphate; 5-Aminoimidazole ribonucleotide; FAD; Guanosine triphosphate; Zinc (II) ion; 5'-Phosphoribosyl-N-formylglycinamide; Diguanosine tetraphosphate; ADP; Deoxyribose 1-phosphate; Oxygen; Guanosine monophosphate; Phosphate; Phosphoribosyl formamidocarboxamide; dGTP; NADH; Ribose 1-phosphate; dADP; AICAR; Deoxyadenosine triphosphate; D-Ribose 5-phosphate; Xanthylic acid; Tetrahydrofolic acid; Carbon dioxide; Glycineamideribotide; Water; Phosphoric acid; Hydrogen peroxide; Heme; 5-Aminoimidazole-4-carboxamide; IDP; 2-(Formamido)-N1-(5-phospho-D-ribosyl)acetamidine; 5-amino-1-(5-phospho-D-ribosyl)imidazole-4-carboxylate; Guanosine 2',3'-cyclic phosphate ; Fe3+
GS1	Urea Cycle	29	0.17	3	3.87E-04	3.75E-02	1.89E-02	Adenosine monophosphate; Ammonia; Argininosuccinic acid; **Fumaric acid**; L-Glutamic acid; L-Alanine; L-Aspartic acid; Oxoglutaric acid; Ornithine; Oxalacetic acid; Pyruvic acid; Pyrophosphate; Urea; Calcium; L-Arginine; Adenosine triphosphate; Hydrogen carbonate; L-Glutamine; **NAD**; **Citrulline**; Carbamoyl phosphate; Manganese; ADP; Phosphate; NADH; Pyridoxal 5'-phosphate; Carbon dioxide; Water; Phosphoric acid
GS2	Arginine and Proline Metabolism	53	1.55	9	8.31E-06	8.15E-04	4.36E-04	Tetrahydrobiopterin; Adenosine monophosphate; Ammonia; **Argininosuccinic acid**; Creatine; **Glycine**; Guanidoacetic acid; **Fumaric acid**; **L-Glutamic acid**; L-Proline; **L-Aspartic acid**; Oxoglutaric acid; Ornithine; NADP; NADPH; Oxalacetic acid; Pyrophosphate; **Succinic acid**; Urea; **L-Arginine**; Adenosine triphosphate; **NAD**; **Citrulline**; S-Adenosylhomocysteine; Carbamoyl phosphate; S-Adenosylmethionine; FAD; 1-Pyrroline-5-carboxylic acid; Manganese; ADP; Pyrroline hydroxycarboxylic acid; Oxygen; Phosphate; NADH; Pyridoxal 5'-phosphate; Phosphocreatine; Flavin Mononucleotide; Carbon dioxide; 4-Hydroxy-2-oxoglutaric acid; L-Glutamic gamma-semialdehyde; Water; Phosphoric acid; 1-Pyrroline-4-hydroxy-2-carboxylate; 4-Hydroxy-L-glutamic acid; Hydrogen peroxide; Heme; Nitric oxide; D-Proline; N-(o)-Hydroxyarginine; 4-Hydroxy-L-proline; L-4-Hydroxyglutamate semialdehyde; 1-Pyrroline-2-carboxylic acid; Hydrogen Ion
GS2	Urea Cycle	29	0.85	7	8.90E-06	8.63E-04	4.36E-04	Adenosine monophosphate; Ammonia; **Argininosuccinic acid**; **Fumaric acid**; **L-Glutamic acid**; L-Alanine; **L-Aspartic acid**; Oxoglutaric acid; Ornithine; Oxalacetic acid; Pyruvic acid; Pyrophosphate; Urea; Calcium; **L-Arginine**; Adenosine triphosphate; Hydrogen carbonate; L-Glutamine; **NAD**; **Citrulline**; Carbamoyl phosphate; Manganese; ADP; Phosphate; NADH; Pyridoxal 5'-phosphate; Carbon dioxide; Water; Phosphoric acid
GS2	Aspartate Metabolism	35	1.03	7	3.39E-05	3.26E-03	1.11E-03	Acetic acid; Adenosine monophosphate; Ammonia; **Argininosuccinic acid**; Beta-Alanine; **Fumaric acid**; **L-Glutamic acid**; **L-Asparagine**; Inosinic acid; **L-Aspartic acid**; Oxoglutaric acid; Oxalacetic acid; Pyrophosphate; **L-Arginine**; Adenylsuccinic acid; Adenosine triphosphate; Magnesium; L-Glutamine; Malonic acid; N-Acetyl-L-aspartic acid; Ureidosuccinic acid; **Citrulline**; Carbamoyl phosphate; Guanosine diphosphate; FAD; Guanosine triphosphate; Zinc (II) ion; Oxygen; Phosphate; Pyridoxal 5'-phosphate; Carbon dioxide; Water; Hydrogen peroxide; D-Aspartic acid; Malonic semialdehyde
GS2	Malate-Aspartate Shuttle	10	0.29	4	1.12E-04	1.06E-02	2.74E-03	**L-Glutamic acid**; **L-Aspartic acid**; Oxoglutaric acid; Oxalacetic acid; Calcium; **Malic acid**; **NAD**; NADH; Pyridoxal 5'-phosphate; Hydrogen Ion
GS2	Ammonia Recycling	32	0.94	6	2.00E-04	1.88E-02	3.92E-03	Biotin; Adenosine monophosphate; Ammonia; **Glycine**; **L-Glutamic acid**; **L-Asparagine**; **L-Histidine**; L-Serine; **L-Aspartic acid**; Oxoglutaric acid; Pyruvic acid; Pyrophosphate; Urocanic acid; Adenosine triphosphate; Magnesium; L-Glutamine; **NAD**; Carbamoyl phosphate; FAD; ADP; Phosphate; (R)-lipoic acid; NADH; Pyridoxal 5'-phosphate; 5,10-Methylene-THF; Tetrahydrofolic acid; Carbon dioxide; Water; Phosphoric acid; Dihydrolipoate; 8-[(Aminomethyl)sulfanyl]-6-sulfanyloctanoic acid; (S)-lipoic acid
GS2	Carnitine Synthesis	22	0.65	4	3.04E-03	2.83E-01	4.88E-02	**Ascorbic acid**; L-Carnitine; **Glycine**; L-Lysine; Oxoglutaric acid; **Succinic acid**; Fe2+; **NAD**; S-Adenosylhomocysteine; 4-Trimethylammoniobutanoic acid; S-Adenosylmethionine; N6,N6,N6-Trimethyl-L-lysine; 4-Trimethylammoniobutanal; Hydrogen; Oxygen; 3-Hydroxy-N6,N6,N6-trimethyl-L-lysine; NADH; Pyridoxal 5'-phosphate; Carbon dioxide; Water; D-Lysine; Hydrogen Ion
GS2	Tyrosine Metabolism	72	2.11	7	3.49E-03	3.21E-01	4.88E-02	p-Hydroxyphenylacetic acid; Iodotyrosine; 3-Methoxytyramine; Tetrahydrobiopterin; **Ascorbic acid**; Ammonia; Acetoacetic acid; Epinephrine; Dopamine; Homovanillic acid; Homogentisic acid; **Fumaric acid**; **L-Glutamic acid**; **L-Tyrosine**; Methylamine; L-Dopa; **L-Aspartic acid**; Oxoglutaric acid; Norepinephrine; NADP; NADPH; Oxalacetic acid; Thyroxine; Liothyronine; Vanillylmandelic acid; **Tyramine**; 3,4-Dihydroxyphenylglycol; Calcium; Magnesium; Copper; 4-Hydroxyphenylpyruvic acid; Normetanephrine; **NAD**; S-Adenosylhomocysteine; Pyrocatechol; S-Adenosylmethionine; Dopaquinone; FAD; 5,6-Dihydroxyindole-2-carboxylic acid; Dehydroascorbic acid; 4-Fumarylacetoacetic acid; 3,4-Dihydroxybenzeneacetic acid; Oxygen; Guaiacol; L-Dopachrome; NADH; Vanylglycol; Pyridoxal 5'-phosphate; 3,4-Dihydroxymandelic acid; Carbon dioxide; Maleylacetoacetic acid; Water; 4a-Hydroxytetrahydrobiopterin; Hydrogen peroxide; 3,5-Diiodo-L-tyrosine; 3,4-Dihydroxyphenylacetaldehyde; 5,6-Dihydroxyindole; 3-Methoxy-4-hydroxyphenylglycolaldehyde; Metanephrine; Leucodopachrome; Melanin; Homovanillin; 3,4-Dihydroxymandelaldehyde; Indole-5,6-quinone; 2-Hydroxy-3-(4-hydroxyphenyl)propenoic acid; Topaquinone; Fe3+; Pyrroloquinoline quinone; Iron; Zinc; Hydrogen Ion; Methylammonium
GS3	Urea Cycle	29	0.54	5	1.13E-04	1.10E-02	7.03E-03	Adenosine monophosphate; Ammonia; **Argininosuccinic acid**; Fumaric acid; **L-Glutamic acid**; L-Alanine; L-Aspartic acid; **Oxoglutaric acid**; Ornithine; Oxalacetic acid; Pyruvic acid; Pyrophosphate; Urea; Calcium; L-Arginine; Adenosine triphosphate; Hydrogen carbonate; L-Glutamine; **NAD**; **Citrulline**; Carbamoyl phosphate; Manganese; ADP; Phosphate; NADH; Pyridoxal 5'-phosphate; Carbon dioxide; Water; Phosphoric acid
GS3	Arginine and Proline Metabolism	53	0.98	6	2.34E-04	2.27E-02	7.03E-03	Tetrahydrobiopterin; Adenosine monophosphate; Ammonia; **Argininosuccinic acid**; Creatine; Glycine; Guanidoacetic acid; Fumaric acid; **L-Glutamic acid**; **L-Proline**; L-Aspartic acid; **Oxoglutaric acid**; Ornithine; NADP; NADPH; Oxalacetic acid; Pyrophosphate; Succinic acid; Urea; L-Arginine; Adenosine triphosphate; **NAD**; **Citrulline**; S-Adenosylhomocysteine; Carbamoyl phosphate; S-Adenosylmethionine; FAD; 1-Pyrroline-5-carboxylic acid; Manganese; ADP; Pyrroline hydroxycarboxylic acid; Oxygen; Phosphate; NADH; Pyridoxal 5'-phosphate; Phosphocreatine; Flavin Mononucleotide; Carbon dioxide; 4-Hydroxy-2-oxoglutaric acid; L-Glutamic gamma-semialdehyde; Water; Phosphoric acid; 1-Pyrroline-4-hydroxy-2-carboxylate; 4-Hydroxy-L-glutamic acid; Hydrogen peroxide; Heme; Nitric oxide; D-Proline; N-(o)-Hydroxyarginine; 4-Hydroxy-L-proline; L-4-Hydroxyglutamate semialdehyde; 1-Pyrroline-2-carboxylic acid; Hydrogen Ion
GS3	Beta-Alanine Metabolism	34	0.63	5	2.49E-04	2.39E-02	7.03E-03	1,3-Diaminopropane; Ureidopropionic acid; Carnosine; Ammonia; **Beta-Alanine**; Dihydrouracil; **L-Glutamic acid**; **L-Histidine**; L-Aspartic acid; Anserine; **Oxoglutaric acid**; Pantothenic acid; NADP; NADPH; Uracil; Calcium; 3-Methylhistidine; Copper; **NAD**; 3-Aminopropionaldehyde; Acetyl-CoA; FAD; Zinc (II) ion; Oxygen; Coenzyme A; NADH; Pyridoxal 5'-phosphate; Flavin Mononucleotide; Carbon dioxide; Water; Hydrogen peroxide; Malonic semialdehyde; Topaquinone; Hydrogen Ion
GS3	Aspartate Metabolism	35	0.65	5	2.87E-04	2.73E-02	7.03E-03	Acetic acid; Adenosine monophosphate; Ammonia; **Argininosuccinic acid**; **Beta-Alanine**; Fumaric acid; **L-Glutamic acid**; L-Asparagine; Inosinic acid; L-Aspartic acid; **Oxoglutaric acid**; Oxalacetic acid; Pyrophosphate; L-Arginine; Adenylsuccinic acid; Adenosine triphosphate; Magnesium; L-Glutamine; Malonic acid; N-Acetyl-L-aspartic acid; Ureidosuccinic acid; **Citrulline**; Carbamoyl phosphate; Guanosine diphosphate; FAD; Guanosine triphosphate; Zinc (II) ion; Oxygen; Phosphate; Pyridoxal 5'-phosphate; Carbon dioxide; Water; Hydrogen peroxide; D-Aspartic acid; Malonic semialdehyde
GS3	Malate-Aspartate Shuttle	10	0.19	3	6.00E-04	5.64E-02	1.18E-02	**L-Glutamic acid**; L-Aspartic acid; **Oxoglutaric acid**; Oxalacetic acid; Calcium; Malic acid; **NAD**; NADH; Pyridoxal 5'-phosphate; Hydrogen Ion
GS3	Glucose-Alanine Cycle	13	0.24	3	1.38E-03	0.13	2.25E-02	Ammonia; D-Glucose; **L-Glutamic acid**; L-Alanine; **Oxoglutaric acid**; NADP; NADPH; Pyruvic acid; **NAD**; NADH; Pyridoxal 5'-phosphate; Water; Hydrogen Ion
GS3	Ammonia Recycling	32	0.59	4	2.19E-03	0.20	3.07E-02	Biotin; Adenosine monophosphate; Ammonia; Glycine; **L-Glutamic acid**; L-Asparagine; **L-Histidine**; L-Serine; L-Aspartic acid; **Oxoglutaric acid**; Pyruvic acid; Pyrophosphate; Urocanic acid; Adenosine triphosphate; Magnesium; L-Glutamine; **NAD**; Carbamoyl phosphate; FAD; ADP; Phosphate; (R)-lipoic acid; NADH; Pyridoxal 5'-phosphate; 5,10-Methylene-THF; Tetrahydrofolic acid; Carbon dioxide; Water; Phosphoric acid; Dihydrolipoate; 8-[(Aminomethyl)sulfanyl]-6-sulfanyloctanoic acid; (S)-lipoic acid
GS3	Tryptophan Metabolism	60	1.11	5	3.60E-03	0.33	4.41E-02	Tetrahydrobiopterin; Formic acid; **L-Glutamic acid**; L-Alanine; Indoleacetic acid; **Oxoglutaric acid**; NADP; NADPH; Quinolinic acid; Pyrophosphate; **Serotonin**; Tryptamine; 5-Hydroxy-L-tryptophan; Adenosine triphosphate; L-Kynurenine; Fe2+; Kynurenic acid; 5-Hydroxyindoleacetic acid; Xanthurenic acid; **NAD**; **L-Tryptophan**; S-Adenosylhomocysteine; 4-(2-Aminophenyl)-2,4-dioxobutanoic acid; 2-Aminobenzoic acid; S-Adenosylmethionine; Indoleacetaldehyde; N'-Formylkynurenine; Acetyl-CoA; N-Acetylserotonin; FAD; 2-Aminomuconic acid semialdehyde; 2-Amino-3-carboxymuconic acid semialdehyde; Oxygen; Melatonin; Coenzyme A; 3-Hydroxyanthranilic acid; NADH; Pyridoxal 5'-phosphate; Carbon dioxide; Water; Molybdopterin; 4a-Hydroxytetrahydrobiopterin; Hydrogen peroxide; Heme; 3'-AMP; 5-Hydroxyindoleacetaldehyde; 5-Hydroxykynurenamine; 4,6-Dihydroxyquinoline; Cinnavalininate; 6-Hydroxymelatonin; 4-(2-Amino-3-hydroxyphenyl)-2,4-dioxobutanoic acid; 5-Hydroxy-N-formylkynurenine; Formylanthranilic acid; 5-Methoxyindoleacetate; Acetyl-N-formyl-5-methoxykynurenamine; N-Methylserotonin; N-Methyltryptamine; L-3-Hydroxykynurenine; 5-Hydroxykynurenine; Formyl-5-hydroxykynurenamine
GS1–3	ND							

Table 5. Correlation coefficients between agronomic traits and metabolites.

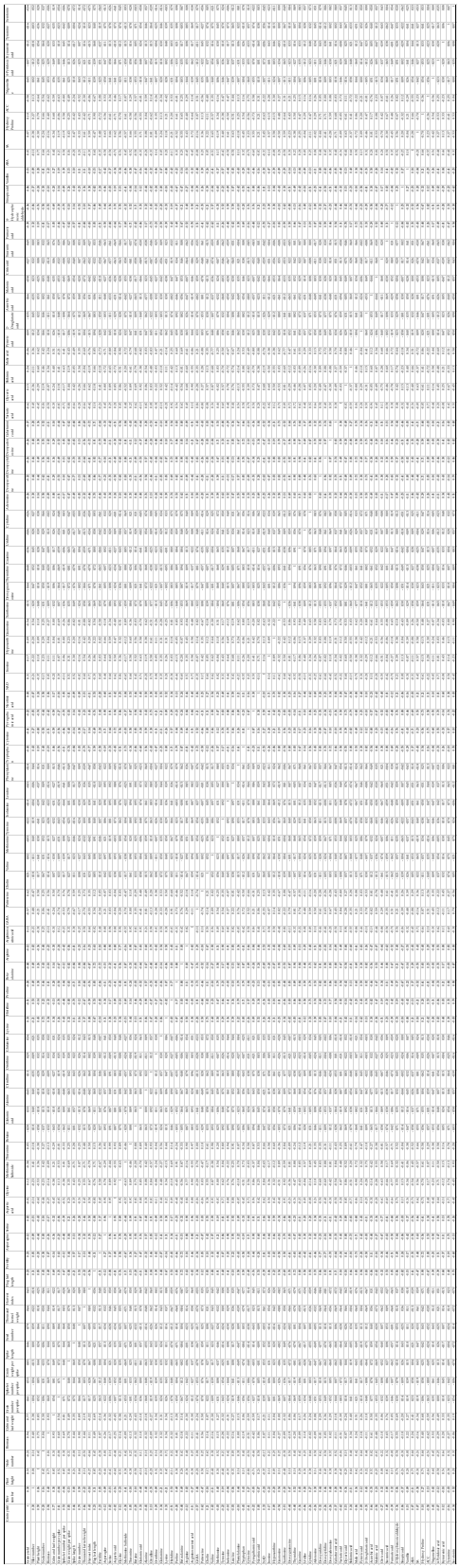

Table 6. *p*-values of the correlation coefficient between agronomic traits and metabolites.

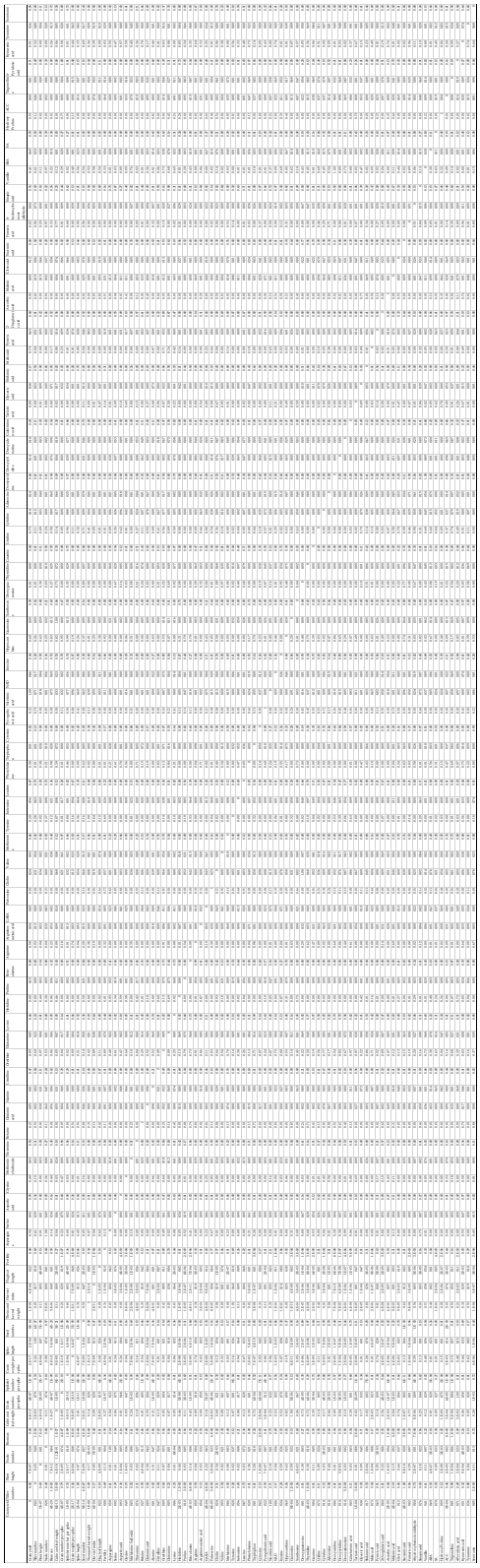

(A)

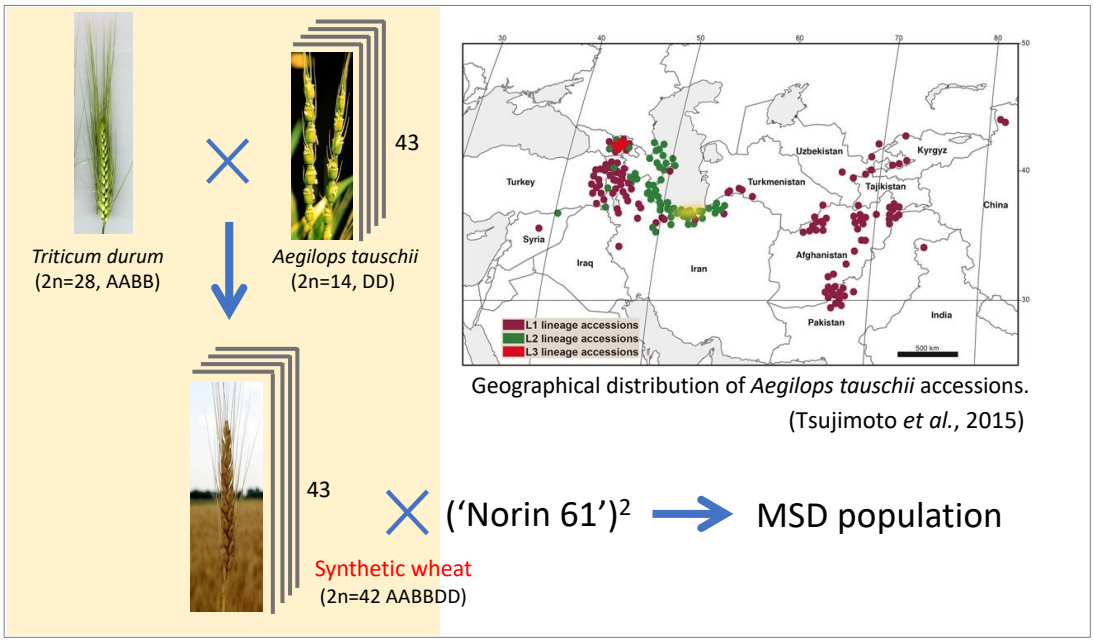

Geographical distribution of *Aegilops tauschii* accessions.
(Tsujimoto *et al.*, 2015)

(B)

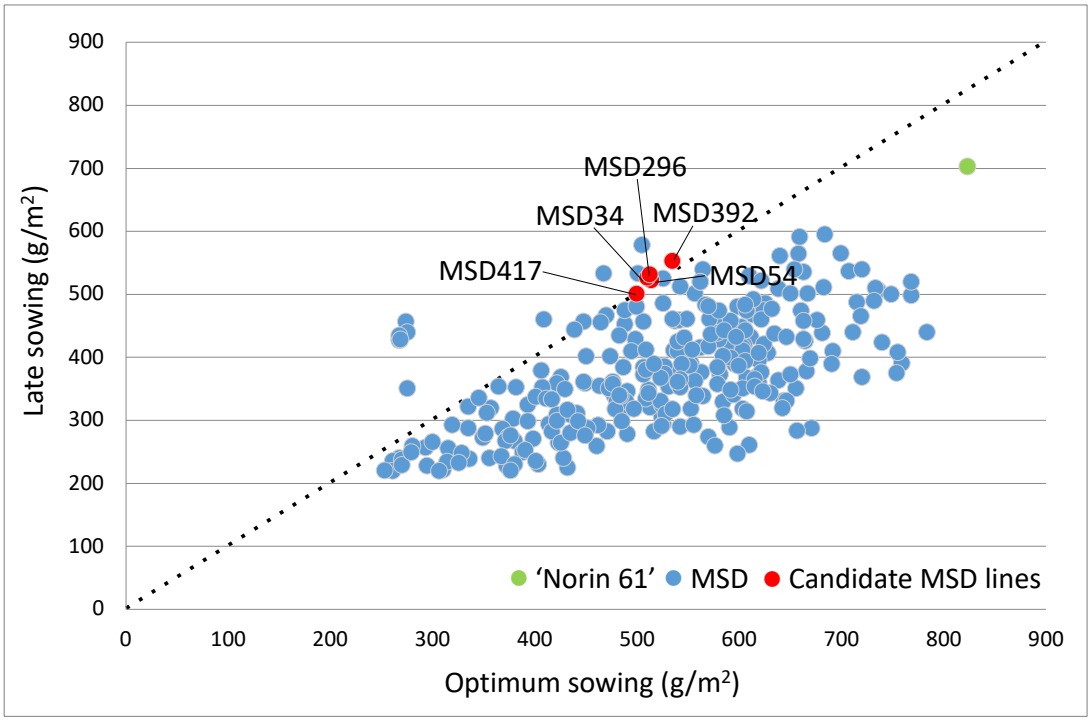

Figure 1. (A) Historical background of the MSD population. (B) Yield plots for normal and late sowing of MSD population (234 lines). Blue dots indicate each MSD lines and red dots indicate 'Norin 61'. Dashed lines indicate Y=X.

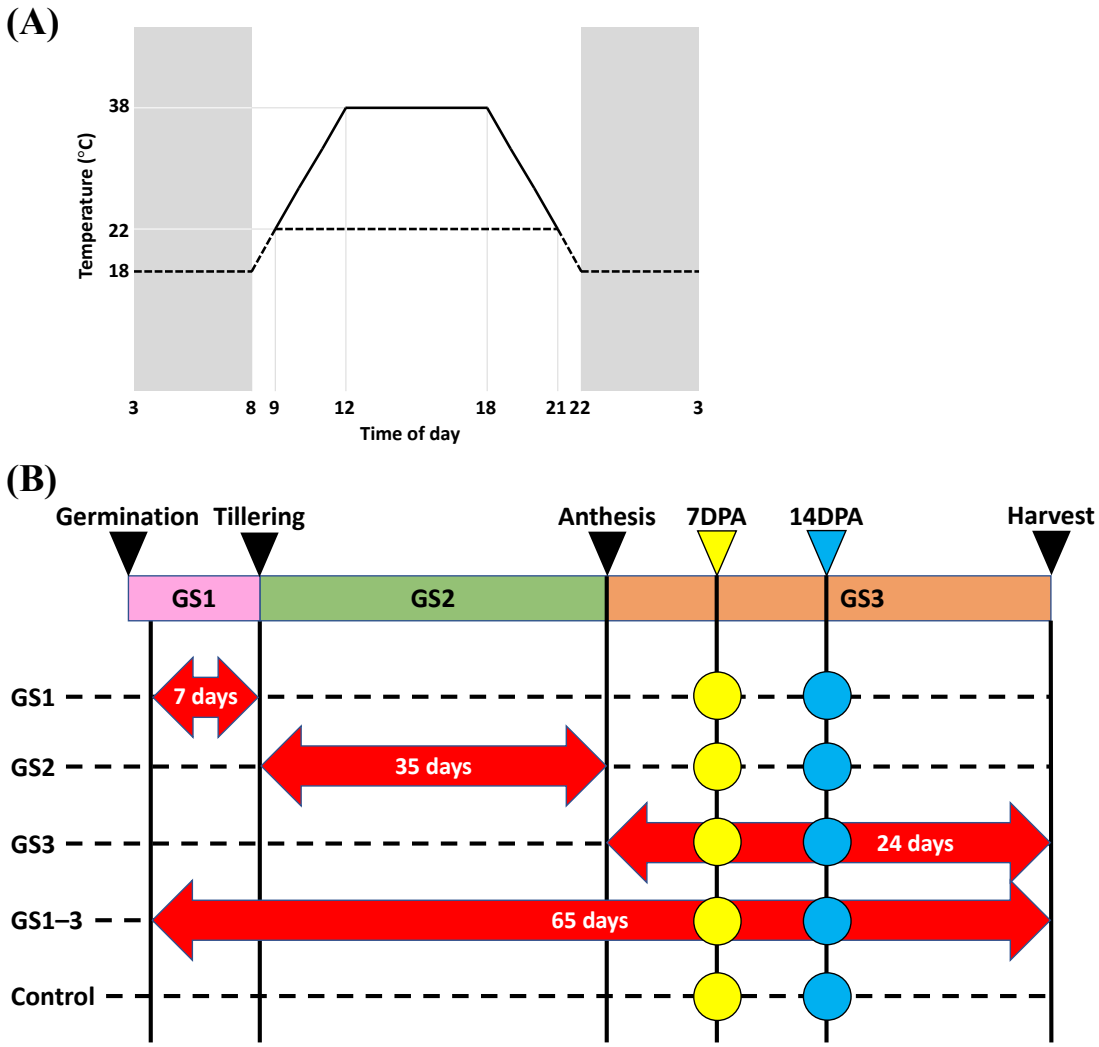

Figure 2. Outline of heat stress experiment. (A) Daily temperature variation. White background, day; gray, night. (B) Timing of the heat treatment (red arrows), metabolite sampling (yellow circles), and photosynthesis measurement (blue circles). Wheat plants were kept at 22°C day/18°C night (Control) or exposed to transient high temperature (Heat) at 38/18°C (day/night) during the indicated growth stages. Red arrows indicate the high-temperature treatment period with treatment days, and dashed lines indicate the period with control temperature. GS, growth stages (1 = heating from germination to tillering; 2 = heating from tillering to flowering; 3 = heating from flowering to full maturity; 1–3 = all stages); DPA, days post-anthesis.

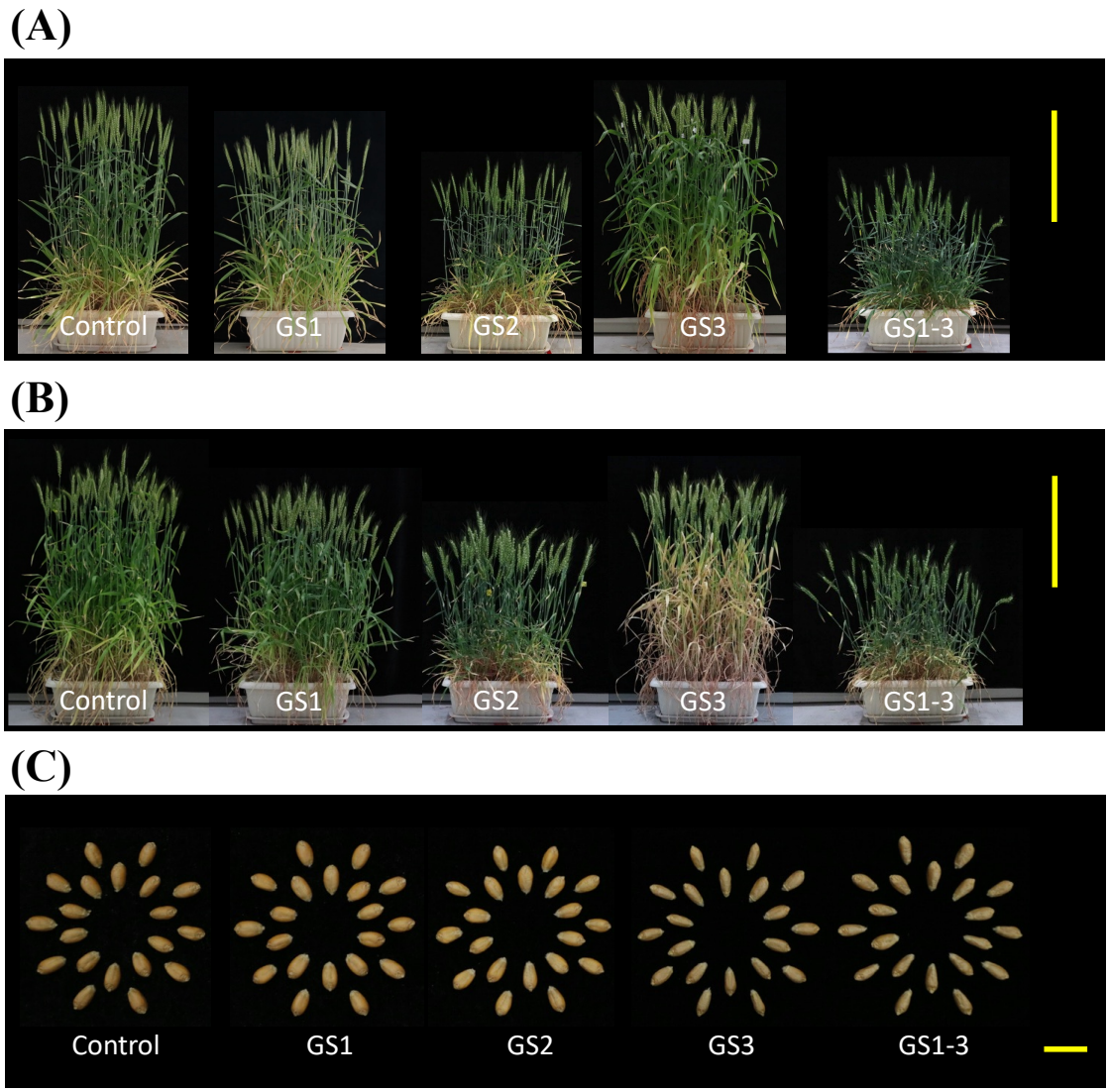

Figure 3. Effect of high temperature during each growth stage on plant and seed morphology. (A, B) Each plant at (A) anthesis and (B) 14 days post-anthesis. (C) Harvested seeds. Bars: plants (A, B), 50 cm; seeds (C), 1 cm.

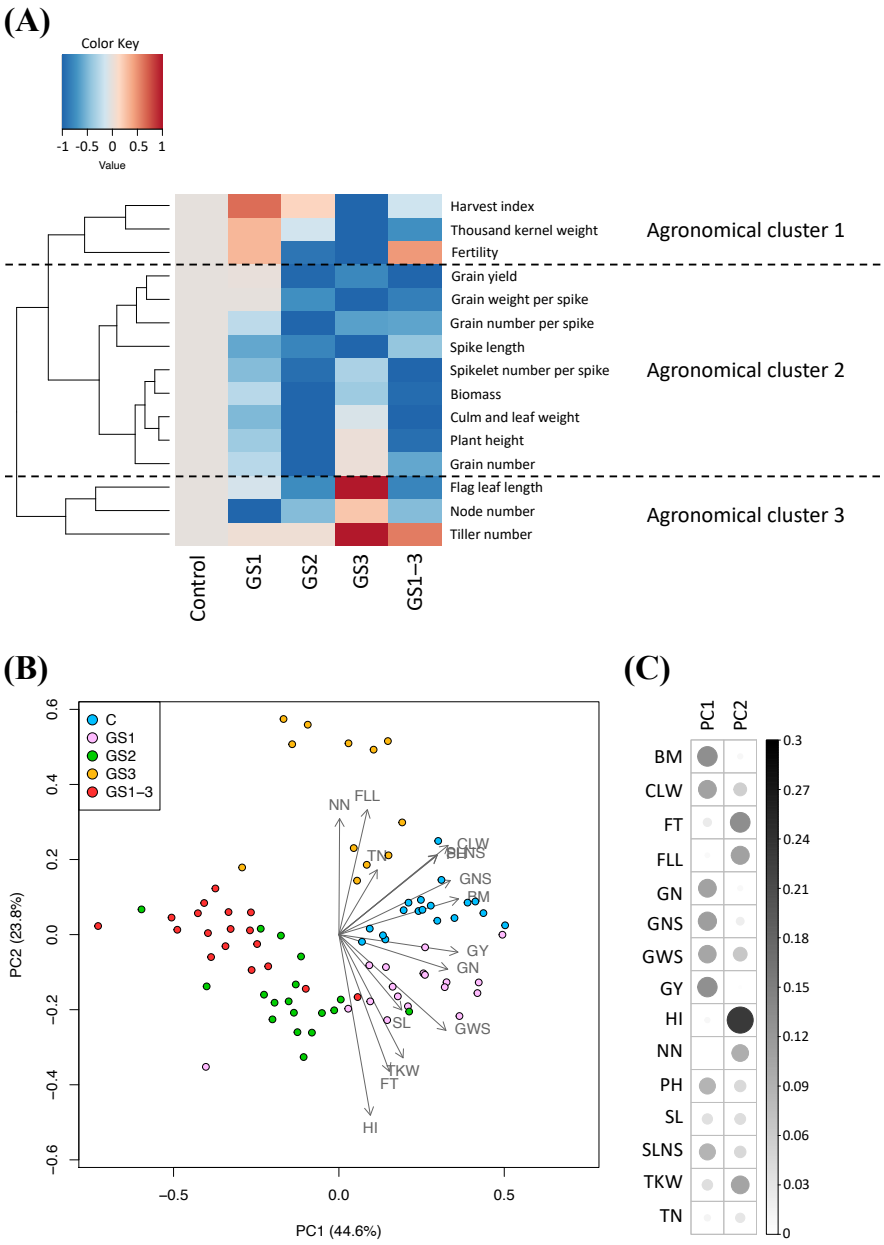

Figure 4. Hierarchical clustering and heat map (A), principal component analysis (PCA) (B) and trait contribution to PC1 and PC2 (C) of agronomic traits in each growing condition (GS1, GS2, GS3, GS1–3 and control indicated by C). Colors in (A) show an increase (red) or decrease (blue) compared with the control. In (C), the strength of the contribution is indicated by the size and intensity of each circle. In (B) and (C), BM, biomass; CLW, culm and leaf weight; FT, fertility; FLL, flag leaf length; GN, grain number; GNS, grain number per spike; GWS, grain weight per spike; GY, grain yield; HI, harvest index; NN, node number; PH, plant height; SL, spike length; SLNS, spikelet number per spike; TKW, thousand kernel weight; TN, tiller number.

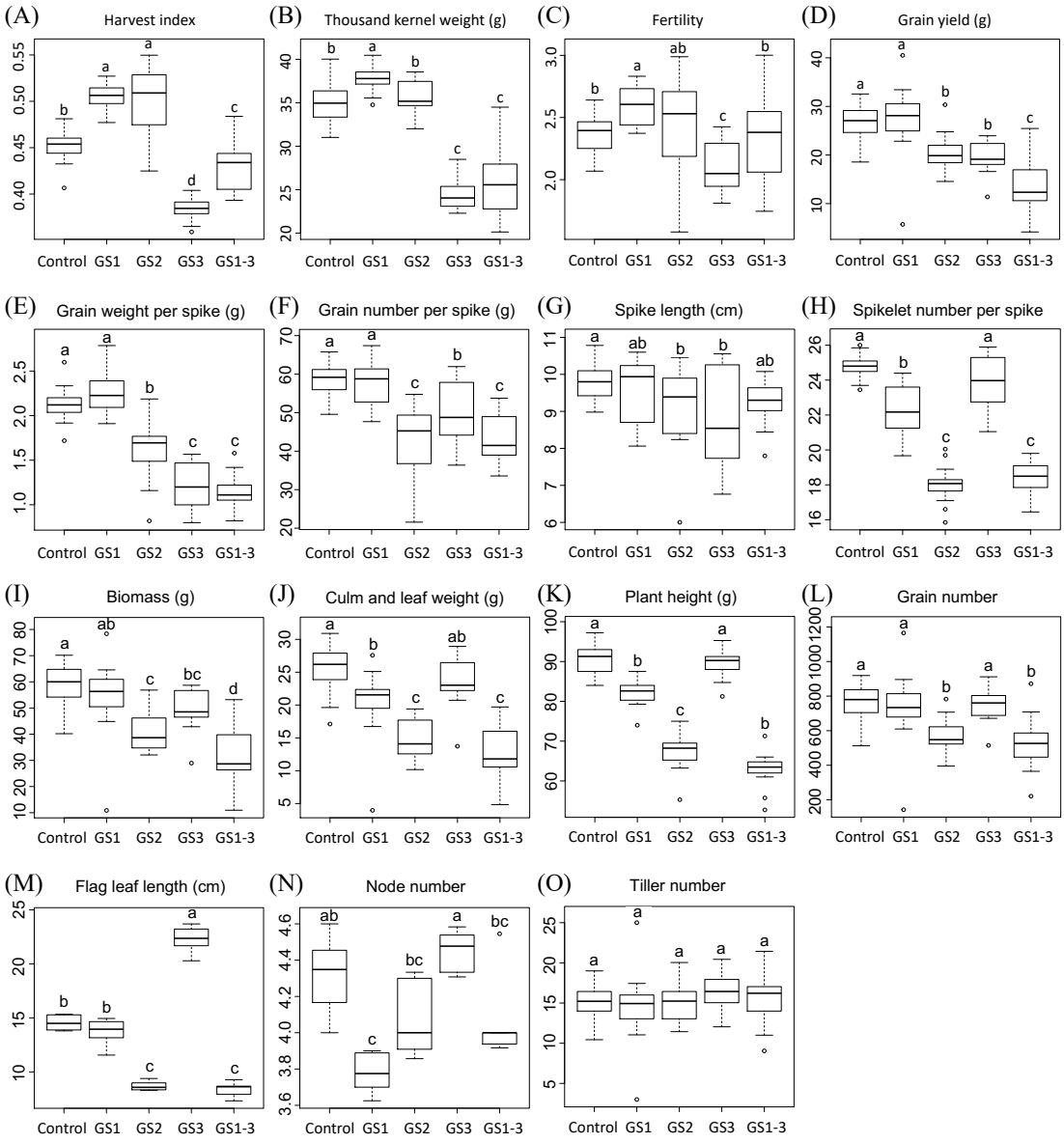

Figure 5. Differences in agronomic traits of heat-treated plants from the control. (A) harvest index, (B) thousand kernel weight (g), (C) fertility, (D) grain yield (g), I grain weight per spike (g), (F) grain number per spike, (G) spike length (cm), (H) spikelet number per spike, (I) biomass (g), (J) culm and leaf weight (g), (K) Plant height (cm), (L) grain number, (M) flag leaf length (cm), (N) node number, and (O) tiller number. The box plots are based on corrected data from two seasons. Bars with the same letter are not significantly different by Tukey's range test ($p < 0.05$). n = 12.

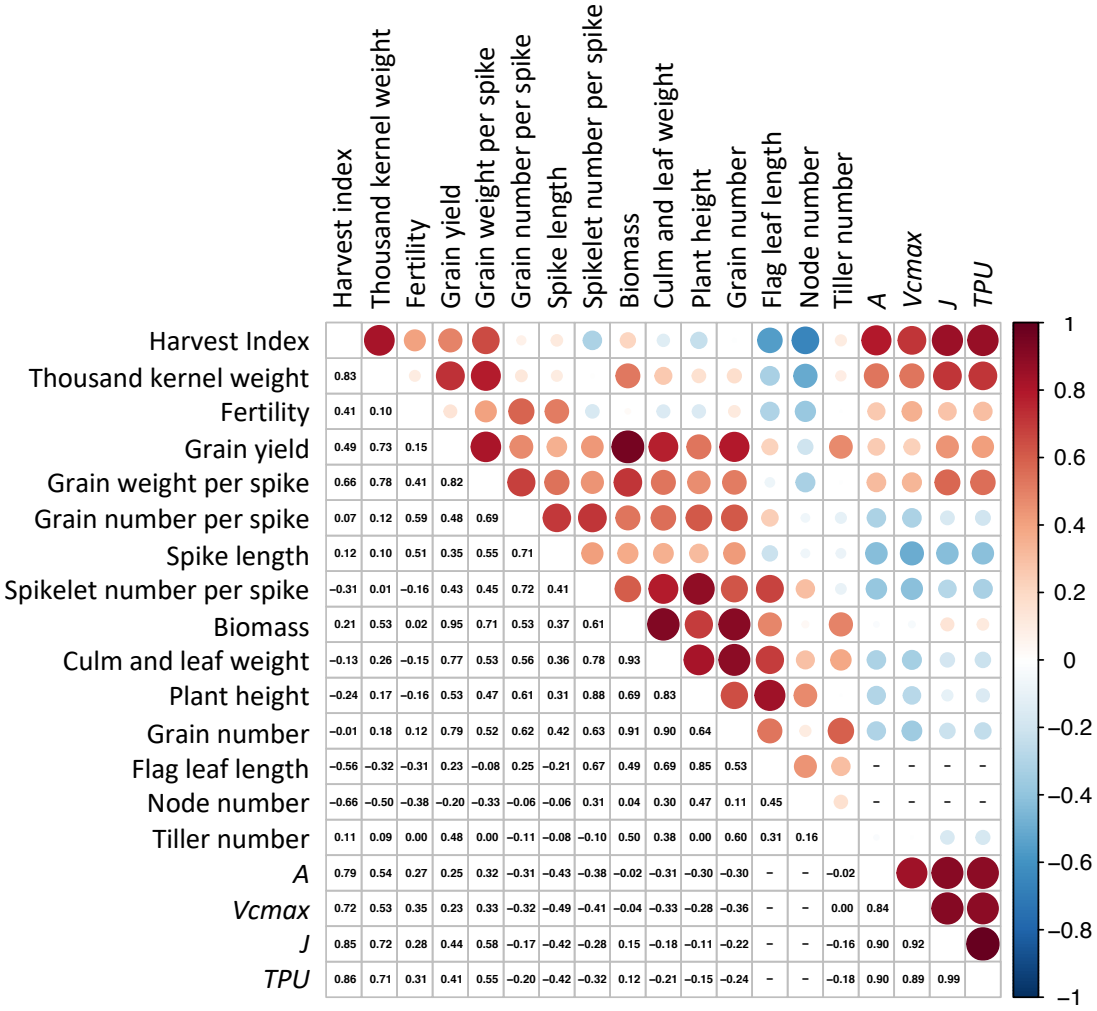

Figure 6. Heat map of the correlation matrix of agronomic traits and physiological traits related to photosynthetic rate. Correlation coefficients were calculated without separating growing conditions. The strength of the correlation is indicated by the color, size, and intensity of each circle: red = positive, blue = negative; larger and darker = higher, smaller and lighter = lower. *A*, photosynthetic CO_2 assimilation; *Vcmax*, the maximum carboxylation rate of rubisco; *J*, the rate of photosynthetic electron transport; *TPU*, the triose phosphate utilization. Bar (-) indicates that the corresponding data do not exist.

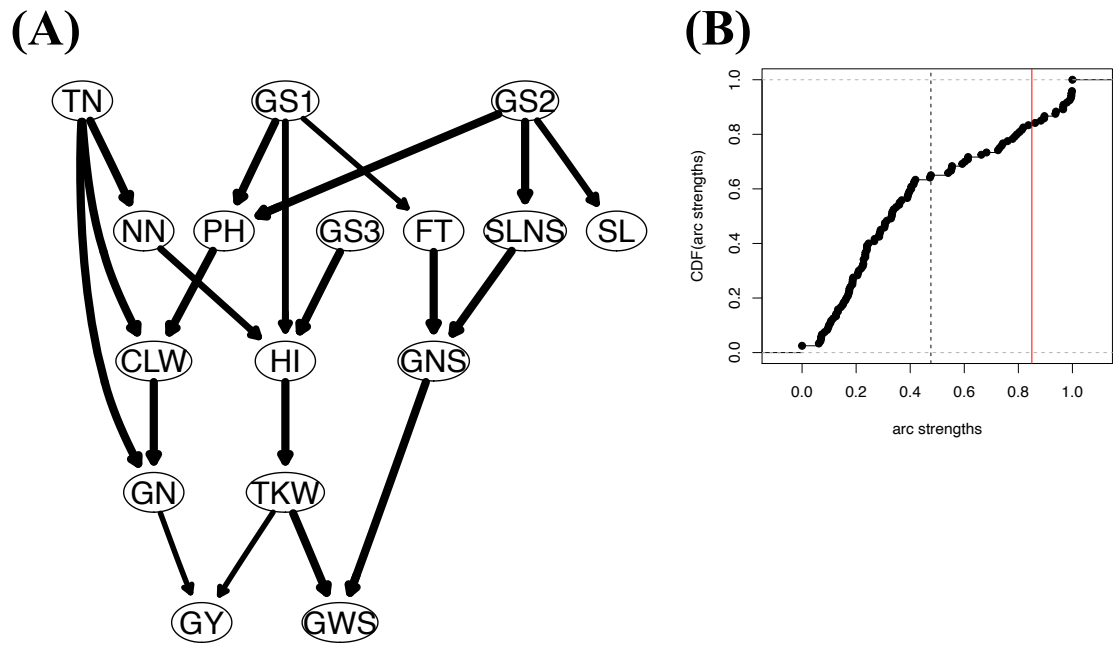

Figure 7. Bayesian network of agronomic traits (A) and edge strengths of the network (B). (A) Widths of arrows indicate strengths of each edge. (B) X-axis and Y-axis indicate edge strengths and CDF (cumulative distribution function) of edges, respectively. A solid line indicates a manual threshold (=0.85) for selecting edges to be drawn in (A). In (A), CLW, culm and leaf weight; FT, fertility; GN, grain number; GNS, grain number per spike; GWS, grain weight per spike; GY, grain yield; HI, harvest index; NN, node number; PH, plant height; SL, spike length; SLNS, spikelet number per spike; TKW, thousand kernel weight; TN, tiller number.

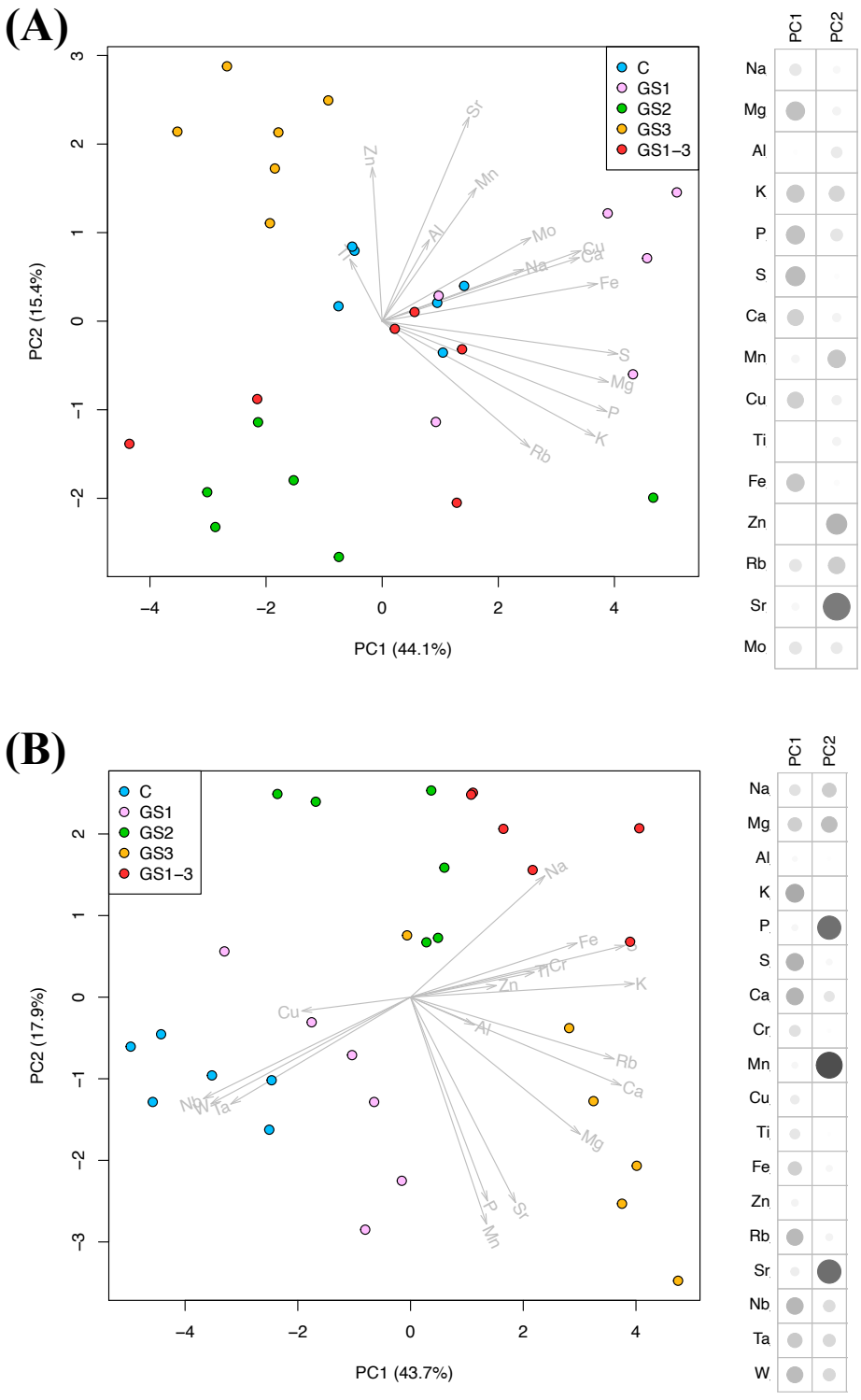

Figure 8. (A, B) Principal component analysis (PCA) of mineral contents in single grain (A) and culm and leaf (B), and trait contribution to PC1 and PC2 of minerals.

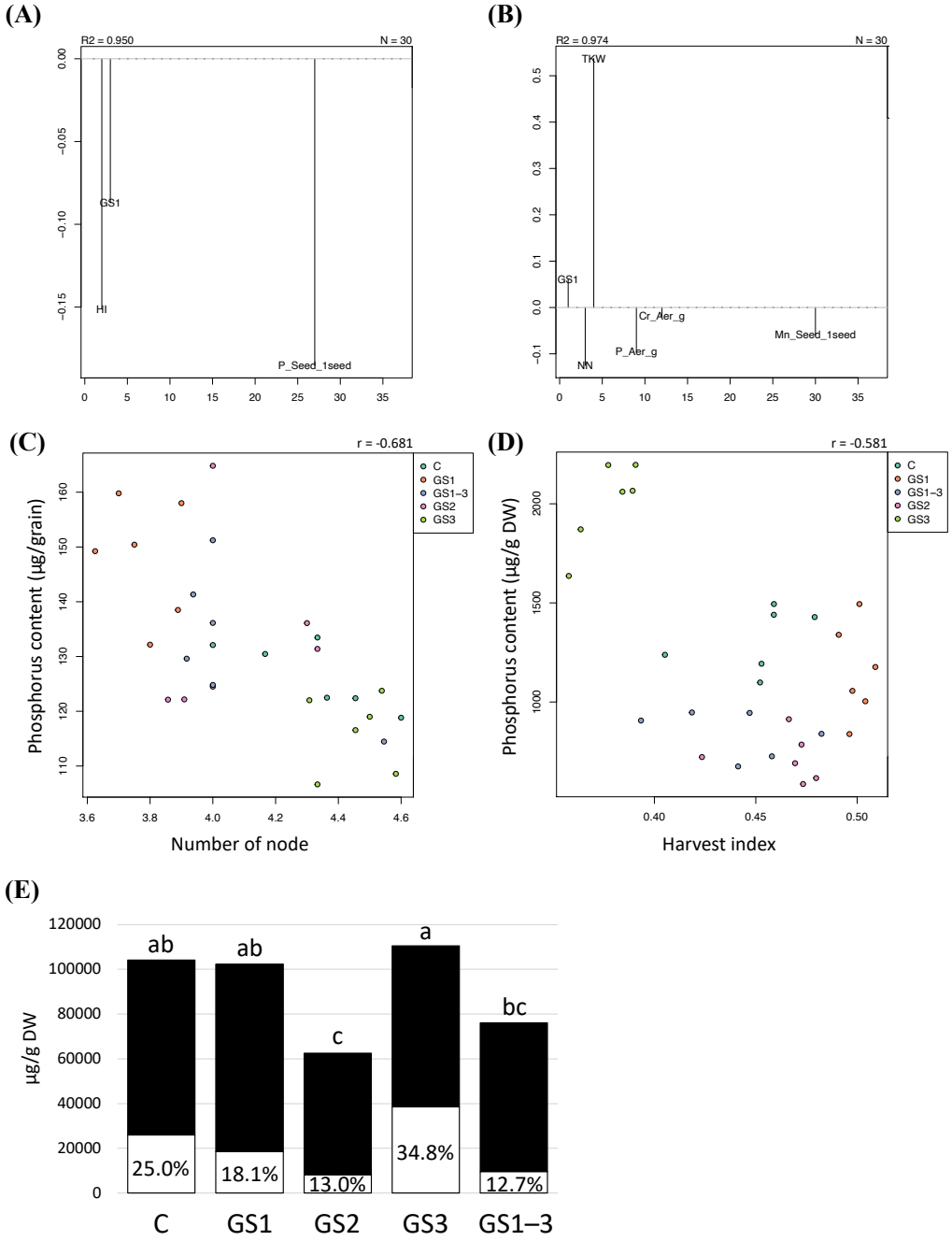

Figure 9. (A, B) barplot of the regression coefficient for number of node (A) and harvest index (B). Y-axis indicates regression coefficients for each trait. Correlation coefficients are shown in the upper left corner. (C, D) Correlation between node number and phosphorus in single grain (C), and harvest index and phosphorus in straw (g) (D). Each point represents 6 replications from each condition, and the color indicates each condition. Correlation coefficients are shown in the upper right corner. (E) The cumulative barplot of phosphorus accumulation in grain (black bar) and culm and leaf (white bar).

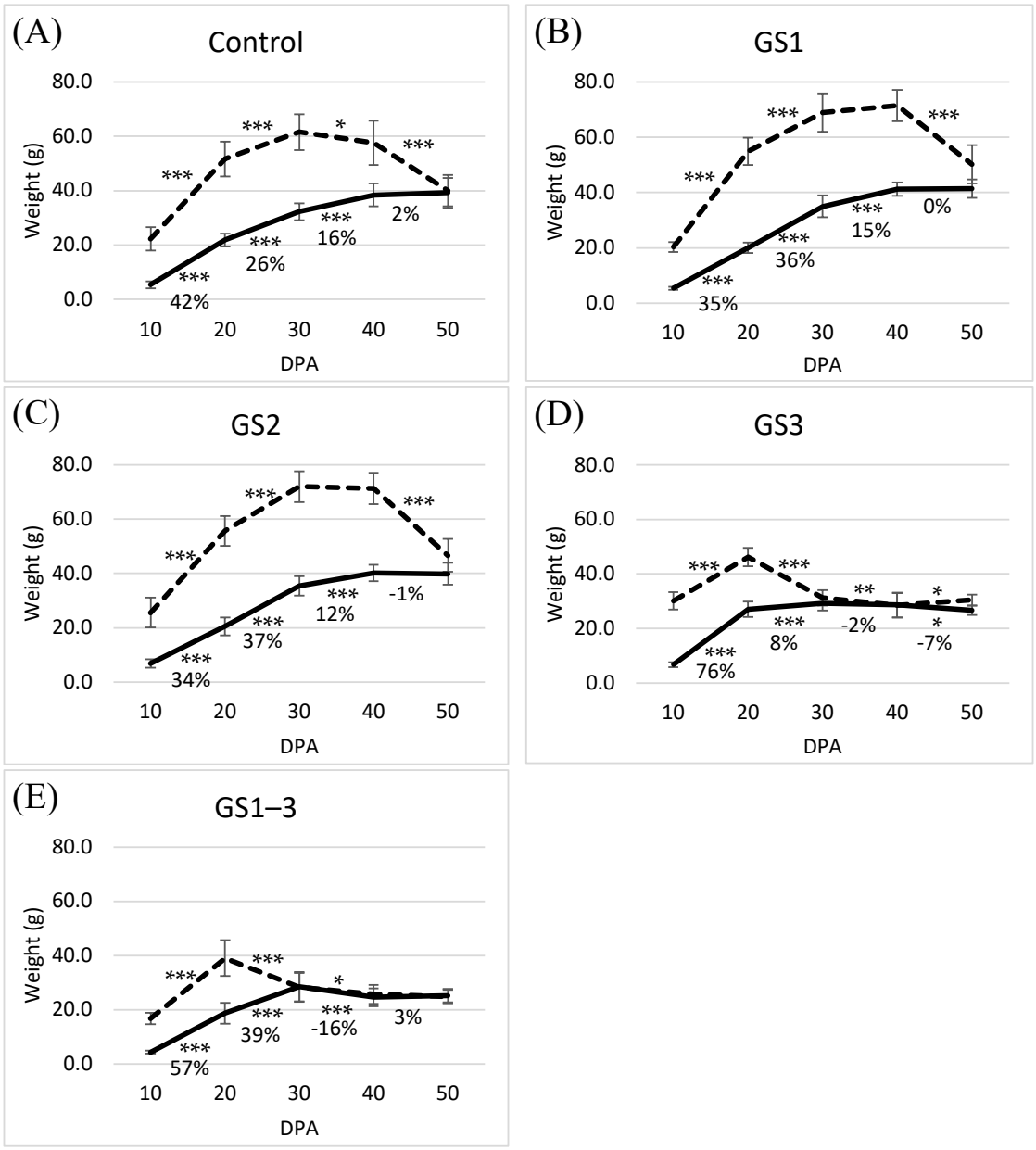

Figure 10. Time-series transition of seed maturity every 10 days from flowering date based on fresh weight (broken line) and dry weight (solid line). * Significant differences between pairs of values (* $p = 0.05$; ** $p = 0.01$; *** $p = 0.001$). Bonferroni's correction was applied to control p-values in multiple comparisons. The percentages indicate the proportion of dry weight at each point calculated with an average dry weight at 50 days post-anthesis of 100%. (A) Control and (B–E) samples treated at high temperature during (B) GS1, (C) GS2, (D) GS3, and (E) all growth stages (GS1–3). n = 3.

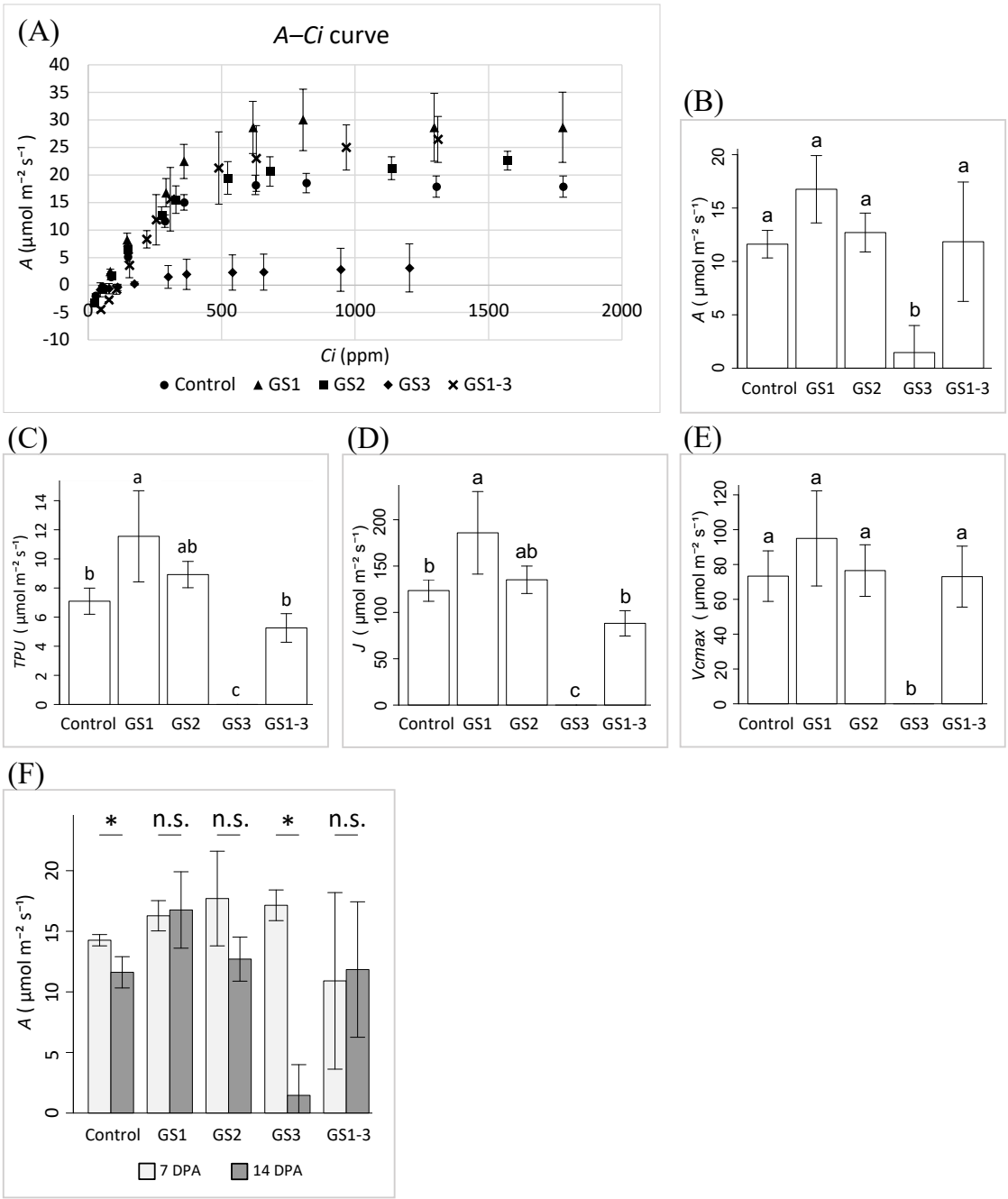

Figure 11. Photosynthetic rate measured at 14 days post-anthesis (DPA). (A) A–Ci curve; (B) carbon assimilation rate, (C) *TPU*, (D) *J*, and (E) *Vcmax* at 400 ppm CO_2; (F) A at 400 ppm CO_2 at 7 and 14 days post-anthesis (* $p = 0.01$). n = 3. Bars with the same letters in B–F are not significantly different by Tukey's range test ($p < 0.05$).

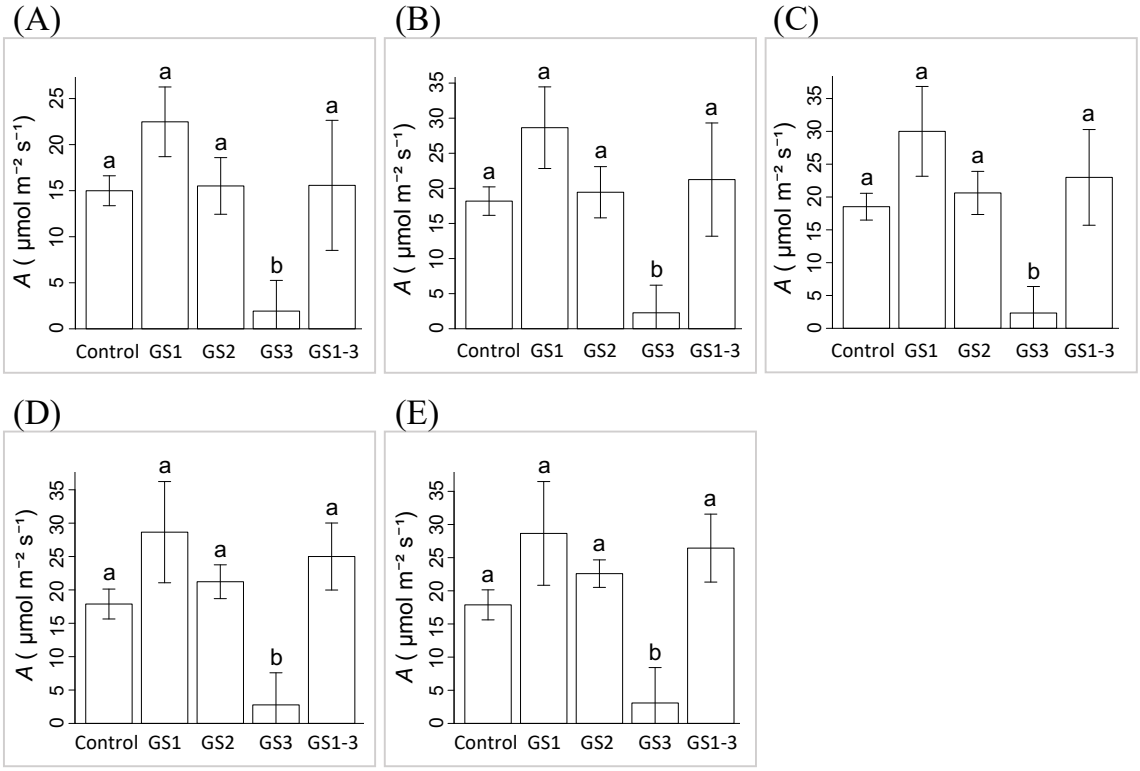

Figure 12. Carbon assimilation rate at CO_2 concentrations of (A) 500 ppm, (B) 800 ppm, (C) 1000 ppm, (D) 1500 ppm, and (E) 2000 ppm. Letters on the bars with the same alphabet indicate no significant difference by Tukey's range test ($p < 0.05$).

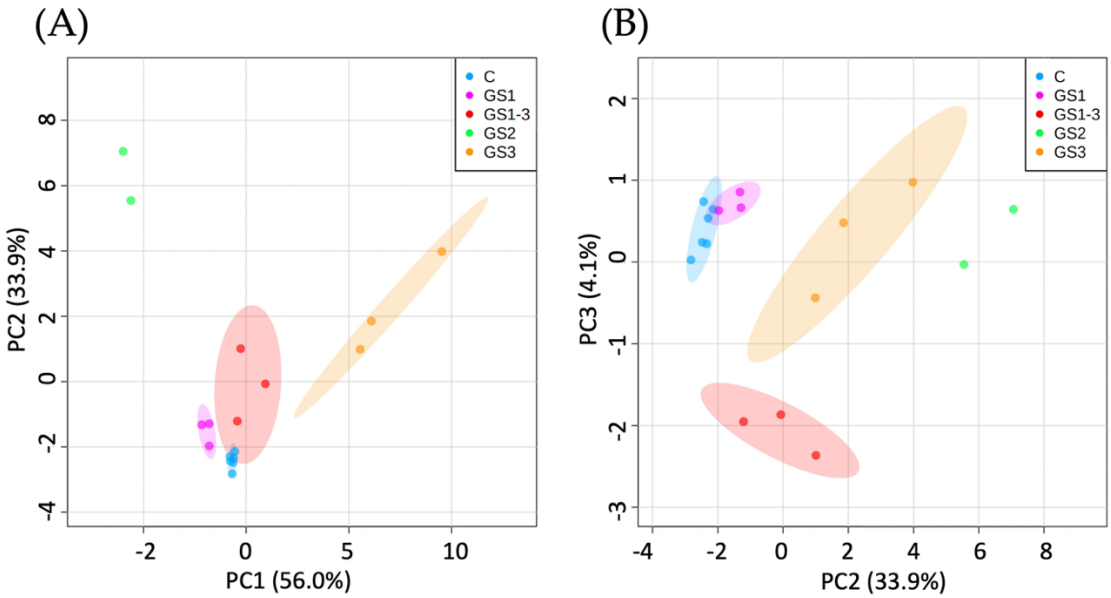

Figure 13. Results of the principal component analysis for the different temperature treatments for (A) principal components PC1 and PC2 and (B) principal components PC2 and PC3. GS represents the growth stages when the high-temperature treatment was applied (C = control, with normal temperatures; GS1 = heating from germination to tillering; GS2 = heating from tillering to flowering; GS3 = heating from flowering to full maturity; GS1–3 = all stages). Stable 69 metabolites were used to perform PCA. The 95% confidence intervals are highlighted by the respective background color. GS2 could not be highlighted because the sample size is less than three replications.

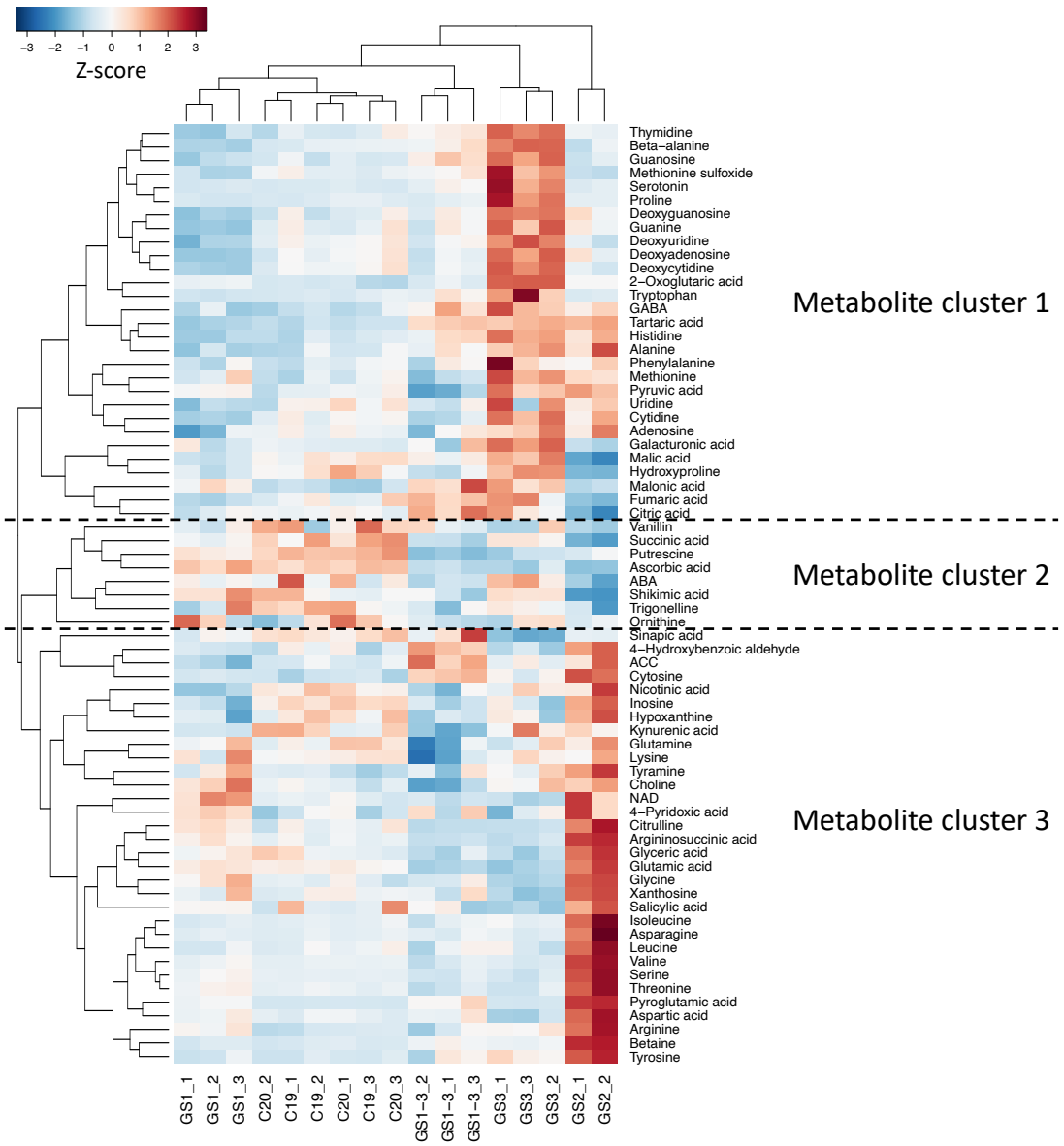

Figure 14. Hierarchical clustering and heat map for the results of high-temperature treatment during different growth stages: C = control, with normal temperatures; GS1 = heating from germination to tillering; GS2 = heating from tillering to flowering; GS3 = heating from flowering to full maturity; and GS1–3 = heating during all growth stages. Colors show increases (red) or decreases (blue) in metabolite levels in *z*-score. Abbreviations: ABA, abscisic acid; ACC, 1-aminocyclopropane-1-carboxylic acid; GABA, gamma-aminobutyric acid; NAD, nicotinamide adenine dinucleotide.

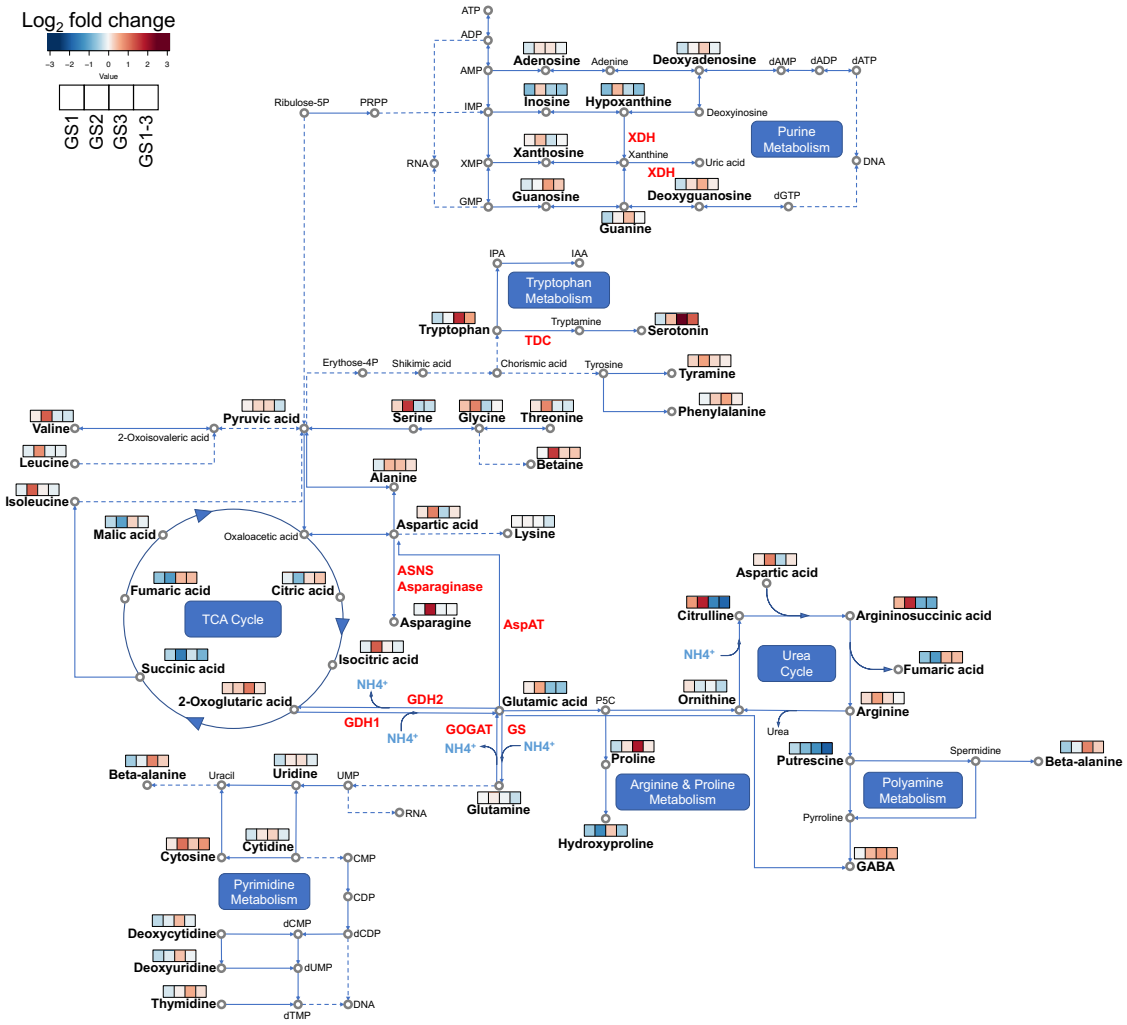

Figure 15. Changes in the metabolite contents of the flag leaves at 7 days post-anthesis under each condition: C = control, with normal temperatures; GS1 = heating from germination to tillering; GS2 = heating from tillering to flowering; GS3 = heating from flowering to full maturity; and GS1–3 = heating during all growth stages. The proposed metabolic pathways are based on the KEGG database (https://www.genome.jp/kegg/). The bars with four cells represent heat treatment during the four growth stages (GS1 to GS1–3, respectively); colors in the cells represent $\log_2$ of the change relative to the control. Abbreviations: XDH, xanthine dehydrogenase/oxidase; TDC, tryptophan decarboxylase; ASNS, asparagine synthetase; AspAT, aspartate aminotransferase; GDH, glutamic acid dehydrogenase; GOGAT, glutamine oxoglutarate aminotransferase; GS, glutamine synthase; GABA, gamma-aminobutyric acid.

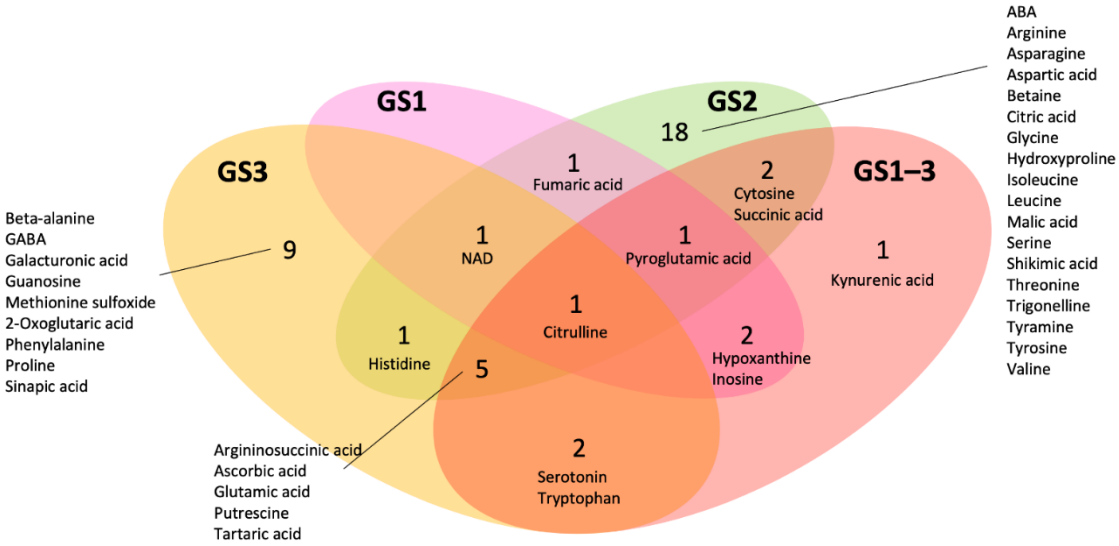

Figure 16. Venn diagram using the metabolites that significantly decreased to less than 0.67 times the control value or significantly increased to more than 1.5 times the control value in the heat-stressed plants ($p < 0.05$). Growth stages: GS1 = heating from germination to tillering; GS2 = heating from tillering to flowering; GS3 = heating from flowering to full maturity; and GS1–3 = heating during all growth stages. Values represent the number of metabolites. Abbreviations: ABA, abscisic acid; GABA, gamma-aminobutyric acid

.

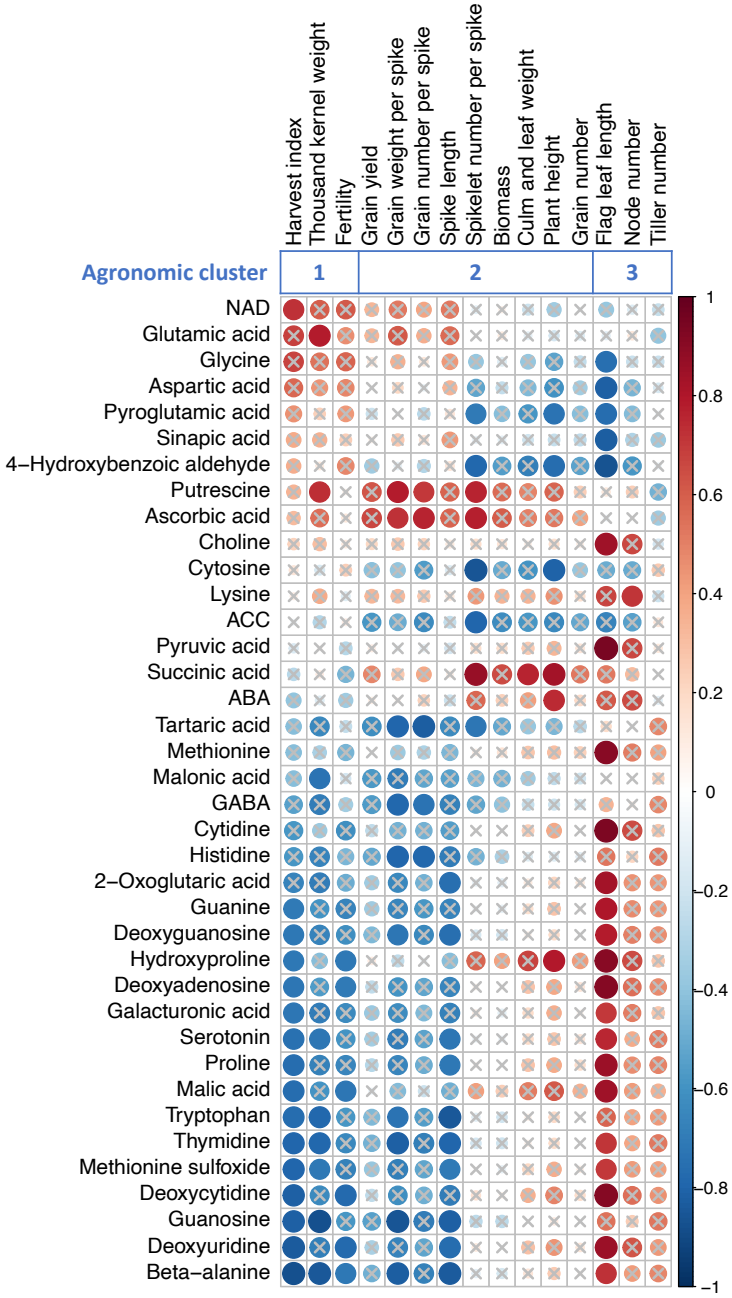

Figure 17. Heatmap of a correlation matrix of agronomic traits and metabolites. Pearson correlation coefficients were calculated using data of all growing conditions. The metabolites that have correlation coefficients greater than 0.7 with at least one agronomic trait are shown. Color and size of circles indicate the value of coefficients (red for positive and blue for negative). Crosses are drawn above circles where absolute values of coefficients are smaller than 0.7 and significant after the Benjamini-Hochberg correction. Abbreviations: NAD, nicotinamide adenine dinucleotide; ACC, 1-aminocyclopropane-1-carboxylic acid; ABA, abscisic acid; GABA, gamma-aminobutyric acid.

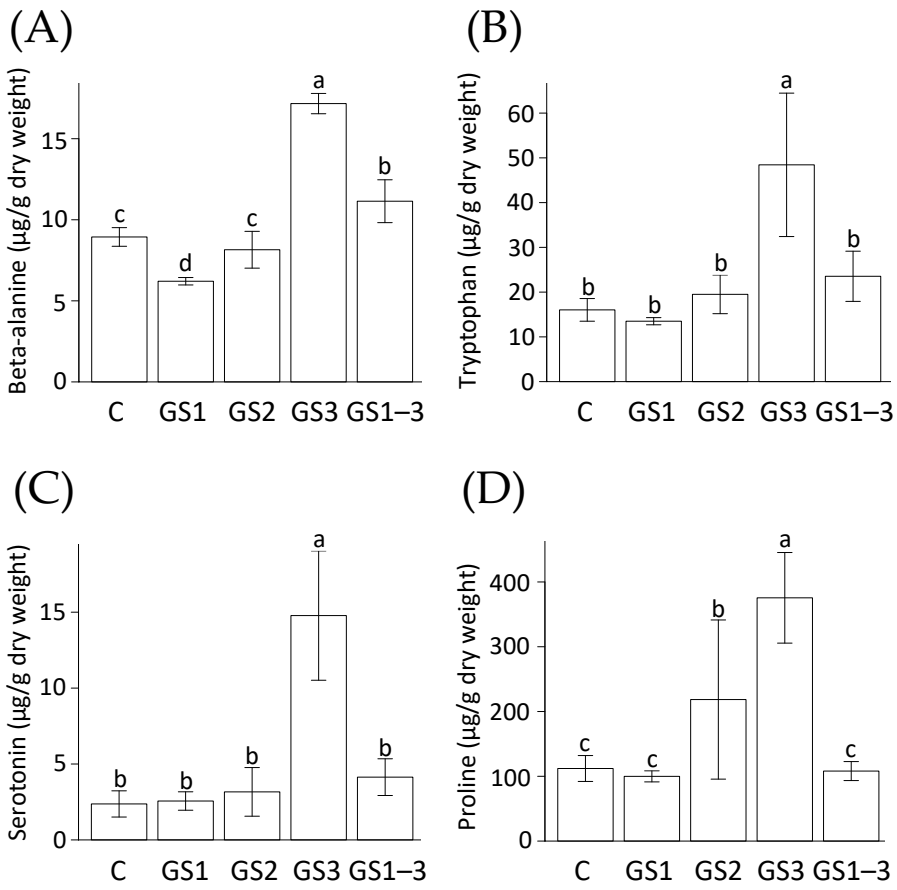

Figure 18. Contents of (A) beta-alanine, (B) tryptophan, (C) serotonin, and (D) proline. Values are means ± SD (n ≥ 2). Growth stages: C = control, with normal temperatures; GS1 = heating from germination to tillering; GS2 = heating from tillering to flowering; GS3 = heating from flowering to full maturity, and GS1–3 = heating during all growth stages. Values of a given metabolite labeled with the same letter did not differ significantly (Tukey's range test, $p < 0.05$).

(A)

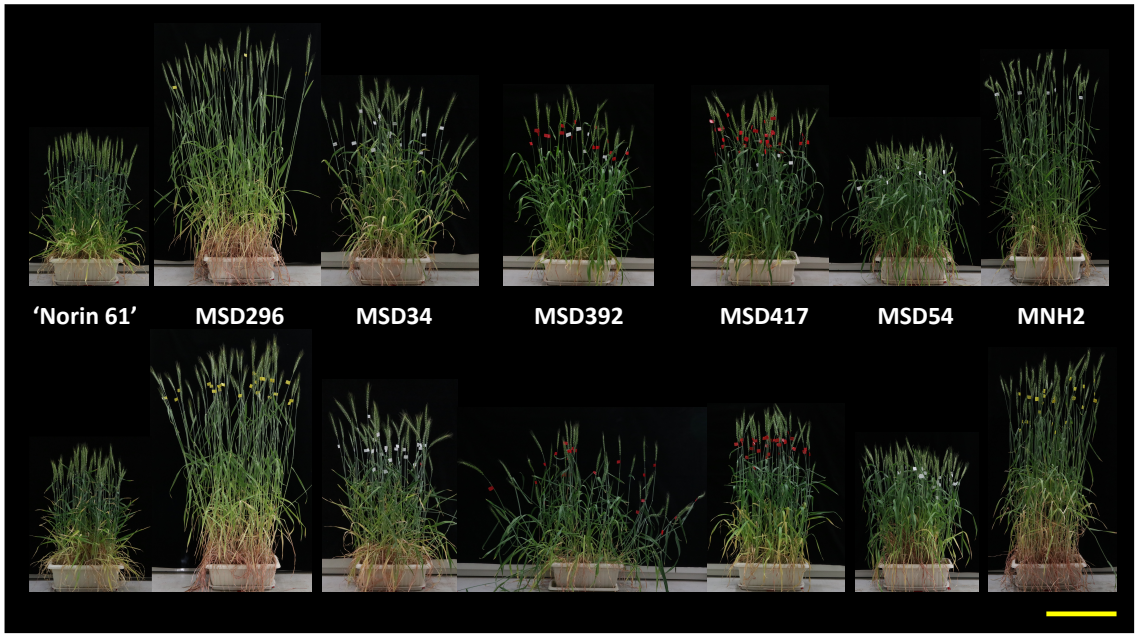

(B)

Figure 19. Effect of high temperature during the reproductive stage on plant and seed morphology. (A, B) Each plant at (A) 7 days post-anthesis. (B) Harvested seeds. Top: Plants/seeds from control condition; bottom: plants/seeds from heat condition. Bars: plants, 50 cm; seeds, 1 cm.

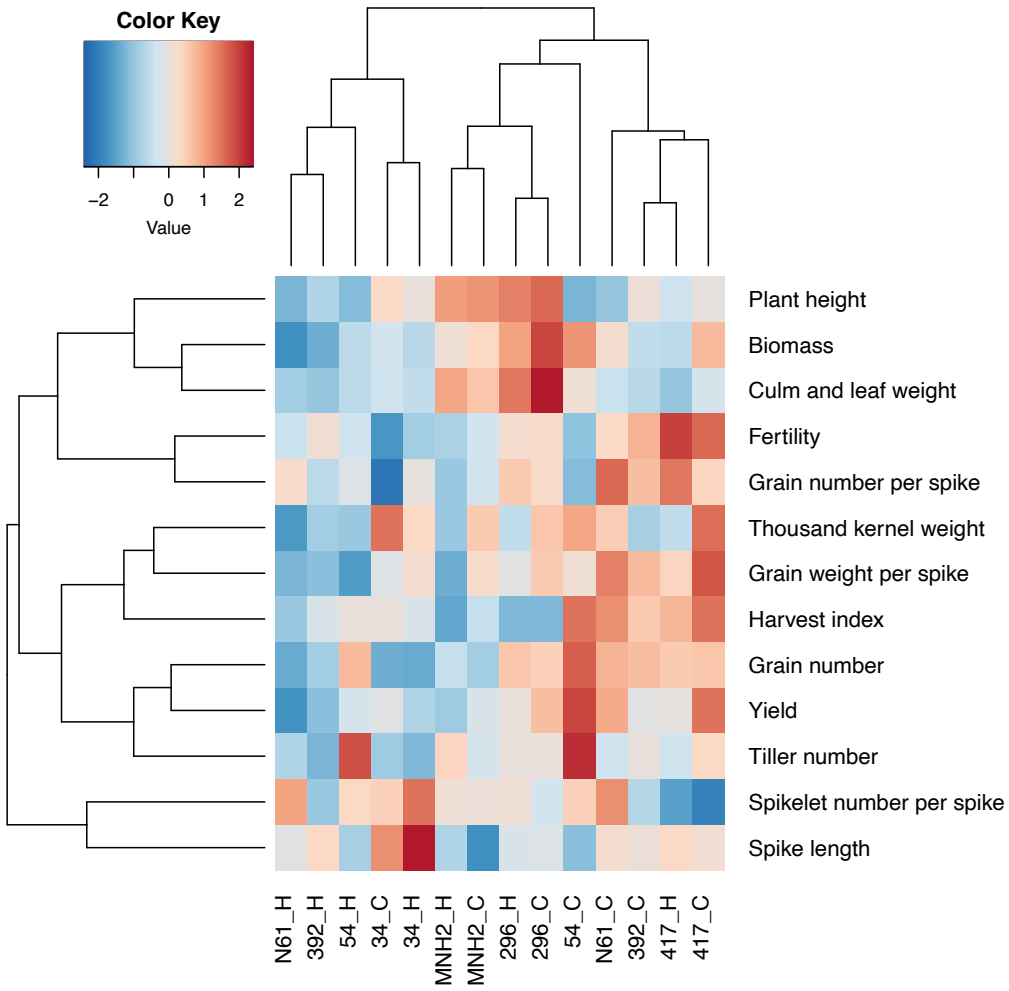

Figure 20. Hierarchical clustering and heat map of agronomic traits in MSD lines (C, Control; H, Heat). Colors in (A) show an increase (red) or decrease (blue) compared with the control.

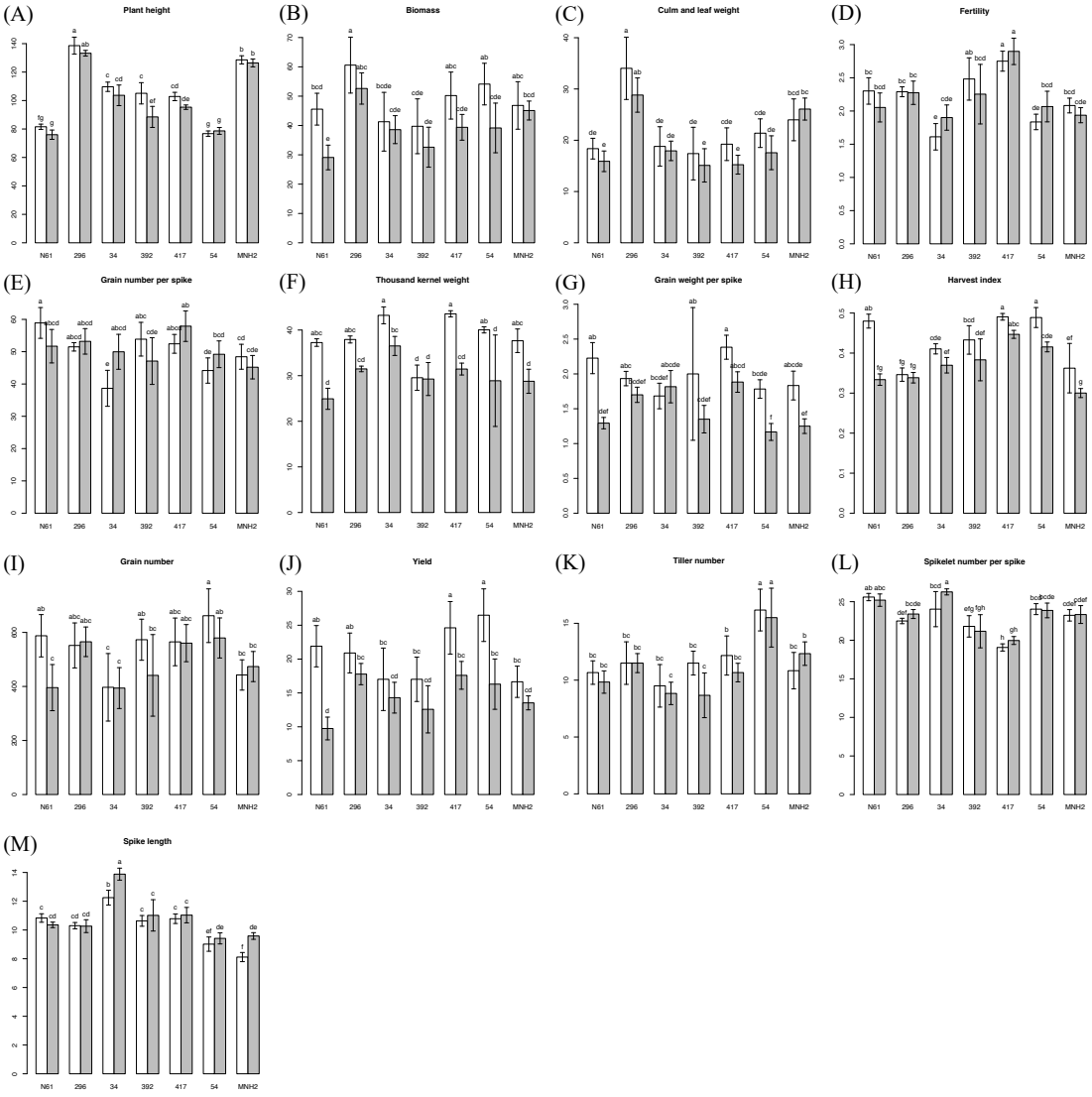

Figure 21. Differences in agronomic traits of heat-treated plants (gray) and the control (white). (A) plant height, (B) biomass, (C) culm and leaf weight, (D) fertility, (E) grain number per spike, (F) thousand kernel weight, (G) grain weight per spike, (H) harvest index, (I) grain number, (J) grain yield, (K) tiller number, (L) spikelet number per spike, (M) spike length. Bars with the same letter are not significantly different by Tukey's range test ($p < 0.05$). n = 6. White, control samples; gray, heat-treated samples.

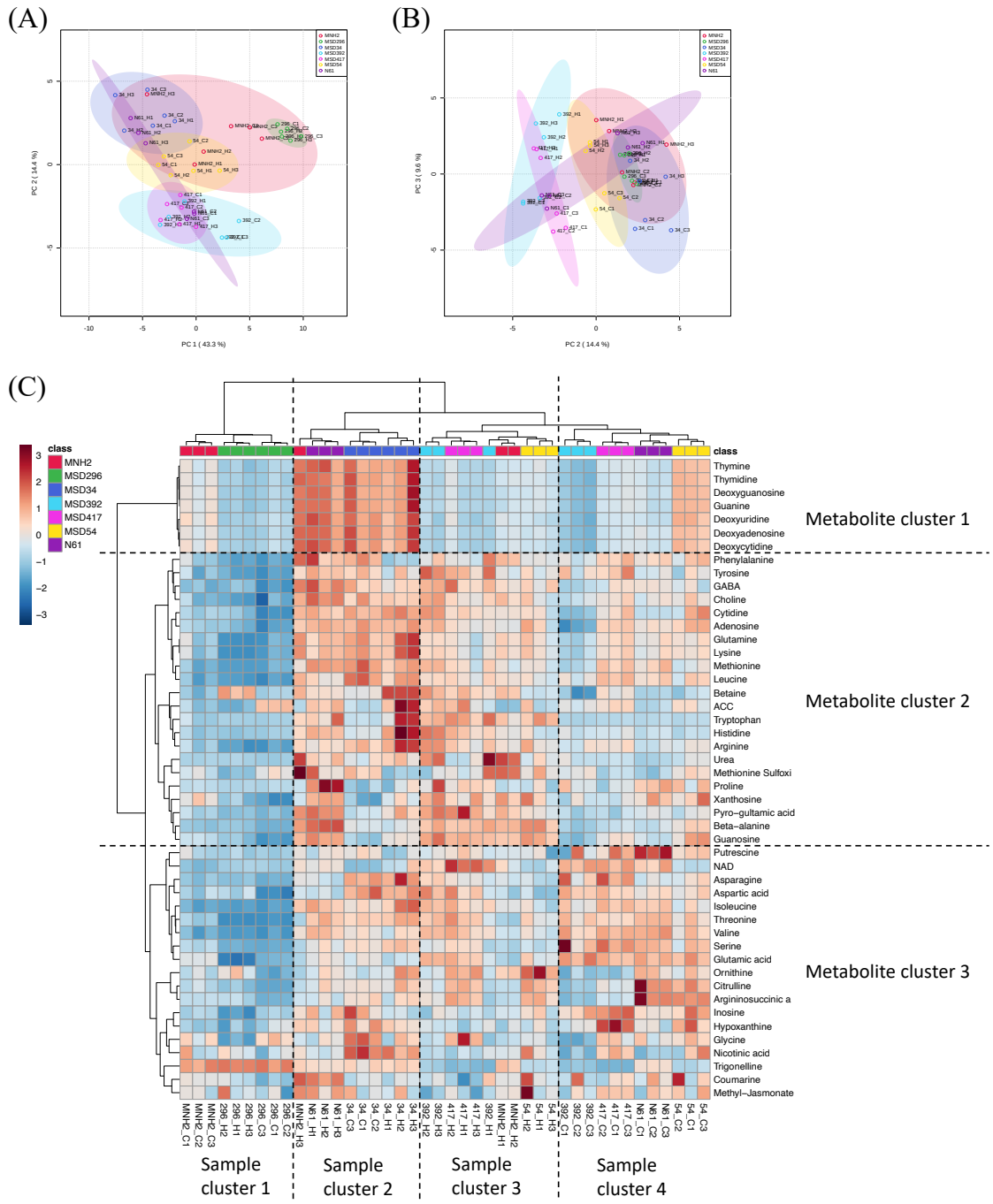

Figure 22. Results of the principal component analysis for the different temperature treatments for (A) principal components PC1 and PC2 and (B) principal components PC2 and PC3. Stable 48 metabolites were used to perform PCA. The 95% confidence intervals are highlighted by the respective background color. (C) Hierarchical clustering and heat map for the results of the sample treated heat (_H) and control (_C).

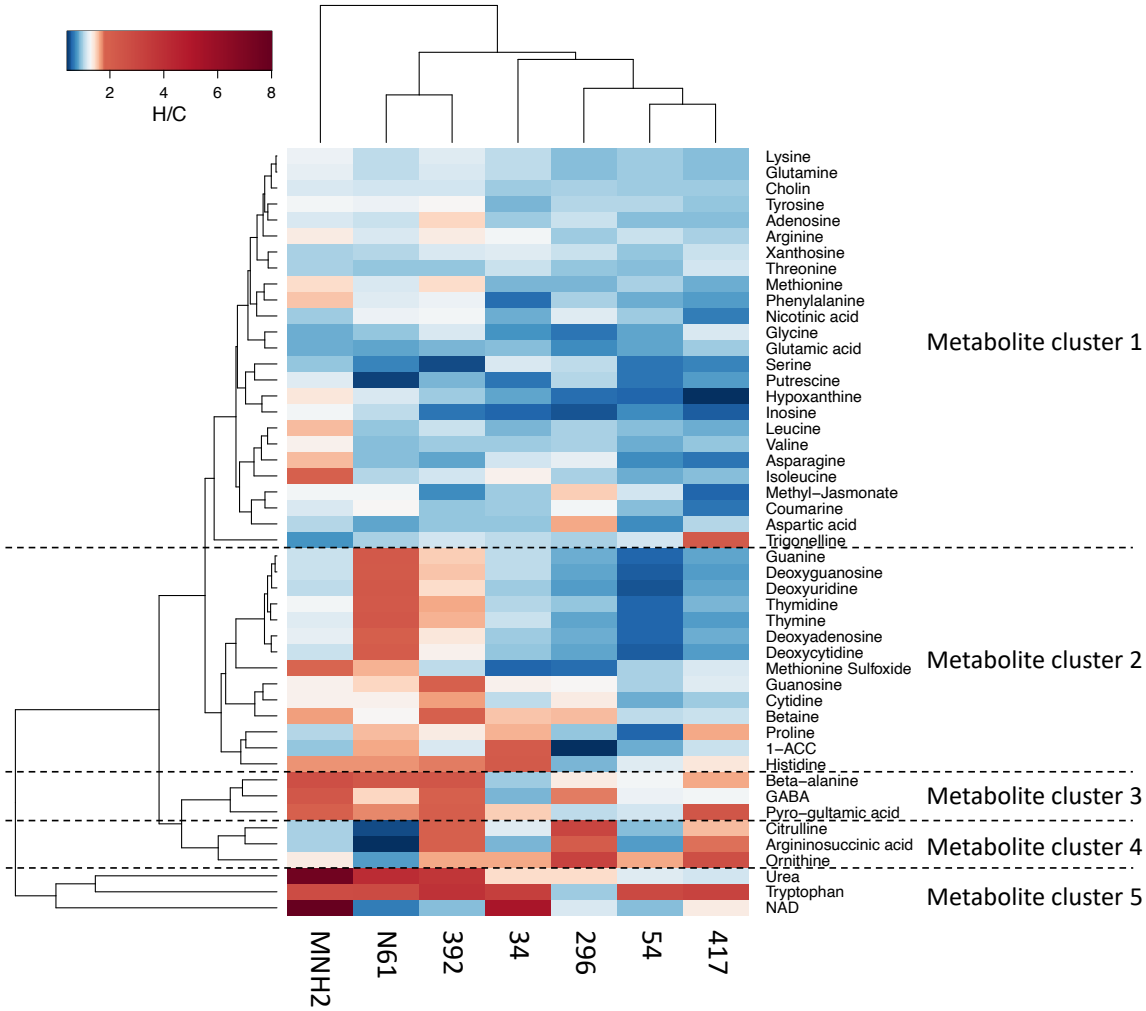

Figure 23. Hierarchical clustering and heat map for the results of the heat-treated plant samples compared with the control. Colors show an increase (red) or decrease (blue) compared with the control condition.

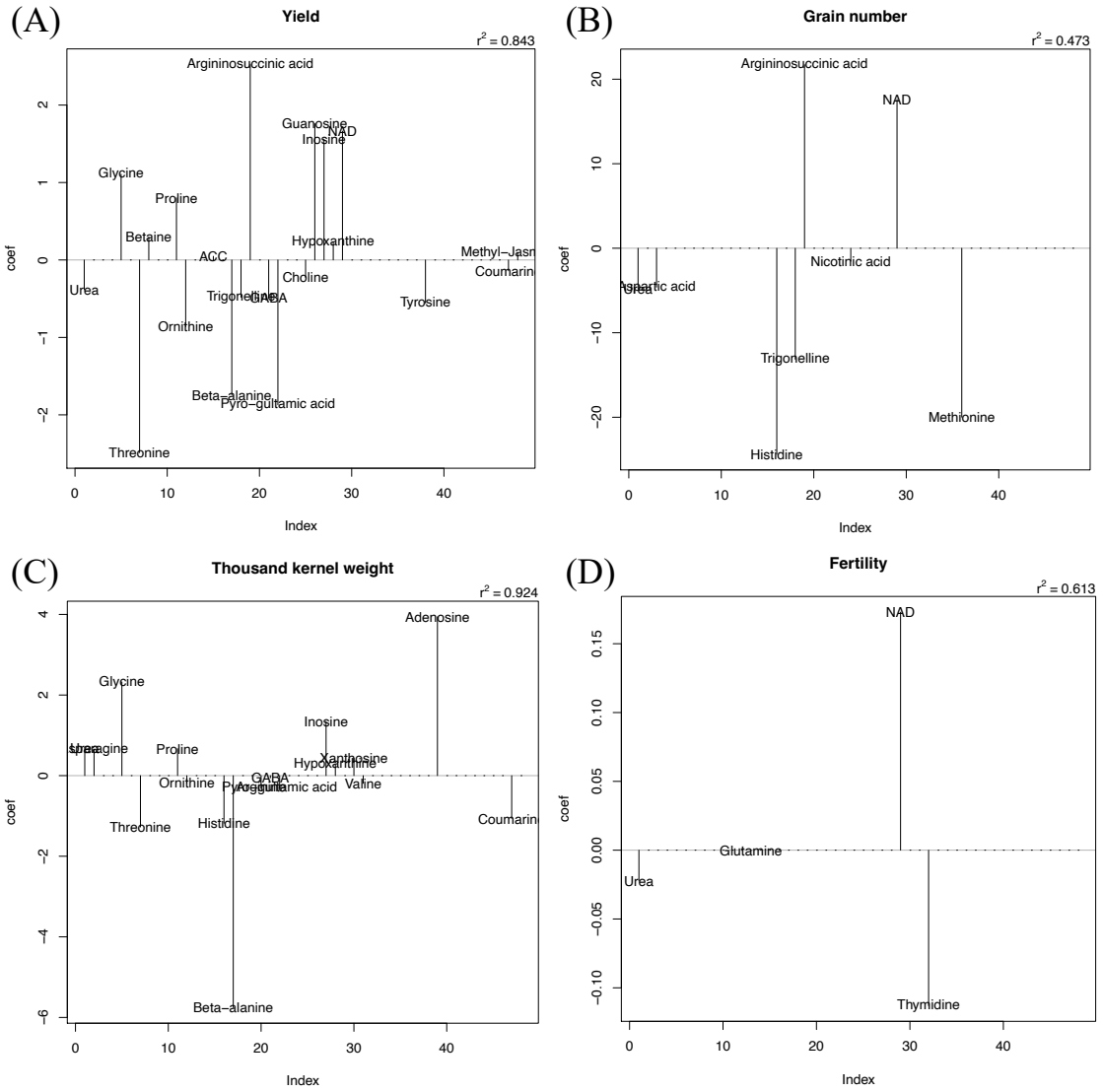

Figure 24. Barplot of regression coefficient with the objective variable as (A) grain yield, (B) grain number, (C) thousand kernel weight, (D) fertility. Y-axis indicates regression coefficients for each trait. Correlation coefficients are shown in the upper left corner.

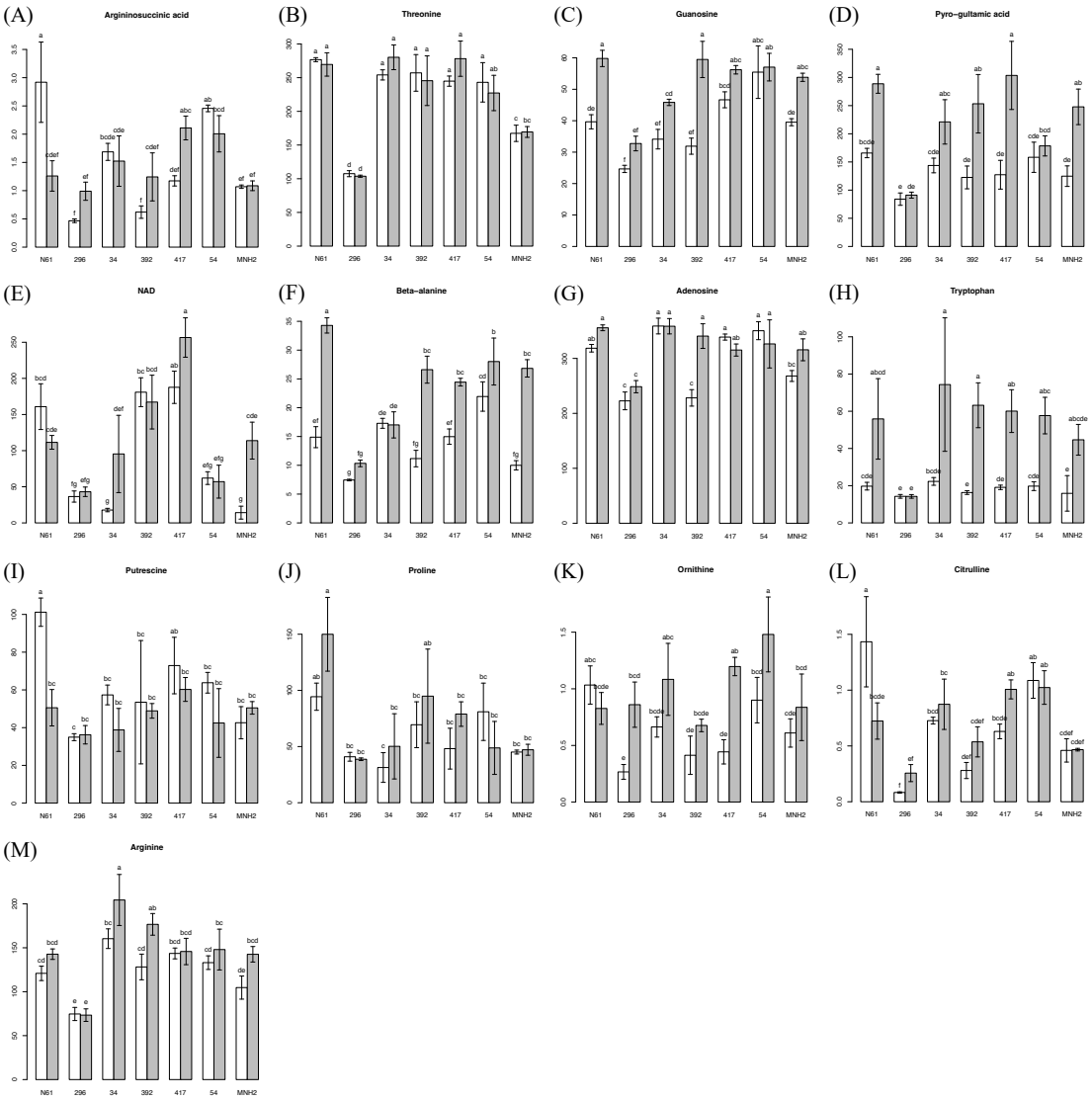

Figure 25. Contents of (A) argininosuccinic acid, (B) threonine, (C) guanosine, (D) pyro-glutamic acid, (E) NAD, (F) beta-alanine, (G) adenosine, (H) tryptophan, (I) putrescine, (J) proline, (K) ornithine, (L) citrulline, and (M) arginine. Values are means ± SD (n = 6). Values of a given metabolite labeled with the same letter did not differ significantly (Tukey's range test, $p < 0.05$). White, control samples; gray, heat-treated samples.

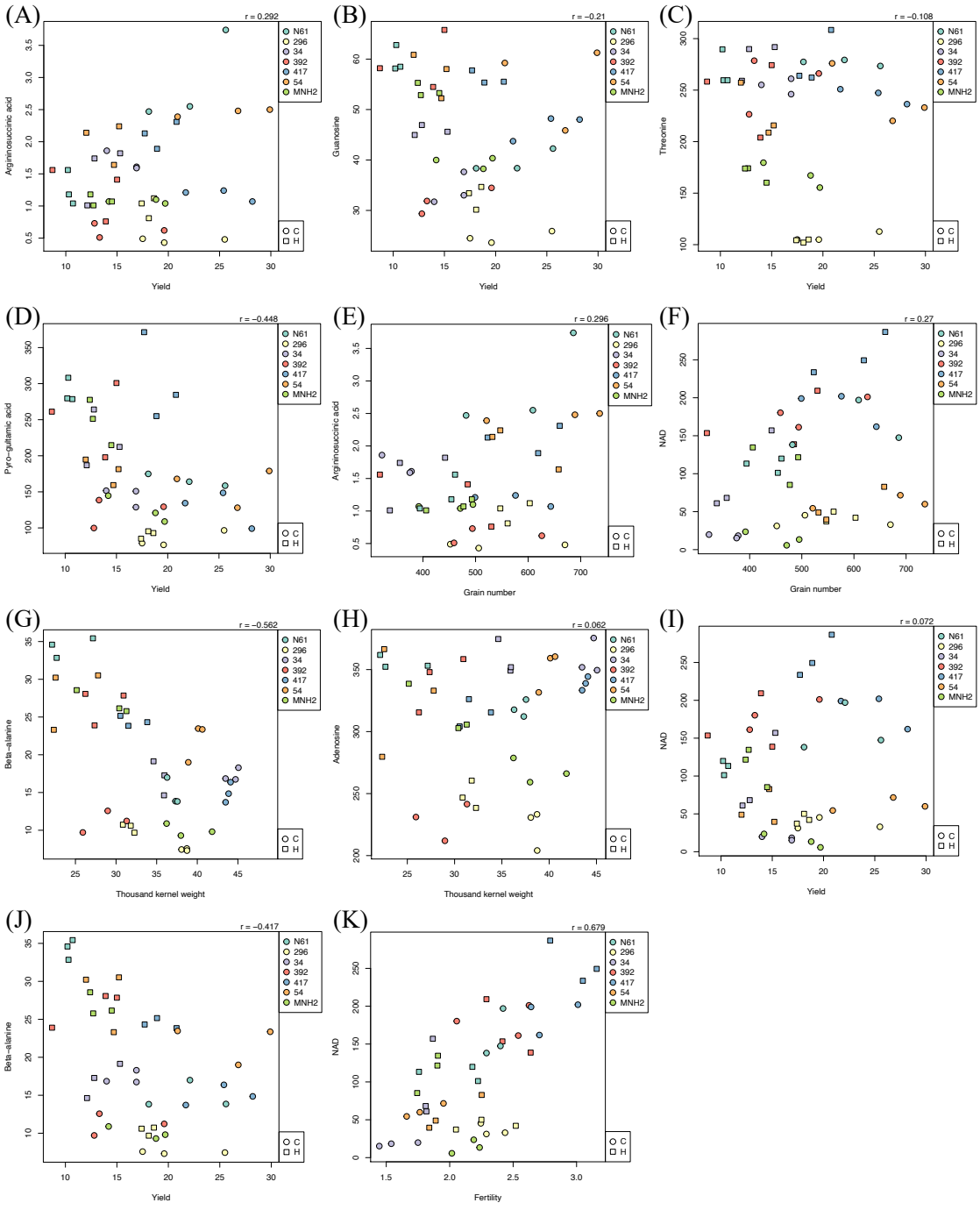

Figure 26. Correlation between (A) argininosuccinic acid and grain yield, (B) guanosine and grain yield, (C) threonine and grain yield, (D) pyro-glutamic acid and grain yield, (E) argininosuccinic acid and grain number, (F) NAD and grain number, (G) beta-alanine and thousand kernel weight, (H) adenosine and thousand kernel weight, (I) NAD and yield, (J) beta-alanine and yield, and (K) NAD and fertility.

Summary

Bread wheat (*Triticum aestivum*) is less adapted to high temperatures than other major cereals, and it is desirable to develop varieties that can produce stable yields even under high-temperature environments. To produce high-temperature tolerant lines, three major factors are required: 1) understanding of high-temperature tolerance throughout the life cycle, 2) diverse genetic resources, and 3) markers to find tolerant lines from these diverse genetic resources. This study aimed at determining these three factors. Previous studies on the effects of high temperature on wheat have focused on the reproductive stage, and there are few reports on yield following high temperature stress in other growth stages. Understanding growth stage-specific responses to high temperature stress would contribute to the development of tolerant varieties suitable for high temperatures at different stages. In addition, the genetic diversity of bread wheat varieties widely used today is limited, and it is believed that many genes have not yet been exploited. To expand the genetic diversity of bread wheat, attention has recently been focused on the genetic diversity of *Aegilops tauschii*, the D genome donor of hexaplod bread wheat, that is known to habor genes for resilience to abiotic stresses. However, methods for verifying how these genetic resources contribute to high-temperature environments and for evaluating resistance have not been established.

Therefore, in this study, I (1) evaluated the growth stage-specific high-temperature response of a representative wheat variety, 'Norin 61', and (2) evaluated the high-temperature tolerance of a candidate high-temperature tolerant line by introducing a gene from a wild species of wheat (*Ae. tauschii*).

The wheat variety 'Norin 61' was exposed to high temperature at three growth

stages: seedling–tillering (GS1), tillering–flowering (GS2), and flowering–maturity (GS3). For each condition, the effect of heat stress on agronomic traits, seed maturity and photosynthesis were compared. The results showed that high temperature treatment at GS2 reduced plant height and number of grains, while the high temperature treatment at GS3 reduced seed formation period and grain weight. However, high temperature treatment at GS1 suppressed senescence, prolonged seed formation period, and induced a "high temperature priming effect" that increased grain weight without reducing yield. In addition, plants exposed to high temperature continuously from the seedling stage to maturity induced "acclimatization," in which senescence was delayed compared to plants exposed to high temperature only after the flowering stage. To elucidate the metabolic mechanism behind the above phenomenon, metabolite analysis was conducted using flag leaves at 7 days after flowering. Beta-alanine, tryptophan, serotonin, proline and putrescine were identified as potential bio-markers for assessing senescence and acclimation, as they showed a strong correlation with agronomic traits such as thousand kernel weight. GS2 and GS3 plants showed the greatest changes in metabolite content under high-temperature stress compared to the control, followed by GS1–3 and GS1. GS3 plants accumulated nucleosides, beta-alanine and serotonin, which are related to the nucleotide salvage pathway. The accumulation of these compounds was significantly lower in GS1 than in the control, suggesting that the accumulation was related to the high-temperature priming effect (inhibition of senescence) observed in the phenotype. GS2 plants accumulated more free amino acids, indicating residual effects of the high temperature treatment and recovery from stress. However, the levels in GS1–3 plants tended to be close to the control, indicating an acclimation response. These data provide fundamental insights into the biochemical and molecular adaptation of bread wheat to

high-temperature stress and have important implications for the development of wheat lines that can respond to high temperatures at different times of the year.

Since the above findings indicate the usefulness of metabolomic analysis for evaluating heat response, I attempted to implement it in the evaluation of wheat lines containing *Ae. tauschii* introgressions. In this study, I used candidate lines for heat tolerance that were expected to maintain or improve yield performance even under high-temperature conditions during the ripening period in a field experiment conducted in Sudan, one of the world's high temperature growing areas for bread wheat. The candidate lines and their backcross parent (‘Norin 61’) were grown in an artificial climate chamber in Japan, and the heat tolerance of each line and its potential for breeding were evaluated by multiple regression analysis of metabolite content and agronomic traits at 7 days post-anthesis; and then evaluated the genotype-specific differences in agronomic traits from metabolic responses. Furthermore, MSD392 and MSD417 were identified as promising candidate lines for high grain yield under heat stress. These findings would provide a useful tool for the efficient breeding of wheat varieties with high yield potential and/or yield stability even in high-temperature environments.

Summary (Japanese)

パンコムギ（*Triticum aestivum*）は、他の主要穀物に比べて高温への適応性が低く、高温環境下でも安定した収穫量が期待される品種の開発が望まれている。高温耐性系統を作出するためには、大きく 3 つの要素が必要である。(1) ライフサイクル全体における高温耐性の理解、(2) 多様な遺伝資源、(3) その多様な遺伝資源から耐性系統を見つけるためのマーカー、である。本研究ではこの 3 つを決定することを目指している。コムギに対する高温の影響に関するこれまでの研究は、登熟期に焦点を当てており、他の生育段階における高温後の収量に関する報告はほとんどない。高温ストレスに対する生育ステージ固有の反応を理解することは、様々なステージでの高温に適した耐性品種の開発に貢献する。また、現在普及しているパンコムギ品種の遺伝的多様性は限られており、未だ利用されていない遺伝子は多く存在すると考えられている。その遺伝的多様性を拡大するために近年、タルホコムギの遺伝的多様性に着目されている。しかし、それら遺伝資源が高温環境にどのように寄与するかの検証や耐性評価の手法は確立されていない。

従って、本研究では①代表品種であるパンコムギ品種「農林 61 号」の生育ステージ特異的な高温応答性評価、②タルホコムギの野生種の遺伝子を導入した高温耐性候補系統の高温耐性評価を実施した。

パンコムギ品種「農林 61 号」を、幼苗期～分蘖期（GS1）、分蘖期～開花期（GS2）、開花期～成熟期（GS3）の 3 つの生育ステージで高温に曝し、それぞれの条件について、農学的形質、種子の成熟度、光合成の結果などを比較した。その結果、GS2 での高温処理は草丈と粒数を減少させ、GS3 での高温処理は種子形成期間と粒重を減少させた。しかし、GS1 での高温処理は老化を抑制し、種子

形成期間を延長させ、収量を減らすことなく粒重を増加させる「高温プライミング効果」を誘発した。また、幼苗期から成熟期まで連続して高温にさらされた植物は、開花期以降にのみ高温にさらされた植物に比べて老化が遅れる「順化」を引き起こした。上記の現象の背後にある植物体内の代謝機構を解明するため、開花 7 日目の止め葉を用いてメタボローム解析を行なった。代謝物質の蓄積傾向によってそのタイミングにおける植物の老化状態や高温への順応、また回復を推定することを可能にし、千粒重などの農学的形質と強い相関関係を示したベータアラニン、トリプトファン、セロトニン、プロリン、プトレシンを、老化や馴化を評価するのに適したバイオマーカーとして同定した。GS2 と GS3 の高温ストレスでは、対照と比較して代謝物の含有量の変化が最も大きく、次いで GS1–3 と GS1 であった。GS3 の植物は、ヌクレオチドサルベージ経路に関連するヌクレオシド、ベータアラニン、セロトニンを蓄積した。これらの化合物の蓄積量は, GS1 ではコントロールに比べて有意に少なく, 表現型に見られる高温プライミング効果（老化の抑制）に関連していることが示唆された。GS2 では遊離アミノ酸の蓄積量が多く、高温処理の影響が残っていることやストレスからの回復が見られた。しかし、GS1–3 の植物ではコントロールに近いレベルになる傾向があり、順応反応が見られた。これらのデータは、高温ストレスに対するパンコムギの生化学的および分子的な適応についての基本的な知見を提供するものであり、1 年のさまざまな時期に高温に対応できる小麦の系統を開発する上で重要な意味を持つ。

上記の知見から、メタボローム解析による高温応答評価の有用性が示されたため、タルホコムギの遺伝子を導入した遺伝資源の耐性評価への実装を試みた。材料として、パンコムギの世界的な高温栽培地であるスーダンの圃場で行なった栽培評価試験で登熟期の高温環境でも収量性の維持および向上が期待された

高温耐性候補系統（MSD296、MSD34、MSD392、MSD417、MSD54、MNH2）を用いた。候補系統とその戻し交配親（農林 61 号）を気温、湿度、照度の制御された人工気象器内で栽培し、開花後 7 日目の止め葉における代謝物質含有量と最終的な農業形質を測定した。それらの結果を用いて重回帰分析を行い、各系統の高温耐性と育種利用への将来性を評価した。系統特異的な農業形質の違いを代謝物質から語ることができ、収量向上に貢献する有力な高温耐性候補系統として、MSD392 と MSD417 を同定した。これらは、それぞれ千粒重と粒数の増加に寄与する遺伝子を有することが期待された。

本研究で得られた知見は、高温環境下でも高い収量性を保持する系統を効率的に育種選抜するツールとして活用できると考えられる。

Acknowledgement

I wish to thank Prof. Hisashi Tsujimoto, Arid Land Research Center, Tottori University, for his kind instruction, plentiful academic advice, stimulus suggestions, discussion providing many insights, critical and patient review of manuscripts and helpful advice for the researcher's life.

I also wish to thank Prof. Masayoshi Shigyo, Faculty of Agriculture, Yamaguchi University, Prof. Kinya Akashi, Faculty of Agriculture, Tottori University, for their academic advice, suggestions, and criticisms.

I deeply appreciate Dr. Yuji Yamasaki and Prof. Benjamin Ewa Ubi, Arid Land Research Center, Tottori University, Dr. Ryosuke Mega, Faculty of Agriculture, Yamaguchi University, and Dr. Yusuke Toda, The University of Tokyo for their kind and accurate instruction, assistance with experiments, constructive suggestions, discussions providing many insights and review of the manuscript.

For all laboratory members of Molecular Breeding, Arid Land Research Center, Tottori University, I would like to express thanks for their cooperation.

Finally, I would like to extend my deepest gratitude to my father and mother, and husband for their endless love, understanding, support throughout my study.

References

Abdelrahman, M.; Burritt, D.J.; Gupta, A.; Tsujimoto, H.; Tran, L.S.P.; Foyer, C. Heat Stress Effects on Source-Sink Relationships and Metabolome Dynamics in Wheat. *Journal of Experimental Botany* **2020**, *71*, 543–554.

Acevedo, E.; Silva, P.; Silva, H. *Wheat Growth and Physiology*; FAO Plant Production and Protection Series No. 30 (eds. B.C. Curtis, S. Rajaram, H. Gómez Macpherson), Food and Agriculture Organization of the United Nations, **2002**, 1–31, ISBN 92-5-104809-6.

Alghabari, F.; Lukac, M.; Jones, H.E.; Gooding, M.J. Effect of Rht Alleles on the Tolerance of Wheat Grain Set to High Temperature and Drought Stress During Booting and Anthesis. *Journal of Agronomy and Crop Science* **2014**, *200*, 36–45, doi:10.1111/jac.12038.

Ashihara, H.; Stasolla, C.; Fujimura, T.; Crozier, A. Purine Salvage in Plants. *Phytochemistry* **2018**, *147*, 89–124, doi:10.1016/J.PHYTOCHEM.2017.12.008.

Asseng, S.; Foster, I.; Turner, N.C. The Impact of Temperature Variability on Wheat Yields. *Global Change Biology* **2011**, *17*, 997–1012, doi:10.1111/j.1365-2486.2010.02262.x.

Avila-Ospina, L.; Clément, G.; Masclaux-Daubresse, C. Metabolite Profiling for Leaf Senescence in Barley Reveals Decreases in Amino Acids and Glycolysis Intermediates. *Agronomy* **2017**, *7*, doi:10.3390/agronomy7010015.

Babben, S., Schliephake, E., Janitza, P. et al. Association genetics studies on frost tolerance in wheat (Triticum aestivum L.) reveal new highly conserved amino acid

substitutions in CBF-A3, CBF-A15, VRN3 and PPD1 genes. *BMC Genomics*, **2018**, 19, 409, doi: 10.1186/s12864-018-4795-6

Balla, K.; Karsai, I.; Bónis, P.; Kiss, T.; Berki, Z.; Horváth, Á.; Mayer, M.; Bencze, S.; Veisz, O. Heat Stress Responses in a Large Set of Winter Wheat Cultivars (*Triticum aestivum L.*) Depend on the Timing and Duration of Stress. *PLoS ONE* **2019**, *14*, e0222639, doi:10.1371/journal.pone.0222639.

Barber, H.M.; Lukac, M.; Simmonds, J.; Semenov, M.A.; Gooding, M.J. Temporally and Genetically Discrete Periods of Wheat Sensitivity to High Temperature. *Frontiers in Plant Science* **2017**, *8*, 51, doi:10.3389/fpls.2017.00051.

Bauwe, H.; Hagemann, M.; Fernie, A.R. Photorespiration: Players, Partners and Origin. *Trends in Plant Science* **2010**, *15*, 330–336, doi:10.1016/j.tplants.2010.03.006.

Bechtel, D.B.; Wilson, J.D. Amyloplast Formation and Starch Granule Development in Hard Red Winter Wheat. *Cereal Chemistry* **2003**, *80*, 175–183, doi:10.1094/cchem.2003.80.2.175.

Blume, C.; Ost, J.; Mühlenbruch, M.; Peterhänsel, C.; Laxa, M. Low CO_2 Induces Urea Cycle Intermediate Accumulation in Arabidopsis Thaliana. *PLOS ONE* **2019**, *14*, e0210342, doi:10.1371/journal.pone.0210342.

Chen, D.; Shao, Q.; Yin, L.; Younis, A.; Zheng, B. Polyamine Function in Plants: Metabolism, Regulation on Development, and Roles in Abiotic Stress Responses. *Frontiers in Plant Science* **2019**, *0*, 1945, doi:10.3389/FPLS.2018.01945.

Duan, G. Effect of Speridine on Protein Contents and Protease during Senescence of Fxicsed Wheat Leaves. *Journal of Sichuan Teachers College* **2000**, *21*, 44–47, doi:10.3969/j.issn.1673-5072.2000.01.009.

Duan, G., Huang, Z., and Lin, H. The Role of Polyamines in the Ontogeny of Higher Plants. *Acta Agriculturae Boreali-occidentalis Sinica* **2006**, *15*, 190–194, doi:10.3969/j.issn.1673-5072.2000.01.009.

Elbashir, A.A.E.; Gorafi, Y.S.A.; Tahir, I.S.A.; Elhashimi, A.M.A.; Abdalla, M.G.A.; Tsujimoto, H. Genetic Variation in Heat Tolerance-Related Traits in a Population of Wheat Multiple Synthetic Derivatives. *Breeding Science* **2017a**, *67*, 483–492, doi:10.1270/jsbbs.17048.

Elbashir, A.A.E.; Gorafi, Y.S.A.; Tahir, I.S.A.; Kim, J.-S.; Tsujimoto, H. Wheat Multiple Synthetic Derivatives: A New Source for Heat Stress Tolerance Adaptive Traits. *Breeding Science* **2017b**, *67*, 248–256, doi:10.1270/jsbbs.16204.

FAOSTAT. Available online: http://www.fao.org/faostat/en/#home (accessed on 5 April 2021).

Fan, Y.; Ma, C.; Huang, Z.; Abid, M.; Jiang, S.; Dai, T.; Zhang, W.; Ma, S.; Jiang, D.; Han, x. Heat Priming during Early Reproductive Stages Enhances Thermo-Tolerance to Post-Anthesis Heat Stress via Improving Photosynthesis and Plant Productivity in Winter Wheat (*Triticum aestivum* L.). *Frontiers in Plant Science* **2018**, *9*, 1–17, doi:10.3389/fpls.2018.00805.

Farooq, M.; Barsa, S.M.A.; Wahid, A. Priming of Field-Sown Rice Seed Enhances Germination, Seedling Establishment, Allometry and Yield. *Plant Growth Regulation* **2006**, *49*, 285–294, doi:10.1007/s10725-006-9138-y.

Ferris, R.; Ellis, R.H.; Wheeler, T.R.; Hadley, P. Effect of High Temperature Stress at Anthesis on Grain Yield and Biomass of Field-Grown Crops of Wheat. *Annals of Botany* **1998**, *82*, 631–639, doi:10.1006/anbo.1998.0740.

Fischer, R.A. Number of Kernels in Wheat Crops and the Influence of Solar Radiation and Temperature. *The Journal of Agricultural Science* **1985**, *105*, 447–461, doi:10.1017/S0021859600056495.

Fischer, R.A.; Rees, D.; Sayre, K.D.; Lu, Z.M.; Condon, A.G.; Larque Saavedra, A. Wheat Yield Progress Associated with Higher Stomatal Conductance and Photosynthetic Rate, and Cooler Canopies. *Crop Science* **1998**, *38*, 1467–1475, doi:10.2135/cropsci1998.0011183X003800060011x.

Gale, M.D.; Youssefian, S. Dwarfing Genes in Wheat. *Progress in Plant Breeding–1* **1985**, 1–35, doi:10.1016/B978-0-407-00780-2.50005-9.

Glaubitz, U.; Erban, A.; Kopka, J.; Hincha, D.K.; Zuther, E. High Night Temperature Strongly Impacts TCA Cycle, Amino Acid and Polyamine Biosynthetic Pathways in Rice in a Sensitivity-Dependent Manner. *Journal of Experimental Botany* **2015**, *66*, 6385–6397, doi:10.1093/JXB/ERV352.

Glutamine, Glutamate, Aspartate, and Asparagine Are Central Regulators of Nitrogen Assimilation, Metabolism, and Transport Available online: https://biocyclopedia.com/index/plant_pathways/glutamine_glutamate_aspartate_and_asparagine.php (accessed on 17 November 2021).

Gorafi, Y.S.A.; Kim, J.S.; Elbashir, A.A.E.; Tsujimoto, H. A Population of Wheat Multiple Synthetic Derivatives: An Effective Platform to Explore, Harness and Utilize Genetic Diversity of *Aegilops tauschii* for Wheat Improvement. *Theoretical and Applied Genetics* **2018**, *131*, 1615–1626, doi:10.1007/s00122-018-3102-x.

Guo, G.; Lv, D.; Yan, X.; Subburaj, S.; Ge, P.; Li, X.; Hu, Y.; Yan, Y. Proteome Characterization of Developing Grains in Bread Wheat Cultivars (*Triticum Aestivum L.*). *BMC Plant Biology* **2012***, 12*, doi:10.1186/1471-2229-12-147.

Guo, R.; Yang, Z.; Li, F.; Yan, C.; Zhong, X.; Liu, Q.; Xia, X.; Li, H.; Zhao, L. Comparative Metabolic Responses and Adaptive Strategies of Wheat (*Triticum Aestivum*) to Salt and Alkali Stress. *BMC Plant Biology 2015 15:1* **2015**, *15*, 1–13, doi:10.1186/S12870-015-0546-X.

Harding, S.A.; Guikema, J.A.; Paulsen, G.M. Photosynthetic Decline from High Temperature Stress during Maturation of Wheat: I. Interaction with Senescence Processes. *Plant Physiology* **1990**, *92*, 648–653, doi:10.1104/pp.92.3.648.

Hasegawa, T.; Kuwagata, T.; Yoshimoto, M.; Fukuoka, M.; Ishimaru, T.; Kondo, M. Spikelet Sterility of Rice Observed in the Record Hot Summer of 2007 and the Factors Associated with Its Variation. *Journal of Agricultural Meteorology* **2011**, *67*, 225–232, doi:10.2480/agrmet.67.4.3.

Hesberg, C.; Hänsch, R.; Mendel, R.R.; Bittner, F. Tandem Orientation of Duplicated Xanthine Dehydrogenase Genes from Arabidopsis Thaliana: DIFFERENTIAL GENE EXPRESSION AND ENZYME ACTIVITIES *. *Journal of Biological Chemistry* **2004**, *279*, 13547–13554, doi:10.1074/JBC.M312929200.

Heyneke, E.; Watanabe, M.; Erban, A.; Duan, G.; Buchner, P.; Walther, D.; Kopka, J.; Hawkesford, M.J.; Hoefgen, R. Characterization of the Wheat Leaf Metabolome during Grain Filling and under Varied N-Supply. *Frontiers in Plant Science* **2017**, 2048, doi:10.3389/FPLS.2017.02048.

Hu, Z.; Song, N.; Zheng, M.; Liu, X.; Liu, Z.; Xing, J.; Ma, J.; Guo, W.; Yao, Y.; Peng, H.; *et al.* Histone Acetyltransferase GCN5 Is Essential for Heat Stress-Responsive Gene Activation and Thermotolerance in Arabidopsis. *The Plant Journal* **2015**, *84*, 1178–1191, doi:10.1111/tpj.13076.

Hyles, J.; Bloomfield, M.T.; Hunt, J.R.; Trethowan, R.M.; Trevaskis, B. Phenology and Related Traits for Wheat Adaptation. *Heredity* **2020**, *125*, 417–430.

Iizumi, T.; Ali-Babiker, I.-E.A.; Tsubo, M.; Tahir, I.S.A.; Kurosaki, Y.; Kim, W.; Gorafi, Y.S.A.; Idris, A.A.M.; Tsujimoto, H. Rising Temperatures and Increasing Demand Challenge Wheat Supply in Sudan. *Nature Food* **2021**, *2*, 19–27, doi:10.1038/s43016-020-00214-4.

Ishihara, A.; Hashimoto, Y.; Tanaka, C.; Dubouzet, J.G.; Nakao, T.; Matsuda, F.; Nishioka, T.; Miyagawa, H.; Wakasa, K. The Tryptophan Pathway Is Involved in the Defense Responses of Rice against Pathogenic Infection via Serotonin Production. *The Plant Journal* **2008**, *54*, 481–495, doi:10.1111/J.1365-313X.2008.03441.X.

Itam, M.; Abdelrahman, M.; Yamasaki, Y.; Mega, R.; Gorafi, Y.; Akashi, K.; Tsujimoto, H. *Aegilops tauschii* Introgressions Improve Physio-Biochemical Traits and Metabolite Plasticity in Bread Wheat under Drought Stress. *Agronomy* **2020a**, *10*, 1588, doi:10.3390/agronomy10101588.

Itam, M.; Mega, R.; Tadano, S.; Abdelrahman, M.; Matsunaga, S.; Yamasaki, Y.; Akashi, K.; Tsujimoto, H. Metabolic and Physiological Responses to Progressive Drought Stress in Bread Wheat. *Scientific Reports* **2020b**, 10, 1–14, doi:10.1038/s41598-020-74303-6.

Ito, H.; Gaubert, H.; Bucher, E.; Mirouze, M.; Vaillant, I.; Paszkowski, J. An SiRNA Pathway Prevents Transgenerational Retrotransposition in Plants Subjected to Stress. *Nature* **2011**, *472*, 115–120, doi:10.1038/nature09861.

Ito, H.; Kim, J.M.; Matsunaga, W.; Saze, H.; Matsui, A.; Endo, T.A.; Harukawa, Y.; Takagi, H.; Yaegashi, H.; Masuta, Y.; *et al.* A Stress-Activated Transposon in

Arabidopsis Induces Transgenerational Abscisic Acid Insensitivity. *Scientific Reports* **2016**, *6*, 1–12, doi:10.1038/srep23181.

Kang, K.; Kim, Y.-S.; Park, S.; Back, K. Senescence-Induced Serotonin Biosynthesis and Its Role in Delaying Senescence in Rice Leaves. *Plant Physiology* **2009**, *150*, 1380, doi:10.1104/PP.109.138552.

Kang, S.; Kang, K.; Lee, K.; Back, K. Characterization of Tryptamine 5-Hydroxylase and Serotonin Synthesis in Rice Plants. *Plant cell reports* **2007**, *26*, 2009–2015, doi:10.1007/S00299-007-0405-9.

Kihara, H. Discovery of the DD–analyzer, one of the analyzers of Triticum vulgare. *Agriculture and Horticulture*, **1944**, 19.1: 889-890.

Law, R. D.; Crafts-Brandner, S. J. Inhibition and Acclimation of Photosynthesis to Heat Stress Is Closely Correlated with Activation of Ribulose-1,5-Bisphosphate Carboxylase/Oxygenase. *Plant Physiology* **1999**, *120*, 173–182, https://doi.org/10.1104/pp.120.1.173.

Le Lay, P.; Isaure, M.P.; Sarry, J.E.; Kuhn, L.; Fayard, B.; le Bail, J.L.; Bastien, O.; Garin, J.; Roby, C.; Bourguignon, J. Metabolomic, Proteomic and Biophysical Analyses of Arabidopsis Thaliana Cells Exposed to a Caesium Stress. Influence of Potassium Supply. *Biochimie* **2006**, 88, 1533–1547, doi:10.1016/J.BIOCHI.2006.03.013.

Liang, C. gang; Chen, L. ping; Wang, Y.; Liu, J.; Xu, G. li; Li, T. High Temperature at Grain-Filling Stage Affects Nitrogen Metabolism Enzyme Activities in Grains and Grain Nutritional Quality in Rice. *Rice Science* **2011**, *18*, 210–216, doi:10.1016/S1672-6308(11)60029-2.

Lu, H.; Hu, Y.; Wang, C.; Liu, W.; Ma, G.; Han, Q.; Ma, D. Effects of High Temperature and Drought Stress on the Expression of Gene Encoding Enzymes and the Activity of

Key Enzymes Involved in Starch Biosynthesis in Wheat Grains. *Frontiers in Plant Science* **2019**, 1414, doi:10.3389/FPLS.2019.01414.

Matsuoka, Y. Evolution of polyploid *triticum* wheats under cultivation: the role of domestication, natural hybridization and allopolyploid speciation in their diversification. *Plant and Cell Physiology*, **2011**, 52(5), 750–764. doi:10.1093/PCP/PCR018

Matsuoka, Y.; Nasuda, S. Durum wheat as a candidate for the unknown female progenitor of bread wheat: An empirical study with a highly fertile F1 hybrid with *Aegilops tauschii Coss*. *Theoretical and Applied Genetics*, **2004**, 109(8), 1710–1717. doi:10.1007/S00122-004-1806-6

Matsuyama, H.; Fujita, M.; Masako, S.; Hisayo, K.; Shimazaki, Y.; Matsunaka, H.; Chono, M.; Hatta, K.; Kubo, K.; Takayama, T.; *et al.* Growth and Yield Properties of Near-Isogenic Wheat Lines Carrying Different Photoperiodic Response Genes. *Plant Production Science* **2015**, *18*, 57–68, doi:10.1626/pps.18.57.

Mcfadden, E. S.; Sears E. R. The artificial synthesis of Triticum spelta. *Records of the Genetics Society of America* **1944**, 13: 26-27.

Mendanha, T.; Rosenqvist, E.; Hyldgaard, B.; Ottosen, C.O. Heat Priming Effects on Anthesis Heat Stress in Wheat Cultivars (*Triticum aestivum* L.) with Contrasting Tolerance to Heat Stress. *Plant Physiology and Biochemistry* **2018**, *132*, 213–221, doi:10.1016/j.plaphy.2018.09.002.

Morot-Gaudry, J.-F.; Job, D.; Lea, P.J. Amino Acid Metabolism. *Plant Nitrogen* **2001**, 167–211, doi:10.1007/978-3-662-04064-5_7.

Nakagawa, A.; Sakamoto, S.; Takahashi, M.; Morikawa, H.; Sakamoto, A. The RNAi-Mediated Silencing of Xanthine Dehydrogenase Impairs Growth and Fertility and

Accelerates Leaf Senescence in Transgenic Arabidopsis Plants. *Plant and Cell Physiology* **2007**, *48*, 1484–1495, doi:10.1093/PCP/PCM119.

Navarro-Reig, M.; Jaumot, J.; Piña, B.; Moyano, E.; Galceran, M.T.; Tauler, R. Metabolomic Analysis of the Effects of Cadmium and Copper Treatment in Oryza Sativa L. Using Untargeted Liquid Chromatography Coupled to High Resolution Mass Spectrometry and All-Ion Fragmentation. *Metallomics* **2017**, 9, 660–675, doi:10.1039/C6MT00279J.

Nguyen, V.L.; Palmer, L.; Roessner, U.; Stangoulis, J. Genotypic Variation in the Root and Shoot Metabolite Profiles of Wheat (*Triticum Aestivum L.*) Indicate Sustained, Preferential Carbon Allocation as a Potential Mechanism in Phosphorus Efficiency. *Frontiers in Plant Science* **2019**, 995, doi:10.3389/FPLS.2019.00995.

Obata, T.; Witt, S.; Lisec, J.; Palacios-Rojas, N.; Florez-Sarasa, I.; Yousfi, S.; Araus, J.L.; Cairns, J.E.; Fernie, A.R. Metabolite Profiles of Maize Leaves in Drought, Heat, and Combined Stress Field Trials Reveal the Relationship between Metabolism and Grain Yield. *Plant Physiology* **2015**, *169*, 2665–2683, doi:10.1104/PP.15.01164.

Oliveira, I.C.; Brenner, E.; Chiu, J.; Hsieh, M.-H.; Kouranov, A.; Lam, H.-M.; Shin, M.J.; Coruzzi, G. Metabolite and Light Regulation of Metabolism in Plants: Lessons from the Study of a Single Biochemical Pathway. *Brazilian Journal of Medical and Biological Research* **2001**, *34*, 567–575, doi:10.1590/S0100-879X2001000500003.

Parthasarathy, A.; Savka, M.A.; Hudson, A.O. The Synthesis and Role of β-Alanine in Plants. *Frontiers in Plant Science* **2019**, *0*, 921, doi:10.3389/FPLS.2019.00921.

Pelagio-Flores, R.; Ortíz-Castro, R.; Méndez-Bravo, A.; Macías-Rodríguez, L.; López-Bucio, J. Serotonin, a Tryptophan-Derived Signal Conserved in Plants and Animals, Regulates Root System Architecture Probably Acting as a Natural Auxin Inhibitor in

Arabidopsis Thaliana. *Plant and Cell Physiology* **2011**, *52*, 490–508, doi:10.1093/PCP/PCR006.

Qu, A.L.; Ding, Y.F.; Jiang, Q.; Zhu, C. Molecular Mechanisms of the Plant Heat Stress Response. *Biochemical and Biophysical Research Communications* **2013**, *432*, 203–207.

Rawson, H.M. An Upper Limit for Spikelet Number per Ear in Wheat as Controlled by Photoperiod. *Aust. J. Agric. Res.* **1971**, *22*, 537–546, doi:10.1071/AR9710537.

Rezaei, E.E. *et al.* Quantifying the response of wheat yields to heat stress: The role of the experimental setup. *Field Crops Research*, **2018**, 217, 93–103. doi:10.1016/J.FCR.2017.12.015.

Rezaei, E.E.; Siebert, S.; Manderscheid, R.; Müller, J.; Mahrookashani, A.; Ehrenpfordt, B.; Haensch, J.; Weigel, H.J.; Ewert, F. Quantifying the Response of Wheat Yields to Heat Stress: The Role of the Experimental Setup. *Field Crops Research* **2018**, *217*, 93–103, doi:10.1016/J.FCR.2017.12.015.

Rivero, R.M.; Shulaev, V.; Blumwald, E. Cytokinin-Dependent Photorespiration and the Protection of Photosynthesis during Water Deficit. *Plant Physiology* **2009**, *150*, 1530–1540, doi:10.1104/pp.109.139378.

Schachtman, D.P., Lagudah, E.S. & Munns, R. The expression of salt tolerance from Triticum tauschii in hexaploid wheat. *Theoretical and Applied Genetics* **1992,** 84, 714–719, doi: 10.1007/BF00224174

Shao, C. G., Wang, H., and Yu-Fen, B.I. Relationship between Endogenous Polyamines and Tolerance in Medicago Sativa L.under Heat Stress. *Acta Agrestia Sinica* **2015**, *23*, 1214–1219, doi:10.11733/j.issn.1007-0435.

Sharkey, T.D.; Bernacchi, C.J.; Farquhar, G.D.; Singsaas, E.L. Fitting Photosynthetic Carbon Dioxide Response Curves for C3 Leaves. *Plant, Cell & Environment* **2007**, *30*, 1035–1040, doi:10.1111/j.1365-3040.2007.01710.x.

Shi, T.; Zhu, A.; Jia, J.; Hu, X.; Chen, J.; Liu, W.; Ren, X.; Sun, D.; Fernie, A.R.; Cui, F.; et al. Metabolomics Analysis and Metabolite-Agronomic Trait Associations Using Kernels of Wheat (*Triticum Aestivum*) Recombinant Inbred Lines. *The Plant Journal* **2020**, *103*, 279–292, doi:10.1111/TPJ.14727.

Shimizu, K.K.; Copetti, D.; Okada, M.; Wicker, T.; Tameshige, T.; Hatakeyama, M.; Shimizu-Inatsugi, R.; Aquino, C.; Nishimura, K.; Kobayashi, F.; *et al.* De Novo Genome Assembly of the Japanese Wheat Cultivar Norin 61 Highlights Functional Variation in Flowering Time and Fusarium Resistance Genes in East Asian Genotypes. *Plant and Cell Physiology* **2020**, *62*, 8–27, doi:10.1093/pcp/pcaa152.

Shin, H., Oh, S., Arora, R., & Kim, D. Proline accumulation in response to high temperature in winter-acclimated shoots of Prunus persica: A response associated with growth resumption or heat stress? *Canadian Journal of Plant Science* **2016**, *96(4)*, 630–638. https://doi.org/10.1139/cjps-2015-0372

Shulaev, V.; Cortes, D.; Miller, G.; Mittler, R. Metabolomics for Plant Stress Response. *Physiologia Plantarum* **2008**, 132, 199–208, doi:10.1111/J.1399-3054.2007.01025.X.

Slafer, G.A.; Rawson, H.M. Does Temperature Affect Final Numbers of Primordia in Wheat? *Field Crops Research* **1994**, *39*, 111–117, doi:10.1016/0378-4290(94)90013-2.

Soltani, A.; Sinclair, T.R. *Modeling Physiology of Crop Development, Growth and Yield*; CABi: Wallingford, UK, **2012**, ISBN 9781845939700.

Stocker, T.F.; Qin, D.; Plattner, G.-K.; Tignor, M.; Allen, S.K.; Boschung, J.; Nauels, A.; Xia, Y.; Bex, V.; Midgley, P.M. *AR5 Climate Change 2013: The Physical Science Basis—IPCC*; Cambridge University Press: Cambridge, UK, **2021**, 1585.

Telfer, P.; Edwards, J.; Bennett, D.; Ganesalingam, D.; Able, J.; Kuchel, H. A Field and Controlled Environment Evaluation of Wheat (Triticum Aestivum) Adaptation to Heat Stress. *Field Crops Research* **2018**, *229*, 55–65, doi:10.1016/J.FCR.2018.09.013.

Templer, S.E.; Ammon, A.; Pscheidt, D.; Ciobotea, O.; Schuy, C.; McCollum, C.; Sonnewald, U.; Hanemann, A.; Förster, J.; Ordon, F.; et al. Metabolite Profiling of Barley Flag Leaves under Drought and Combined Heat and Drought Stress Reveals Metabolic QTLs for Metabolites Associated with Antioxidant Defense. *Journal of Experimental Botany* **2017**, *68*, 1697–1713, doi:10.1093/jxb/erx038.

Tian, H.; Lam, S.M.; Shui, G. Metabolomics, a Powerful Tool for Agricultural Research. International Journal of Molecular Sciences 2016, 17, doi:10.3390/IJMS17111871.

Timm, S.; Florian, A.; Wittmiß, M.; Jahnke, K.; Hagemann, M.; Fernie, A.R.; Bauwe, H. Serine Acts as a Metabolic Signal for the Transcriptional Control of Photorespiration-Related Genes in Arabidopsis. *Plant Physiology* **2013**, *162*, 379, doi:10.1104/PP.113.215970.

Todaka, D.; Zhao, Y.; Yoshida, T.; Kudo, M.; Kidokoro, S.; Mizoi, J.; Kodaira, K.S.; Takebayashi, Y.; Kojima, M.; Sakakibara, H.; et al. Temporal and Spatial Changes in Gene Expression, Metabolite Accumulation and Phytohormone Content in Rice Seedlings Grown under Drought Stress Conditions. *Plant Journal* **2017**, *90*, 61–78, doi:10.1111/tpj.13468.

Tsujimoto H.; Sohail Q.; Matsuoka Y. Broadening the Genetic Diversity of Common and Durum Wheat for Abiotic Stress Tolerance Breeding. *In*: Ogihara Y., Takumi S.,

Handa H. (eds) Advances in Wheat Genetics: From Genome to Field. Springer, Tokyo. **2015**, 233–38

Voss, I.; Sunil, B.; Scheibe, R.; Raghavendra, A.S. Emerging Concept for the Role of Photorespiration as an Important Part of Abiotic Stress Response. *Plant Biology* **2013**, *15*, 713–722, doi:10.1111/J.1438-8677.2012.00710.X.

Wahid, A.; Gelani, S.; Ashraf, M.; Foolad, M.R. Heat Tolerance in Plants: An Overview. *Environmental and Experimental Botany* **2007**, *61*, 199–223.

Walkowiak, S.; Gao, L.; Monat, C.; Haberer, G.; Kassa, M.T.; Brinton, J.; Ramirez-Gonzalez, R.H.; Kolodziej, M.C.; Delorean, E.; Thambugala, D.; *et al.* Multiple Wheat Genomes Reveal Global Variation in Modern Breeding. *Nature* **2020**, *588*, 277–283, doi:10.1038/s41586-020-2961-x.

Wang, W.; Chen, Q.; Hussain, S.; Mei, J.; Dong, H.; Peng, S.; Huang, J.; Cui, K.; Nie, L. Pre-Sowing Seed Treatments in Direct-Seeded Early Rice: Consequences for Emergence, Seedling Growth and Associated Metabolic Events under Chilling Stress. *Scientific Reports* **2016**, *6*, 1–10, doi:10.1038/srep19637.

Wang, X.; Xin, C.; Cai, J.; Zhou, Q.; Dai, T.; Cao, W.; Jiang, D. Heat Priming Induces Trans-Generational Tolerance to High Temperature Stress in Wheat. *Frontiers in Plant Science* **2016**, *7*, 501, doi:10.3389/fpls.2016.00501.

Watanabe, S.; Nakagawa, A.; Izumi, S.; Shimada, H.; Sakamoto, A. RNA Interference-Mediated Suppression of Xanthine Dehydrogenase Reveals the Role of Purine Metabolism in Drought Tolerance in Arabidopsis. *FEBS Letters* **2010**, *584*, 1181–1186, doi:10.1016/J.FEBSLET.2010.02.023.

Wheeler, T.R.; Batts, G.R.; Ellis, R.H.; Hadley, P.; Morison J.I.L. Growth and Yield of Winter Wheat (*Triticum aestivum*) Crops in Response to CO2 and Temperature. *The Journal of Agricultural Science* **1996a**, *127*, 37–48.

Wheeler, T.R.; Hong, T.D.; Ellis, R.H.; Batts, G.R.; Morison, J.I.L.; Hadley, P. The Duration and Rate of Grain Growth, and Harvest Index, of Wheat (*Triticum aestivum* L.) in Response to Temperature and CO2. *Journal of Experimental Botany* **1996b**, *47*, 623–630, doi:10.1093/jxb/47.5.623.

Witte, C.-P.; Herde, M. Nucleotide Metabolism in Plants. *Plant Physiology* **2020**, *182*, 63–78, doi:10.1104/PP.19.00955.

Worland, A.J.; Börner, A.; Korzun, V.; Li, W.M.; Petrovíc, S.; Sayers, E.J. The Influence of Photoperiod Genes on the Adaptability of European Winter Wheats. *Euphytica* **1998**, *100*, 385–394, doi:10.1023/a:1018327700985.

Yamaji, N.; Ma, J.F. The Node, a Hub for Mineral Nutrient Distribution in Graminaceous Plants. *Trends in Plant Science* **2014**, *19*, 556–563, doi:10.1016/j.tplants.2014.05.007.

Yamaji, N.; Takemoto, Y.; Miyaji, T.; Mitani-Ueno, N.; Yoshida, K. T.; Ma, J. F. Reducing phosphorus accumulation in rice grains with an impaired transporter in the node. *Nature* **2017**, 541(7635), 92–95. doi:10.1038/nature20610

Yamasaki, Y.; Gao, F.; Jordan, M.C.; Ayele, B.T. Seed Maturation Associated Transcriptional Programs and Regulatory Networks Underlying Genotypic Difference in Seed Dormancy and Size/Weight in Wheat (*Triticum aestivum* L.). *BMC Plant Biology* **2017**, *17*, 1–18, doi:10.1186/s12870-017-1104-5.

Yang, H.; Gu, X.; Ding, M.; Lu, W.; Lu, D. Heat Stress during Grain Filling Affects Activities of Enzymes Involved in Grain Protein and Starch Synthesis in Waxy Maize. *Scientific Reports* **2018**, *8*, 1–9, doi:10.1038/s41598-018-33644-z.

Yang, Y., and Yang, X. Effect of Temperature on Endogenous Polyamine Content in Leaves of Chinese Kale Seedlings. *Journal of South China Agicultural University* **2002**, *23*, 9–12, doi:10.3969/j.issn.1001-411X.2002.03.003.

Yuan, L.; Tang, L.; Zhu, S.; Hou, J.; Chen, G.; Liu, F.; Liu, S.; Wang, C. Influence of Heat Stress on Leaf Morphology and Nitrogen-Carbohydrate Metabolisms in Two Wucai (Brassica Campestris L.) Genotypes. *Acta Societatis Botanicorum Poloniae* **2017**, 86, doi:10.5586/ASBP.3554.

Zadoks, J.C.; Chang, T.T.; Konzak, C.F. A Decimal Code for the Growth Stages of Cereals. *Weed Research* **1974**, *14*, 415–421, doi:10.1111/j.1365–3180.1974.tb01084.x.

Zampieri, M.; Ceglar, A.; Dentener, F.; Toreti, A. Understanding and Reproducing Regional Diversity of Climate Impacts on Wheat Yields: Current Approaches, Challenges and Data Driven Limitations. *Environmental Research Letters* **2018**, *13*, 021001, doi:10.1088/1748-9326/AAA00D.

Published Paper

First article: Result section (3.1, 3.2, 3.4, 3.5)

Title: Stage-Specific Characterization of Physiological Response to Heat Stress in the Wheat Cultivar Norin 61

Authors: Sachiko Matsunaga; Yuji Yamasaki; Yusuke Toda; Ryosuke Mega; Kinya Akashi; Hisashi Tsujimoto

Journal with Volume, Number and Pages: International Journal of Molecular Sciences, 22(13), 6942

Accepted Date: June 2021

Second article: Result section (3.6 – 3.10)

Title: Metabolome Profiling of Heat Priming Effects, Senescence, and Acclimation of Bread Wheat Induced by High Temperatures at Different Growth Stages

Authors: Sachiko Matsunaga; Yuji Yamasaki; Ryosuke Mega; Yusuke Toda; Kinya Akashi; Hisashi Tsujimoto

Journal with Volume, Number and Pages: International Journal of Molecular Sciences, 22(23), 13139

Accepted Date: December 2021